

Mathematical models of stress and epidemiology

An alternative format thesis submitted to The University of Sheffield for
the degree of Doctor of Philosophy (PhD)

Ross Dean Booton

Department of Animal and Plant Sciences

November 2018

Abstract

This thesis is concerned with using mathematical models to investigate the impacts of stress and epidemiology on ecological frameworks. First we focus on the effects of stress on honey bee colony decline. We establish a mathematical model to describe the regulatory processes governing the hive and general stressors impacting the colony. We analyse this model in order to understand how these regulatory processes counteract stressors and find that increasing a density-dependent Allee stressor effect can cause sudden and unexpected dynamical changes in behaviour.

Our second study examines honey bee hive infection with multiple routes of transmission. We study a mathematical model of infection with multiple transmission routes in order to understand how these routes can impact the spread of disease within a colony. We use published data taken from the literature and examine the respective contributions to total disease burden by each route. We demonstrate the presence of a synergistic interaction between both infection pathways compared to each infection route acting alone.

Our third study examines the interaction between two interacting stressors. Toxicant stress can have both immunosuppressive and lethal direct effects on non-target organisms. We study a model which describes the within-host processes of cellular health, infection and immunity and anal-

yse this model under the effects of increasing toxicant stress. We show that sublethal toxicant stress can promote within-host infection and that this infection is maximised by an intermediate level of toxicant, rather than linearly increasing as the toxicant load is increased.

We expand upon this within-host framework to include population level processes. We do this since infection not only spreads within the host organism but also spreads between those individuals within a population. We formulate a nested model to describe the within-host processes and the between-host epidemiological dynamics under stress to understand how toxicants impact the spread of population-level disease. We show that infection outbreak at the population level is determined by the interaction with stress and that the epidemic is maximised by an intermediate level of toxicant.

Finally we summarise the findings of this thesis and discuss potential future avenues for research.

Acknowledgements

I would first like to thank my principal supervisor, Dr. Dylan Childs for the opportunity to work under his direction. In particular, I appreciate his guidance and time, and his advice steering me away from mathematics for the sake of mathematicians. I would also like to thank my secondary supervisor, Prof. James Marshall for his support and guidance particularly towards the first half of my PhD, and later, his constructive comments on journal articles.

I'm grateful to have spent two summers working under the guidance of Yoh Iwasa in Japan, and I am thankful to JSPS for funding these research trips. I would like to thank Prof. Iwasa for the passion he has in supporting young researchers - his legacy in mathematical biology will live on because of this.

I would like to thank the various lab groups I have been involved within: the Childs lab group, past and present members of the BET group, and the mathematical biology lab at Kyushu. In particular I would like to thank Ryo Yamaguchi for the various projects we worked on and his friendship during the time I spent in Japan. Likewise, to Prof. Shingo Iwami for the opportunity to work in his group and I look forward to visiting Japan again soon.

I would like to thank the new friends I gained in Sheffield, who have

supported me throughout my PhD. A special thanks to the city of Sheffield for putting up with us and leaving such a lasting impression on me. It has truly been some of the best years of my life.

Thank you to my sixth form maths teacher Mr. Bonser for inspiring me to pursue mathematics and teaching me the valuable lesson of independence.

I don't get the opportunity to thank my parents very often. First, I would like to thank my Mum for everything she has done. I remember the effort she put into my education and learning and I am forever grateful. She dedicated her life to raising us and I am so appreciative of her. Second, I would like to thank my Dad for instilling in me a belief that I could do anything I wanted in this world. When I was growing up, he regularly showed me the alternative future where I worked with him if I didn't work hard at school. It is because of this that I was able to pursue academic interests and gain my PhD.

Finally, I cannot give enough appreciation to my fiancée Sophie who has been there with me throughout everything I have done. Without her love, support and unlimited encouragement I could not have completed this work. I look forward to hopefully becoming Dr and Dr Booton in 2019.

Contents

1	Introduction	1
1.1	Stressors	2
1.2	Mathematical models	5
1.3	Motivation and aims	11
1.4	Overview of Thesis	13
2	Stress-mediated Allee effects can cause the sudden collapse of honey bee colonies	17
2.1	Abstract	18
2.2	Introduction	19
2.3	Methods	22
2.4	Results	29
2.5	Discussion	38
3	Multiple routes of transmission synergistically increase infection within the honey bee hive	43

3.1	Abstract	44
3.2	Introduction	45
3.3	Methods	47
3.4	Results	49
3.5	Discussion	57
4	Interactions between immunotoxicants and parasite stress: implications for host health	62
4.1	Abstract	63
4.2	Introduction	64
4.3	Methods	67
4.4	Results	71
4.5	Discussion	82
5	How do toxicants affect epidemiological dynamics?	87
5.1	Abstract	88
5.2	Introduction	89
5.3	Methods	93
5.4	Results	100
5.5	Discussion	113
6	Discussion	120
6.1	Summary	120
6.2	Future work	122

Bibliography **127**

A Appendix for Chapter 2 **152**

B Appendix for Chapter 3 **160**

C Appendix for Chapter 4 **166**

D Appendix for Chapter 5 **174**

List of Figures

1.1	Outline of a SIR model	7
1.2	Outline of the immune response model	10
1.3	Outline for a generalised nested model	11
2.1	Dynamics of the honey bee stress population model	24
2.2	The effects of stress and high density on in-hive mortality . .	28
2.3	Numerical simulations for increasing stress and sensitivity . .	33
2.4	The saddle-node bifurcation through parameter μ	35
2.5	Two levels of stress on the in-hive-forager phase plane	36
2.6	The location of the limit point in 2D parameter space	37
3.1	Outline of the honey bee disease dynamics model	50
3.2	Simulations of the honey bee disease model for p^*	54
3.3	Contributions to disease outbreak in each season	56
3.4	Simulations of the disease model for a range of R_I and R_D . .	58
4.1	Outline of the within-host stress model	69

4.2	Within-host processes under increasing toxicant exposure . . .	76
4.3	Within-host processes under $Q = 0$ and $Q = 0.5$	78
4.4	Within-host processes under increasing toxicant and $r = 0$. . .	79
4.5	Within-host processes under increasing toxicant and $r > h$. . .	80
4.6	The behaviour of the model within $r - h$ space	81
5.1	Outline of the nested multilevel model	99
5.2	The baseline dynamics of the nested model with $Y^* = 0$. . .	103
5.3	5 phases of an infected population under increasing Q	106
5.4	The predicted phase outcome for varying ζ_1 and ζ_2	108
5.5	The predicted phase outcome for varying ϵ and θ	109
5.6	The predicted phase outcome for varying Λ and u	110
5.7	3 phases under increasing Q with $\zeta_1 = 0$	112
5.8	3 phases under increasing Q with $\zeta_1 > \zeta_2$	113
A1	The saddle-node bifurcation through m	155
A2	The saddle-node bifurcation through α	156
A3	The reversed direction saddle-node bifurcation through σ . .	156
A4	The reversed direction saddle-node bifurcation through L . .	157
A5	Model comparison	158
A6	In-hive and forager population bifurcations	159
B1	Data from WebPlotDigitizer and Higes et al. 2008	161

- C1 Pairwise range of sublethal and lethal effects on density . . . 171
- C2 Pairwise range of sublethal and lethal effects on infection . . . 172
- C3 Within-host processes under a density-dependent assumption 173

List of Tables

2.1	Parameter values used in the honey bee stress population model	30
3.1	Parameter values used in the honey bee disease dynamics model	51
4.1	Parameter values used in the within-host stress model	71
4.2	Net change in within-host processes for $Y = 0$ and $Y > 0$	73
5.1	Parameter values used in the nested multilevel model	100

Alternative Format Thesis:

Published parts of the thesis, author contributions and copyright

All co-authors agree to the use of published material in this thesis and signed the following statements (which are attached to the end of this thesis) which summarise co-author contributions: *Please allow Ross Booton to include the following paper(s) which have been published (or submitted for publication), of which I was a co-author in his doctoral thesis. I confirm that Ross Booton conceived the initial idea for the paper(s) and was the primary contributor to the design and conduct of the reported research. All authors contributed its development. Ross Booton constructed the model(s) and analysed and interpreted the material. Ross Booton wrote the manuscript(s), with contributions from all authors.*

The following chapters featured within this thesis have been published previously in peer-reviewed international journals:

- Chapter 2 is based on RD Booton, Y Iwasa, JAR Marshall, and DZ Childs. Stress-mediated Allee effects can cause the sudden collapse of honey bee colonies. *J. Theor. Biol.*, 420:213–219, 2017.
- Chapter 4 is based on RD Booton, R Yamaguchi, JAR Marshall, DZ Childs, and Y Iwasa. Interactions between immunotoxicants and parasite

stress: implications for host health. *J. Theor. Biol.*, 445:120–127, 2018.

The following chapters are currently under consideration/ review in peer-reviewed international journals:

- Chapter 3 is based on R. Booton, D. Childs, R. Yamaguchi, Y. Tachiki, and S. Iwami. Multiple routes of transmission synergistically increase infection within the honey bee hive: a mathematical model. *Manuscript submitted for publication*, 2018.
- Chapter 5 is based on R. Booton, Y. Iwasa, and D. Childs. How do toxicants affect epidemiological dynamics? *Manuscript submitted for publication*, 2018.

Permission has been obtained where appropriate to include material which has been published. This was obtained from the Copyright Clearance Center RightsLink: *Please note that, as the author of this Elsevier article, you retain the right to include it in a thesis or dissertation, provided it is not published commercially. Permission is not required, but please ensure that you reference the journal as the original source.*

Additional papers published during the thesis

The following papers were published during the completion of this thesis but are not included within this thesis:

- R. Booton, R. Yamaguchi, and Y. Iwasa. A population model for diapausing multivoltine insects under asymmetric cannibalism. *Population Ecology*, in press, 2018.
- A. Goldfield, R. Booton, and J. Marston. Modeling the role of fire and cooking in the competitive exclusion of Neanderthals. *Journal of Human Evolution*, in press, 2018.
- B. Oiestad et al. Longitudinal course of physical function in people with symptomatic knee osteoarthritis: Data from the multicenter osteoarthritis study and the osteoarthritis initiative. *Arthritis care and research*, 68(3): 325-331, 2016.

Chapter 1

Introduction

Each chapter in this alternative format thesis has a standalone introduction, which summarises the empirical and theoretical studies relevant to each respective chapter in journal publication style. However, none of these chapters discuss the broader themes underpinning this thesis as a whole. Here I will briefly give a general overview of different types of biotic and abiotic stressors and their impacts on populations of host organisms. Second, I will provide an overview of commonly used mathematical models and their applications, in order to provide context for the models chosen within this thesis. Finally I will provide the motivation for, and an overview of the contents of this thesis.

1.1 Stressors

Throughout this thesis, we define the term *stressor* to be any natural or environmental factor which has a detrimental impact on the individual. *Stressors* are the external factors impacting the host, while *stress* is the internal state induced by those stressors [3]. Stress acts on a relative scale to the normal functioning of the organism and is species-specific, for example, the lack of air is completely normal to fish, but would indeed be extremely stressful to other animals [3]. Within ecological systems, organisms face a plethora of stressors [4], ranging from heat stress, freezing temperatures, desiccation, oxygen depletion, environmental pollutants and parasites [5]. In this thesis we focus upon two common stressors; environmental stress and parasites.

Environmental stress and ecotoxicology

Toxic chemicals released into the environment damage and cause stress to biological organisms at the individual level, with consequences for populations and communities. The field of ecotoxicology is a branch of toxicology which examines the effects of these chemical pollutants on organisms [6] and ecotoxicological studies have experienced a substantial growth in recent years [7]. Toxicants are usually introduced into the environment directly by or as a by-product of human activity e.g. for a substance intended

to control pests. The use of toxicants such as pesticides to control agricultural pests continues to increase globally [8–10]. These anthropogenic toxicants are known to affect a wide range of non-target species including birds and mammals [11], aquatic invertebrates and fish [7, 12], and insects such as butterflies, moths and bees [9].

Toxicants can have both lethal [13–17] and sublethal effects [18, 19]. Sublethal effects often impact the behavioural or developmental traits of an organism such as growth, mobility, feeding, learning and memory, while lethal effects are often quantified as the lethal concentration (LC_{50}) expected to kill 50% of the population. In general, the individual-level impacts of toxicants on organisms are well studied, but the effects on higher scale population processes are largely unknown [20]. Many toxicology studies focus on single-species toxicity tests [7] or on the molecular, physiological and cellular effects of toxicants [20], or on simply monitoring the decline in population as toxicant exposure increases [20]. Therefore quantifying only the lethal and sublethal thresholds of toxicant exposure [7] leads to uncertainty for the population-level consequences of toxicant-exposed individuals [21]. Very few studies address the interface between toxicant stress and population level processes [22, 23].

Parasites

There are different definitions of the term *parasite* dependent upon the scientific field. In the parasitological literature, the term *parasite* will usually refer to the more strict definition of macroscopic organisms e.g. parasitic worms and protozoans [24]. However, ecologists tend to have a broader definition of the term *parasite*: any small organism (including bacteria, viruses, fungi, worms and protozoans) living in close association with a respective host organism, which reduces the fitness of the host at the individual or population level through infection [24]. Throughout this thesis we will use this broader definition of the term *parasite* in reference to stress.

The field of parasitology is concerned with the impacts that parasites have on population dynamics, sexual selection and life-history evolution [25]. There are a substantial number of different parasite taxa, to which hosts have developed a substantial number of adaptations to stop these infections [25]. This field is extremely broad, and within this thesis we will stay within the population dynamics and parasite ecology sub-fields, rather than focussing on other important questions relating to parasite evolution and selection.

Multiple Stressors

Effects of stressors are usually tested individually, however in natural systems, organisms are frequently exposed to multiple stressors simultaneously [26]. When acting in combination, these stressors can either increase overall host stress through synergistic interactions or reduce stress through antagonistic interactions [5] (Synergism occurs when the cumulative effect of both stressors is greater than the individual additive effects, antagonism occurs when the combined effect is less than additive). Interactions between stressors often lead to effects which are not predictable from understanding the underlying impacts of the individual stressors [27]. For example, non-additive interactions between pairs of stressors can have considerable impacts on survival, intrinsic rate of natural increase and first-brood offspring [27].

1.2 Mathematical models

Mathematical models are commonly used to study complicated biological systems. Here I will give a summary of the general types of deterministic models used throughout this thesis.

Susceptible-infected-recovered (SIR) models

Modelling the spread of disease within a population was first conceptualised by Kermack and McKendrick [28], by dividing the population into susceptible (S), infective (I) and recovered (R) compartments. Susceptible individuals are those who are currently uninfected, but may become later infected, while recovered individuals are those who can no longer contract any infection. They used the following simple set of ordinary differential equations

$$\frac{dS}{dt} = -\beta SI \quad (1.1a)$$

$$\frac{dI}{dt} = \beta SI - \alpha I \quad (1.1b)$$

$$\frac{dR}{dt} = \alpha I \quad (1.1c)$$

alongside the assumptions that each individual within each compartment has identical characteristics, infected individuals transmit the infection with rate βN where $N = S + I + R$ and recovery from the infection occurs at rate α . This simple model has been used and adapted to describe a wide range of diseases and has been verified by and used extensively to fit epidemic data [29].

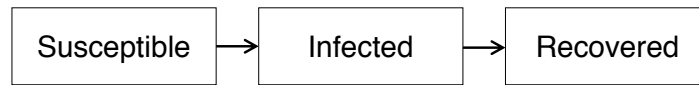


Figure 1.1: The flow diagram for the SIR model. Upon infection, susceptible individuals leave the susceptible compartment and move into the infected compartment. Upon recovery, they move from the infected to the recovered compartment.

Many extensions to the SIR model framework [28] are used in modern epidemiology, such as incorporating treatment (infected individuals become susceptible again) or including birth and death rates of the population to simulate population dynamics. Ecological disease models were pioneered by Anderson and May [30, 31] to further include the host population as a dynamical variable rather than a constant, and to include life cycles of the host and their respective parasite infections. In this thesis we will mainly use the basic susceptible-infected framework within these extensions. However, recent models have investigated a wide variety of such extensions to the initial SIR framework, including more stages and compartments of infection, vector transmission, vaccination, vertical transmission, spatiality, quarantine and explicit age structure [32]. These approaches have been developed to answer questions relating to diseases such as HIV/AIDS, syphilis, rabies, herpes, smallpox, measles, rubella and malaria (see review by Hethcote [32]).

Immune response models

Modelling the within-host interaction between pathogens, cells and the immune system relies on many assumptions dependent upon the specific biology of the species and pathogen in question [33]. However, a simple general model for the relationship between the immune response of an individual and a pathogen was formulated by Nowak and May [33], which considers four variables: uninfected cells (X), infected cells (Y), virus particles (V) and immune response (Z):

$$\frac{dX}{dt} = \lambda - \beta XV - dX \quad (1.2a)$$

$$\frac{dY}{dt} = \beta XV - aY - pYZ \quad (1.2b)$$

$$\frac{dV}{dt} = kY - uV \quad (1.2c)$$

$$\frac{dZ}{dt} = c - bZ \quad (1.2d)$$

where infected cells are produced from uninfected and virus particles at rate βXV , die at rate aY , and are removed by the immune response at rate pYZ . Uninfected cells are produced at rate λ and die at rate d . Virus is produced from infected cells at rate kY and dies at rate uV . Immunity is produced at rate c and dies at rate bZ . The model works under the assumption that $c > 0$ if $Y > 0$, otherwise $c = 0$. Other assumptions involving the acquisition of immunity are possible (such as increasing relative to parasite density [33]), but throughout this thesis we assume the simplest possible

immune response above. This model predicts two outcomes: either $R_0 < 1$ and clearance of infection, or $R_0 > 1$ and the persistence of the infection. The immune response reduces the equilibrium status of infected cells and likewise increases the equilibrium number of uninfected cells. These types of deterministic models have been used to understand different immune responses to various diseases [34], such as HIV [35], hepatitis B [36] and influenza [37], or the immune response to infection within a honey bee colony [38].

In order to simplify this model further, in this thesis we assume fast dynamics of virus replication compared to the replication of other within-host cells or immunity, which results in the formulation of the model without virus particles:

$$\frac{dX}{dt} = \lambda - \beta XY - dX \quad (1.3a)$$

$$\frac{dY}{dt} = \beta XY - aY - pYZ \quad (1.3b)$$

$$\frac{dZ}{dt} = c - bZ \quad (1.3c)$$

This model is similar to system (1.2), but assumes that infected cells are produced from uninfected and infected cells at rate βXY . This assumption means that the variable Y now represents a cell occupied by a parasitic infection rather than the cell itself.

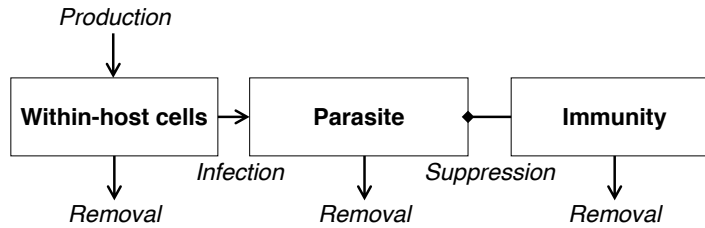


Figure 1.2: The flow diagram for the immune response model. Within-host cells are infected by the parasite and immune suppression reduces the infection. Production and removal of within-host cells, and the natural removal of parasite and immunity are also considered.

Nested models

Bridging the gap between multi-scale biological processes can be achieved using nested deterministic mathematical models [39, 40]. Nested mathematical models often embed the characteristics of smaller scales of organisation into a wider larger-scale framework. These models are commonly used to link within- and between-host levels of infection dynamics in many areas of epidemiology, for example modelling HIV and hepatitis C, and fitness evolution and viral diversity [40]. This approach allows epidemiological parameters to be determined by the dynamics of within-host parameters such as parasite load, immune status and cellular health. Nested models are particularly useful when relationships between the within- and between-host processes are unknown [40] and as such can be formalised from the subsequent analysis of these models. Recently the use of nested modelling approaches has been increasing, providing important biological

mechanistic predictions particularly within inherently multi-scale epidemiology [39, 41–45]. For example, a nested model describing the relationship between epidemiological and immunological dynamics [41] predicted that unexpected complex dynamical properties can emerge as the result of coupling two models. Additionally a model linking the within- and between-host dynamics under an environmentally-driven *Toxoplasma gondii* infection predicted that population-level disease can occur even when the isolated between-host reproduction number R_0 was less than one [44].

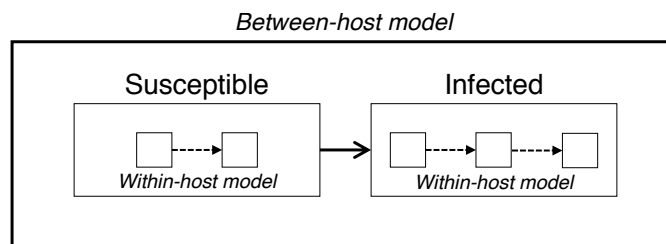


Figure 1.3: The flow diagram for a generalised nested model. The between-host model has 2 compartments: susceptible and infected. Within-host models are embedded within both susceptible and infected individuals. The particular within-host processes modelled depend entirely upon the particular infection and can vary dependent upon the between-host compartment. For example, we may want to model more processes within an infected individual, or the within-host processes impacting those of the between-host.

1.3 Motivation and aims

Before giving an overview of the contents of this thesis, I will briefly explain the main motivation and aims for each chapter, and for the entire body of work.

The original starting point for this body of work was to understand how different stressors impact honey bee colony dynamics. The motivation for this lies within the recent rapid decline in honey bee populations [10, 46], and the subsequent implications for the pollination industry, food security and biodiversity [47]. However, empirical research has yet to find a single causal factor for these honey bee declines [48]. This pressing issue provided the motivation for our original study, combined with the potential for simple theoretical models to shed new light on important biological problems.

As a consequence of completing the work contained within Chapters 2 and 3 on honey bee modelling, we found additional motivation in applying these kind of models to the wider eco-epidemiological field. Many such organisms are exposed to a wide array of stressors, which sometimes act multiplicatively [5]. Multi stressor approaches have the potential to not only explain honey bee colony losses, but could also be useful in the context of any organism undergoing stress. This is why we generalise our results to the wider stress ecology and epidemiological fields later in this thesis.

Therefore the main questions we are interested in answering within this thesis relate to both honey bee colonies and the wider, eco-epidemiological field, and are as follows:

- How do sublethal stressors impact honey bee colony dynamics? How do simple regulatory functions of honey bee colonies respond to

stress?

- How does a disease stressor with multiple routes of infection impact the spread of disease within a honey bee colony?
- How does seasonality affect the spread of Nosema disease in honey bee colonies? What are the implications of treating this disease at different points in the colony life cycle?
- What are the effects of multiple stressors (toxicant-parasite interactions) on within-host health? How do these stressors affect each other at the within-host level?
- What are the effects of multiple stressors (toxicant-parasite interactions) on population dynamics?
- Which within-host processes determine the outcome of population epidemiology?
- How does toxicant stress impact epidemiological population dynamics?

1.4 Overview of Thesis

This thesis is comprised of four main chapters which have been adapted from their corresponding peer-reviewed journal articles, followed by a discussion chapter.

In Chapter 2, *Stress-mediated Allee effects can cause the sudden collapse of honey bee colonies*, we will focus on the effects of generalised external stress on an important ecological problem; honey bee colony decline. These organisms face a multitude of sublethal stressors and research has yet to identify a cause for colony disappearance. Here we establish a mathematical model of the essential regulatory processes governing the hive and the general stressors impacting the colony. In particular, we analyse how these regulatory processes interact with and counteract stress. We find that increasing stress acting through a density-dependent Allee effect can cause sudden dramatic switches in the underlying dynamical behaviour of the hive. This chapter was published in the *Journal of Theoretical Biology* [1]: RD Booton, Y Iwasa, JAR Marshall, and DZ Childs. Stress-mediated Allee effects can cause the sudden collapse of honey bee colonies. *J. Theor. Biol.*, 420:213–219, 2017.

In Chapter 3, *Multiple routes of transmission synergistically increase infection within the honey bee hive: a mathematical model*, we examine the effects of a stressor which acts through multiple pathways. Again, we apply this to the ecological field of honey bee decline. In this chapter we study a mathematical model of general infection stress with multiple transmission routes. We do this to better understand how stressors with multiple pathways impact the spread of disease. We carefully parameterise the model according to the data and honey bee literature. We examine the respec-

tive contributions to disease spread and outbreak by each route and show that the combination of both pathways synergistically contribute a much greater risk of infection compared to each route acting alone. This chapter is currently under review.

In Chapter 4, *Interactions between immunotoxicants and parasite stress: implications for host health*, we examine the interaction between two interacting stressors; toxicant exposure and parasite infection. Toxicants can have both sublethal immunosuppressive and lethal direct effects on non-target organisms. We formulate a model which describes the within-host dynamics of immunity, infection and health and examine the effect of increasing toxicant exposure on these within-host processes. We demonstrate that sublethal toxicant exposure can promote an already-present infection through the suppression of the immune system. In particular, we show that within-host parasite density is maximised by intermediate toxicant stress, rather than simply increasing through a linear relationship. This chapter was published in the *Journal of Theoretical Biology* [2]: RD Booton, R Yamaguchi, JAR Marshall, DZ Childs, and Y Iwasa. Interactions between immunotoxicants and parasite stress: implications for host health. *J. Theor. Biol.*, 445:120–127, 2018.

In Chapter 5, *How do toxicants affect epidemiological dynamics?*, we expand upon the within-host framework provided in Chapter 4 to include population level epidemics. We do this since infection not only spreads within

the host organism but also spreads between those individuals within a population. Here we formulate a multilevel model of the within-host processes of immunity and infection and the between-host epidemiological dynamics of a population under lethal and sublethal stressors. We do this to better understand how toxicants impact the spread of disease within a population. We demonstrate that disease outbreak at the population level is dependent upon the level of stress and that epidemics can be maximised by an intermediate level. The within-host processes described in Chapter 4 also determine the outcome of the population epidemic. This chapter is currently under review.

Finally, in Chapter 6 we will summarise our key findings and propose future work which could extend upon the ideas contained within this thesis.

Overall this thesis contributes to the fields of stress ecology and eco-epidemiology through the careful theoretical formulation of biological frameworks. In particular, the mathematical models contained here show real, important applications within ecology: whether it be the dramatic collapse of population dynamics under general stressors found in Chapter 2, the synergism between multiple routes of infection stress in Chapter 3, the maximisation of host infection stress under intermediate levels of toxicant in Chapter 4, or the phase-based relationship between population epidemics and within-host stressors found in Chapter 5.

Chapter 2

Stress-mediated Allee effects can cause the sudden collapse of honey bee colonies

This chapter has previously been published as RD Booton, Y Iwasa, JAR Marshall, and DZ Childs. Stress-mediated Allee effects can cause the sudden collapse of honey bee colonies. *J. Theor. Biol.*, 420:213–219, 2017. As author of this Elsevier article, I retain the right to include it in a thesis or dissertation, provided it is not published commercially. Permission is not required, but I reference the Journal of Theoretical Biology as the original source. The full published version is available on Science Direct.

2.1 Abstract

The recent rapid decline in global honey bee populations could have significant implications for ecological systems, economics and food security. No single cause of honey bee collapse has yet to be identified, although pesticides, mites and other pathogens have all been shown to have a sublethal effect. We present a model of a functioning bee hive and introduce external stress to investigate the impact on the regulatory processes of recruitment to the forager class, social inhibition and the laying rate of the queen. The model predicts that constant density-dependent stress acting through an Allee effect on the hive can result in sudden catastrophic switches in dynamical behaviour and the eventual collapse of the hive. The model proposes that around a critical point the hive undergoes a saddle-node bifurcation, and that a small increase in model parameters can have irreversible consequences for the entire hive. We predict that increased stress levels can be counteracted by a higher laying rate of the queen, lower levels of forager recruitment or lower levels of natural mortality of foragers, and that increasing social inhibition can not maintain the colony under high levels of stress. We lay the theoretical foundation for sudden honey bee collapse in order to facilitate further experimental and theoretical consideration.

2.2 Introduction

The pollination industry generates a total economic value of 153 billion euros per year [49] and 75% of the leading global fruit, vegetable and seed crops rely on animal pollination, accounting for 35% of total global food production [47]. The Western honey bee *Apis mellifera* L. is the most common pollinator, providing an additional service to native pollinators through managed colonies [50, 51]. Hence, there are major concerns for the effects that decreasing honey bee colonies will have on future biodiversity and agriculture [52–55]. Furthermore, it is normal for beekeepers to lose 15% of the total honey bee population per year [56], but more recently this decline has accelerated alarmingly to 30% per year [57]. This has led to the definition of the term Colony Collapse Disorder (CCD) to describe the sudden mass disappearance of the worker honey bee population leading to colony failure [56].

Many potential stressors thought to cause CCD have been identified, although there has been no definitive explanation for every known symptom of collapsing hives. Pesticides [13, 58–60], viruses [61–64], fungal diseases [63, 65–68], microbes [69], mite infections [48, 70, 71], poor nutrition [72, 73] and starvation [74] have all been shown to have adverse effects on honeybees. Recently the possibility of causes involving several co-factors have been investigated. It has been suggested that CCD could have its origins in

multiple abiotic and biotic stressors interacting with each other [54, 75, 76]. For example, the parasitic mite *Varroa destructor* and the viruses it transmits [38, 77], the interactions between multiple pesticides having a synergistic effect on development and mortality rate [78–81], and pesticides increasing the effect of pathogens in larvae and adult bees, increasing the colony death rate [82].

Honey bee social behaviour and the mechanisms that govern this are widely understood. Eusocial insects are typically defined by their intricate advanced division of labour [83], and within honey bee colonies specific individuals have different roles in the hive [84]. Life for the honey bee begins with the queen laying eggs, from which a proportion will eclose within three weeks dependent upon the size of the adult workforce [85]. The rate that a colony can grow is impacted by two central factors, the total number of adult workers and the laying rate of the queen [86]. One of the most fundamental honeybee colony dynamics is the ability to structure the workforce according to age of the individuals, although this division of labour can change [87] in response to stressors and in order to ensure colony survival. This regulation system, known as temporal polyethism allows honey bees to respond to stressors by either reverting to previous roles or taking on new ones. This flexibility in age structured task allocation is socially regulated [88]. Young honey bees tend to work on in-hive tasks such as cleaning, tending brood and eating pollen [89] while remaining

protected from potential outside stressors. Older adults will begin foraging at around 2-3 weeks [85], where natural mortality will most likely occur due to forager exhaustion [90] and the risks affiliated with foraging [91]. Therefore, natural mortality in individual honey bees is age-dependent.

While an abundance of empirical work has been conducted addressing the individual effects of stressors, relatively few theoretical approaches have considered the underlying dynamics of collapse and the mechanisms regulating honey bee population dynamics. A simple model of in-hive and forager worker bees and the transitions between these showed that beneath a critical death rate of foragers, the colony can survive [92]. Developments upon this framework to include more complicated aspects of the hive were analysed with similar results [93]. Seasonal and annual fluctuations within another model predicted that death rates, food and transitions from in-hive to foraging tasks can influence colony survival [94]. Population based Allee effects were shown to induce failure of the hive [95] and investigations into the effects of sublethal stress on colony function demonstrated that positive density dependence can cause either exponential growth or failure of the colony [96]. Other models incorporating the effects of stressors have been shown to cause colony failure such as infection [97], American Foulbrood disease [98] and the interaction between *Varroa destructor* and Acute Bee Paralysis Virus [99].

While previous theoretical studies capture some elements of CCD and

failure of the colony, particularly the existence of thresholds where the colony will either grow or fail, real collapse dynamics appear to be sudden [100] rather than the gradual decline observed in most modelling studies. Bistability, or the presence of two alternate stable states, where one state corresponds to a stable positive population equilibrium, and the other to the extinction of the hive, could be crucial to understanding the suddenness observed in CCD. That is, CCD could be caused by sudden switches in stability around a critical point. We present a model that exhibits these positive-extinction stable states. We consider a generalised density-dependent stressor causing adult worker bees to disappear from the hive, and density-dependent mortality acting on high-density populations. We investigate the codependence of stress with the major regulatory functions in bee hives, such as the laying rate of the queen, recruitment to the forager class, natural mortality and social inhibition, and how these regulatory functions can counteract high stress levels in honey bee colony units.

2.3 Methods

The structure of the honey bee hive is complex [89], and many mathematical models have tried to express and explain the major regulatory systems observed in real hives. The model we present in Fig. 2.1 extends previous

model frameworks in Khoury et al. [92] from which we formulate the basic processes governing the hive. We make the simplification to consider only the in-hive worker (H) and outside-of-the-hive worker or forager (F) populations, and assume all bees can be classified in this way. Because in-hive mortality is extremely low compared to that among foragers [91], we assume that all natural mortality occurs in the forager class, at a rate m . Honey bees enter the hive through the eclosion function E , and are recruited into the forager class through the recruitment function R . We assume that a proportion of the colony is lost to a generalised stress function, which induces a lethal effect [101], through an individual's total disappearance from the colony caused by the effects of pesticides causing navigational problems for foragers never returning back to the hive [102], or that of density dependent in-hive worker bee mass disappearance, present in CCD situations [103].

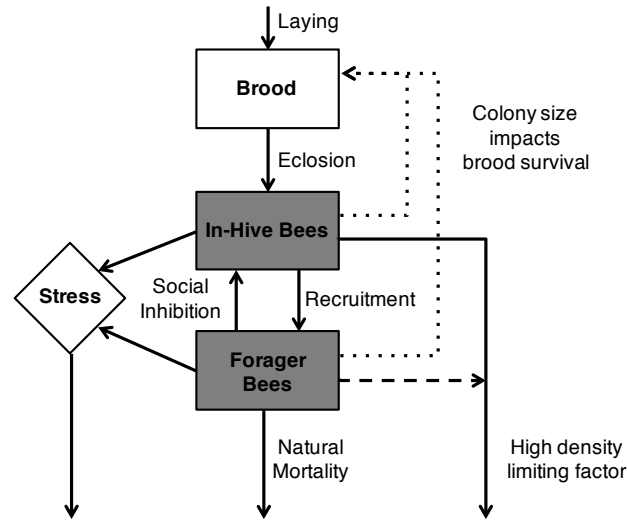


Figure 2.1: Dynamics of the model. The queen lays eggs which eclose into adult in-hive bees. Total adult population size impacts brood survival. A proportion of the in-hive bees are recruited into the foraging class by the natural age-dependent structure of the hive. Forager bees are able to make the switch back to the in-hive class via social inhibition. Natural mortality occurs within the forager class, but high density mortality occurs within the in-hive class. The generalised stress term acts over both adult classes and causes both in-hive and forager mortality or disappearance from the hive.

We assume that stress S as a function of time t acts across both in-hive and forager compartments, as an Allee effect. As each individual stressor impacts different classes of honey bee in a different way, we make this assumption to simplify all stresses into a single function. We did this under the knowledge that the location of stress within the model does not impact the qualitative dynamics of the model (Appendix Fig. A6). We also model density-dependent limiting effects at large colony sizes via the function C . We can express the model with this additional general stressor term and additional large colony limiting effect as a two dimensional system of

differential equations:

The rate of change of the in-hive population as functions of eclosion E , recruitment R , stress S and limiting function C

$$\frac{dH}{dt} = E(H, F) - R(H, F)H - S(H, F)H - C(H, F)H \quad (2.1)$$

The rate of change of the forager population as functions of recruitment R , natural mortality m and stress S

$$\frac{dF}{dt} = R(H, F)H - mF - S(H, F)F \quad (2.2)$$

Following Khoury et al. [92], we assume that the maximum eclosion of brood is equivalent to the laying rate L of the queen, and converges to L as $H + F$ gets large. Maximum eclosion occurs when the total size of the colony is large, representing the case when the total adult honey bee population is able to raise all eggs to adulthood [85]. The parameter ω sets the speed at which total eclosion tends towards the maximum eclosion L . We make this assumption because the total number of eclosing eggs in honey bee hives is proportional to the number of adult bees in the colony [104, 105].

$$E(H, F) = L \frac{H + F}{\omega + H + F} \quad (2.3)$$

The recruitment function $R(H, F)$ captures the effects of both natural age-dependent transitions to foraging and that of social inhibition. In-hive bees are recruited to the foraging class at rate α , and can switch back to in-hive tasks via social inhibition at a rate σ , proportional to the relative foraging capacity of the colony. We introduce a term k , which represents the rate at which the proportion of reverting foragers approaches the maximum social inhibition rate σ . Similarly to Khoury et al. [92], the recruitment function can be modelled as

$$R(H, F) = \alpha - \sigma \frac{F}{k + F + H} \quad (2.4)$$

Stress is modelled as a positive density-dependent mortality Allee effect, similarly to Bryden et al. [96],

$$S(H, F) = \frac{\mu}{\phi + H + F} \quad (2.5)$$

where per capita mortality is inversely proportional to the operational colony size. The rate of stress can be expressed as μ , and the low colony mortality can be controlled via ϕ . The limiting function at high densities is proportional to the total colony size

$$C(H, F) = \gamma(H + F) \quad (2.6)$$

We choose this high density effect γ to be extremely small. This large

colony size limiting function represents the biological nature of hives, as populations do not grow indefinitely, with a typical colony size around 20000 worker bees [89], and often managed hives have limited comb space which are maintained by beekeepers. In addition, populations of honey bees often swarm, preventing the total population from growing indefinitely. The total combined mortality effect for the in-hive population ($S(H, F) + C(H, F)$) and the individual effects of both can be seen in Fig. 2.2, where the overall mortality is very high for lower number of bees, and decreases before increasing again for large colony sizes.

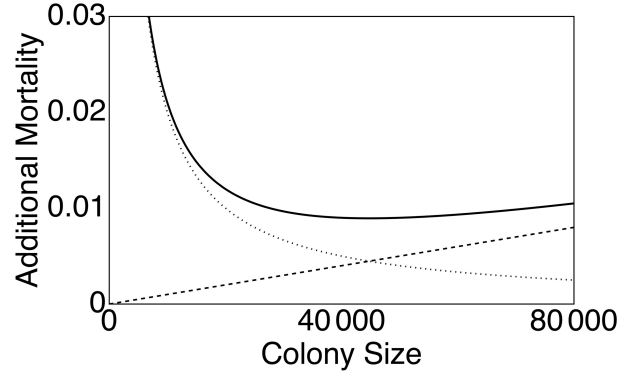


Figure 2.2: The effects of stress $S(H, F)$ (dotted) and high density function $C(H, F)$ (dashed) on in-hive mortality, and the combined effect (black), as the colony size ($H+F$) increases. Parameters are $\mu = 200$, $\phi = 0.402$, $\gamma = 0.0000001$. In our model, the stress function $S(H, F)$ acts strongly at very small populations, whereas the large population size limiting factor $C(H, F)$ is small at low populations. At high population sizes, the limiting effect reduces the population which results in the population declining rapidly whereas the stress term has a small effect. The combined impact is high additional mortality at low population sizes, then a decrease for intermediate population sizes before higher mortality again at high population sizes.

The final system of differential equations is therefore

$$\frac{dH}{dt} = L \frac{H+F}{\omega + H+F} - H \left(\alpha - \sigma \frac{F}{k+F+H} \right) - \frac{\mu H}{\phi + H+F} - \gamma(H+F)H \quad (2.7a)$$

$$\frac{dF}{dt} = H \left(\alpha - \sigma \frac{F}{k+F+H} \right) - mF - \frac{\mu F}{\phi + H+F} \quad (2.7b)$$

These equations were analysed using the standard methods from dynam-

ical systems theory. The equations were solved numerically with Wolfram Mathematica version number 10.0.2.0. Numerical bifurcation plots were produced using the package MatCont in MATLAB version number 8.6 R2015b. We parameterise the model according to previous empirical and theoretical studies as shown in Table 2.1.

2.4 Results

There are two fixed points in system (2.7)

$$(H, F) = (0, 0) \tag{2.8a}$$

$$(H, F) = (H^*, F^*) \tag{2.8b}$$

with $H^*, F^* > 0$. Let us define the following functions

$$g_1(H, F) = \frac{dH}{dt} \tag{2.9a}$$

$$g_2(H, F) = \frac{dF}{dt} \tag{2.9b}$$

We calculate the Jacobian matrix for system (2.7) evaluated at the fixed point $(H, F) = (0, 0)$

$$J = \begin{pmatrix} \left(\frac{dg_1}{dH}\right)_{(0,0)} & \left(\frac{dg_1}{dF}\right)_{(0,0)} \\ \left(\frac{dg_2}{dH}\right)_{(0,0)} & \left(\frac{dg_2}{dF}\right)_{(0,0)} \end{pmatrix} = \begin{pmatrix} -\alpha - \frac{\mu}{\phi} + \frac{L}{\omega} & \frac{L}{\omega} \\ \alpha & -m - \frac{\mu}{\phi} \end{pmatrix} \tag{2.10}$$

<i>Parameter</i>	<i>Description</i>	<i>Value</i>	<i>Reference</i>
L	Laying rate of the queen	2000	[106]
α	Recruitment to forager class	0.25	[107]
σ	Social inhibition	0.75	[107]
ω	Rate at which eclosion tends to maximum	27000	[92]
ϕ	Control of low colony mortality	0.402	[96]
m	Natural mortality	0.1	<i>chosen to be small</i>
k	Rate at which social inhibition tends to maximum	0.1	<i>arbitrary</i>
γ	High density effect	0.0000001	<i>chosen to be very small</i>
μ	Stress	[0, 2000]	<i>varying</i>

Table 2.1: Parameter values used in the honey bee stress population model

Calculating eigenvalues gives the condition for stability of the extinction of the population of honey bees. This happens when (2.11a) and (2.11b) hold true

$$0 < \omega < \frac{L(m + \alpha)}{m\alpha} \quad \& \quad (2.11a)$$

$$\mu > \frac{L\phi + \omega \left(-\phi(m + \alpha) + \sqrt{\frac{\phi^2(L^2 + 2L\omega(m + \alpha) + (m - \alpha^2)\omega^2)}{\omega^2}} \right)}{2\omega} = \mu_{crit} \quad (2.11b)$$

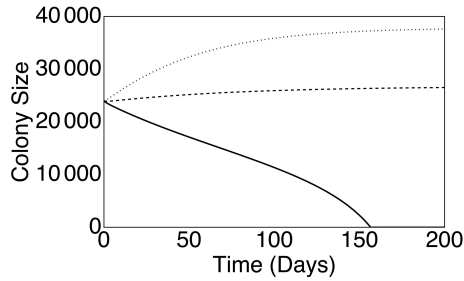
or, when (2.12) holds true

$$\omega \geq \frac{L(m + \alpha)}{m\alpha} \quad (2.12)$$

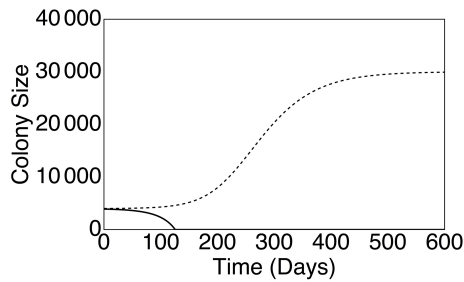
i.e. the population goes extinct when either the laying rate is too low (2.12) or when the laying rate is sufficiently high (2.11a) and the stress μ is higher than a critical level μ_{crit} (2.11b).

Two qualitatively distinct dynamical outcomes are possible within our model. Either the colony size over time reaches a positive stable equilibrium which represents the optimal size of the colony or the population decreases rapidly around a critically low density colony size and the hive collapses. These two possibilities are dependent on initial conditions and parameter choice. This dynamical behaviour is summarised in Fig. 2.3(a), which shows the effect of increasing the stress parameter μ on the total numbers of the adult in-hive and forager bees. In the stress free popula-

tion and for stress levels less than the critical level, the model predicts that the population will reach equilibrium if the initial density is high enough. As the stress parameter μ is increased, total density drops, and then we observe a tipping point at the critical level of stress. If initial population sizes are below the unstable population size (Fig. 2.3(b)), then we predict the extinction of the hive. Otherwise, all populations will grow and tend towards the stable branch, and remain stable (Fig. 2.3(b)).



(a)



(b)

Figure 2.3: Numerical simulations of the model for (a) increasing stress levels and (b) sensitivity of initial conditions. In (a) we plot 3 stress levels $\mu = 0$ (dotted), $\mu = 200$ (dashed) and $\mu = 400$ (solid). Failure of the colony is initiated by the high stress level ($\mu = 400$). Initial conditions are $H(0) = 16000$, $F(0) = 8000$. In (b), dependence upon initial conditions is illustrated with a fixed stress $\mu = 150$ for $H(0) = 3000$, $F(0) = 1000$ (dashed) and $H(0) = 2900$, $F(0) = 1000$ (solid). A decrease in 100 initial in-hive bees causes the colony to fail. Parameters are taken from Table 2.1.

Fig. 2.4 shows the saddle-node bifurcation present in our system, highlighting the location of the stable and unstable branches with respect to the stress parameter for the in-hive population. This shows the way that the total in-hive population changes as a function of stress, and where the limit

point is formed as the stable and unstable equilibria branches collide and disappear, leaving only the stable zero solution. This dynamical behaviour and the presence of the stable-unstable-stable equilibria is related to initial conditions (Fig. 2.5), for both low and high stress levels. For lower stress levels all solutions tend towards either stable equilibria dependent upon initial conditions, and for high stress levels all solutions tend towards the stable extinction of the hive. Other saddle-node bifurcations can be caused by changes to the parameters representing the natural mortality of foragers (Appendix Fig. A1), and recruitment to the forager class (Appendix Fig. A2). The direction of the saddle-node bifurcation is reversed for the laying rate of the queen (Appendix Fig. A4), and is also reversed for the bifurcation of the social inhibition parameter (Appendix Fig. A3).

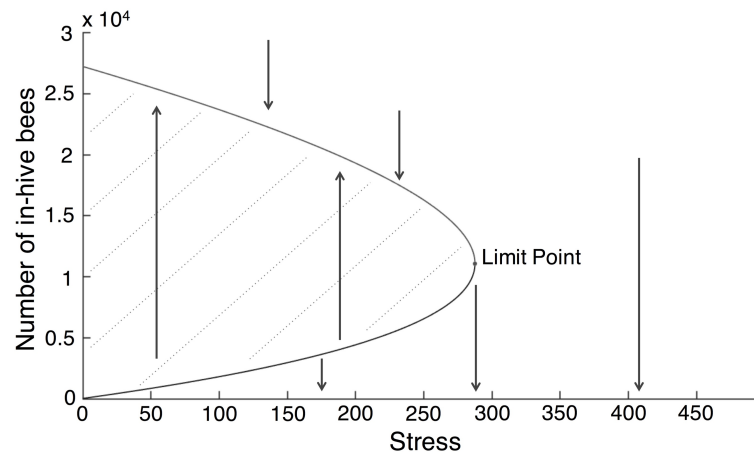


Figure 2.4: The saddle-node bifurcation through the stress parameter μ for the total numbers of in-hive honey bees. Parameters are taken from Table 2.1. The location of the limit point represents a critical stress level after which the total number of in-hive bees will become 0. The existence of the unstable branch pushes all solutions onto the stable branch, unless initial conditions lie below this unstable branch. Around the critical stress level, we see a rapid decline in the number of in-hive bees.

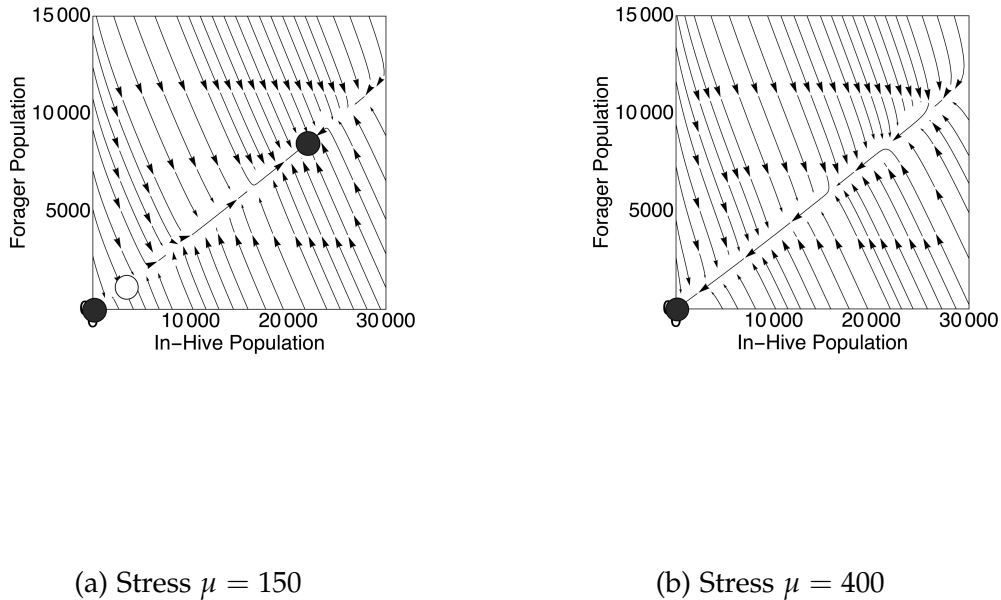


Figure 2.5: The comparison of two levels of stress on the in-hive - forager phase plane. Parameters are taken from Table 2.1. At the lower level of stress $\mu = 150$, the populations tend towards the positive stable equilibrium at $(H, F) = (21643, 8380)$ or to the stable origin $(H, F) = (0, 0)$ (black dots). The existence and location of the unstable equilibrium (white dot) suggests that for these parameters there can be a minimum of 2927 in-hive and 1064 foragers before extinction of the hive. In (b), all solutions tend towards $(0, 0)$ (black dot), regardless of the initial conditions suggesting that this level of stress $\mu = 400$ will cause extinction in all cases.

Fig. 2.6 shows the point of colony failure as a function of stress and other critical parameters, highlighting the relationship between the major regulatory functions of the honey bee hive and the hive's response to stress. Higher levels of laying by the queen, lower levels of forager recruitment and lower natural forager mortality can all counteract high levels of stress impacting the colony. Interestingly, our model predicts that varying the

level of social inhibition can not save the colony from extinction at high stress levels.

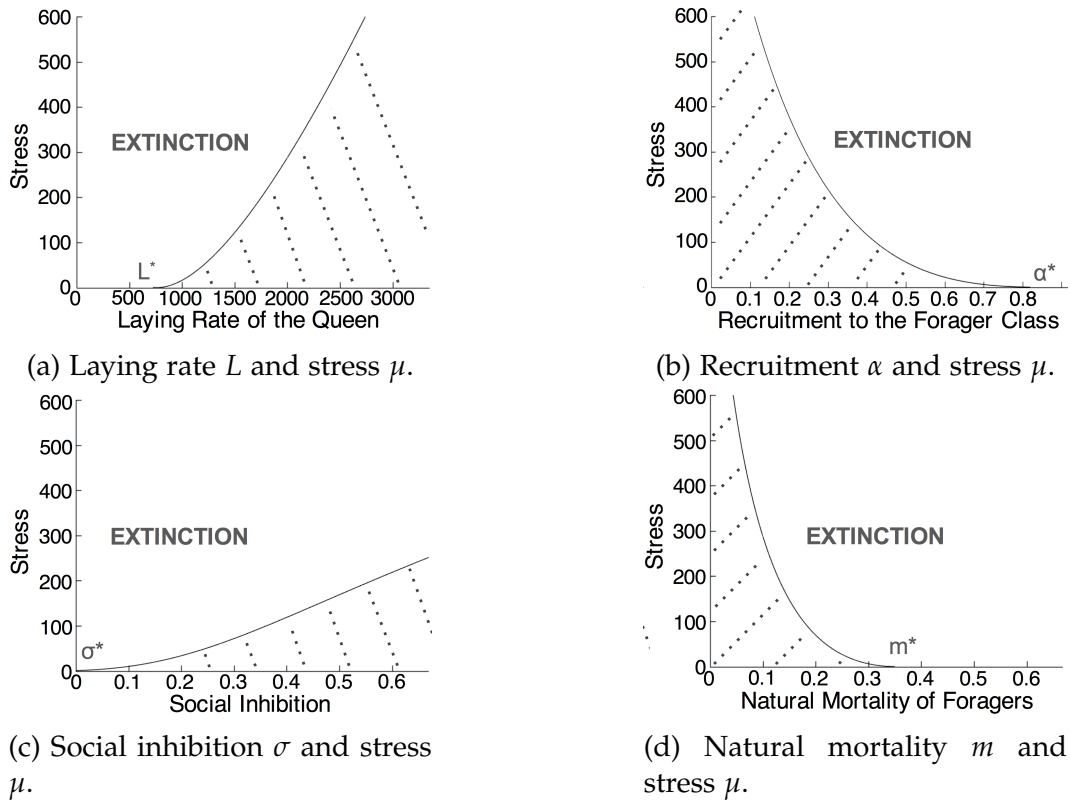


Figure 2.6: The location of the limit point present in the saddle-node bifurcation within two dimensional parameter space (black line), and the conditions for extinction and persistence (dotted), with parameters taken from Table 2.1. In (a), the higher laying rate L counteracts stress and extremely high laying rates require exponential stress levels to cause failure. In (b), low levels of forager recruitment α can maintain the colony. This can be thought of as lower levels of 'panic' switching between tasks counteracting high stress levels. In (c), extinction of the hive is possible for all values of social inhibition σ . Low levels of social reversion are close to the limit point, even in the stress free hive. In (d), collapse of the hive is not possible for extremely low natural mortality m of foragers. Past the critical death rate all colonies will fail regardless of the stress level.

2.5 Discussion

In this paper we show how stress-mediated Allee effects bring about sudden collapse in the population dynamics of honey bee colonies. The stress induced bistability created by our model forced dependence on the initial population sizes of both in-hive and forager bees. This led to a sensitive threshold around the unstable population size where colonies would either persist or fail. In addition, we show that CCD can be triggered by small perturbations in regulatory hive functions through changes in hive parameters indicating that the honey bee hive is highly sensitive to such changes under density-dependent stress.

The regulatory functions governing honey bee hives are well understood. It is well documented that the hive will respond to higher levels of mortality of foragers by speeding up recruitment to form a workforce primarily made of precocious foragers [88], a process that is thought to be one of the symptoms of CCD [92]. It is also understood that the queen is influenced by many factors including seasonality, total available resources, queen age, temperature in the hive, and photoperiod [108, 109]. Therefore regulatory functions could have significant implications in maintaining the colony under stress, and could also be influenced by these stresses. Through investigating the relationship between stress and the major regulatory functions of honey bee hives, we make predictions reflecting the na-

ture of colony collapse. Near the critical threshold inherent in our model, both an increase in recruitment to the forager class or a decrease in social inhibition can cause sudden colony failure. This suggests that CCD can be promoted by a breakdown in these simple regulatory functions that usually maintain honey bee hives under stress. We also predict that fluctuations in the queen's laying rate are highly sensitive in failing colonies. A small decrease in the laying rate of the queen subject to these natural fluctuations close to the bifurcation point could result in drastic switches in the dynamics of the hive, although colonies will normally replace the queen if she is not adequately laying enough brood [85], which could potentially occur before this critical point. In addition, the model proposes that a small increase in natural mortality can cause the sudden collapse of the colony, although the occurrence of mortality fluctuations are unlikely in summer conditions given the observed constant probability of death per unit time spent away from the hive [91], thus making natural mortality less likely to be subject to bifurcation-causing fluctuations.

The intrinsic bistability and sensible ecological behaviour present within our model implies an alternative route to colony collapse through the presence of a saddle-node bifurcation, not seen in other theoretical studies of honey bee population dynamics [92, 96]. Although some empirical replications of CCD have observed sudden declines in honey bee populations exposed to stressors such as the neonicotinoid imidacloprid [100], an insec-

ticide thought to cause abnormal foraging behaviour [110], further work is needed to understand the mechanisms governing honey bee failure. Our generalised approach to modelling stress can, in theory, be thought of as acting through any possible mortality-based hive-wide stressor, such as other pesticides [58], the mite *Varroa destructor* [48] or the pathogen *Nosema ceranae* [62]. If it shown that honey bee hives exhibit bistability, we may be able to forecast the period leading up to the critical transition, and provide new ways of detecting imminent CCD.

There are many potential extensions to the modelling framework we present. We do not consider the effects of seasonality, instead concentrating on the colony in the favourable spring and summer conditions. Indeed, it has been shown that honey bee survival depends upon the time of year [74] and that the proportion of brood reared to adulthood depends upon the supply of pollen which decreases in the autumn and winter seasons [111]. In order to better understand how the risk of colony collapse varies across the seasons, we suggest extending the model to include seasonality in similar ways in which other models have proven useful in this context [94, 99]. This combination of known ecological behaviour and bistability within our model could provide insight into the mechanisms governing colonies which commonly collapse in winter conditions [103].

Currently, we concentrate on the two most significant distinct adult classes [89], the in-hive and forager worker bees. We make this simplifica-

tion as there is a clear distinction in mortality rates and behaviour between these two populations, and together they express the most important regulatory processes in the hive [89]. However we could extend the model to include the population dynamics of bees from either the nest centre (cleaning and feeding) or nest periphery (receiving, packing and storing nectar) [89]. For example, we did not consider the regulatory processes governing receiver honey bees for which the dynamics are well known. Forager bees collect nectar and transfer it to receiver bees who then proceed to store this material in cells [112]. Under higher influxes of nectar, the colony can allocate more honey bees into the receiver bee class [113], and thus can be thought of as another regulatory process maintaining the colony. This introduction of a new classification of honey bee into our modelling framework would help describe the breakdown in regulatory processes of a honey bee hive under CCD conditions in more detail.

In recent years, researchers have become interested in forecasting transitions of state in the underlying dynamics of a wide range of systems [114–118]. If bistability is important in understanding the general mechanisms governing a honey bee hive under stress, then we should be able to predict the onset of colony collapse. The model described in this paper has the required properties needed to detect critical transitions before they drastically alter the population dynamics of the system. The existence of a set of predictors called early warning signals (EWS) can be applied to any

system with sudden changes in state [118]. When a system undergoes significant change from one state into another state, just before the transition it approaches the tipping point or critical threshold, as shown in the dynamics of our model. Sometimes these changes in state can be catastrophic and widespread, having a detrimental ecological impact on the system as a whole [118, 119], with the system sometimes never returning to its original state, even after pre-collapse conditions have been restored [118]. The potential implications and applications of these EWS combined with our model are numerous and may provide the much needed insight into the complex problem of CCD.

Chapter 3

**Multiple routes of transmission
synergistically increase infection
within the honey bee hive**

3.1 Abstract

Honey bee populations are frequently exposed to the microsporidian parasite *Nosema*, thought to be a potential aggravator of population decline. Transmission of *Nosema* occurs in two ways: via either an oral-oral (trophalaxis feeding) or oral-fecal (contamination) pathway. Here, we quantify the relative contributions to honey bee disease outbreak by both oral-oral and fecal-oral pathways. We do this to understand how multiple routes of infection acting in combination impact the spread of disease. We study a mathematical model of infection with multiple transmission routes in a honey bee colony. Using parameters taken from the honey bee literature and using *Nosema* disease as our motivating example, we examine the relative effects of multiple routes of transmission and their respective contributions to the basic reproduction number. We run simulations to determine the expected % infected and % level of contamination present in a honey bee hive for each transmission pathway acting alone and the combination of both. We show that the combination of both transmission routes synergistically contribute a much greater risk of infection compared to each route acting alone. In general, the combination of both routes causes much greater contamination within the hive and higher infection load across the colony. We consider seasonality based infection, showing that the greatest risk occurs in spring and show that *Nosema* is easier to treat in autumn and winter.

These results are consistent with the empirical data available in the literature. The findings of this study indicate that examining multiple routes of transmission may be key to understanding honey bee colony losses. Our results also suggest that by limiting a singular transmission route from a honey bee population, infection can be managed. In addition, we also suggest that these results may be applied to any honey bee disease with more than one route of transmission.

3.2 Introduction

Honey bee (*Apis mellifera*) populations continue to decline [10, 46], causing widespread concern for the impact this will have on the pollination industry, global food security and biodiversity [47, 120]. In particular, honey bees play a vital role within the pollination industry, pollinating an array of commercial crops [121] which are crucially important for global food security. However, a single causal factor of honey bee population decline has yet to be found [48].

One such potential aggravator of honey bee decline is the microsporidian parasite *Nosema*, one of the most prevalent honey bee diseases found all over the world [66, 122]. *Nosema* is caused by two genetically distinct pathogens, *Nosema apis* and *Nosema ceranae*, which infect the midgut of honey bees causing nosemosis. Honey bees ingest *Nosema* spores in either

food or fecal material, after which germination causes the proliferation within the midgut epithelial cells [123]. Common symptoms of *N. apis* include trembling, abdomen dilation, faecal stains on comb walls and dead bees found around the hive [122]. This results in a decrease in population size [122], honey production [124] and crop pollination [125].

Transmission of Nosema occurs from the ingestion of Nosema spores. Honey bees frequently perform hygienic behavioural tasks such as cleaning the hive [126], resulting in the acquisition of Nosema spores via an oral-fecal pathway [122, 127, 128]. Furthermore, Nosema can be found within the stored pollen and brood food [129, 130], providing another source of contamination. An additional route of transmission occurs via trophallaxis [131, 132], an oral-oral pathway and method of mouth-to-mouth liquid exchange and feeding.

Disease within honey bee colonies has been studied in the context of theoretical models. Betti et al. [133] showed that general infectious diseases can lead to colony collapse using *Nosema* as an example. Other models focus on other specific diseases or have a more generalised approach, such as Varroa mites [134–136], American foulbrood [98], contagions [97] or general stressors [1]. Ratti et al. [135] examined virus transmission in the context of a susceptible-infected framework, a commonly used model to examine disease transmission. However, current general theoretical models neglect important disease dynamics, such as possible multiple routes of

transmission, contamination or treatment.

In this paper we construct a mathematical model to describe the seasonal epidemiology found in a honey bee colony under multiple routes of transmission. We carefully parameterise and simulate this model based on published data in order to understand the role of multiple transmission routes in honey bee disease and wider honey bee colony losses. We use *Nosema* disease as the motivating example for the model, and we consider the role of both contamination (fecal-oral route) and trophallaxis feeding (oral-oral route) in the spread of general disease in a honey bee colony. In particular we examine the risk of infection outbreak in a seasonal honey bee population, and study the total contributions to infection load by both contamination and trophallaxis transmission routes. We also examine the minimum treatment necessary under these conditions to control the infection.

3.3 Methods

Mathematical model

Within our mathematical model, all individual honey bees can be classified as either healthy (X) or infected (Y). The fraction of contaminated material within the hive is represented by state variable Z which takes a value between 0 and 1. A value of 0 represents a fully uncontaminated in-hive

environment and a value of 1 represents an entirely contaminated in-hive environment. The total population ($X + Y$) grows logistically with carrying capacity $M_i \leq 1$, where i can take a value representing spring (1), summer (2), autumn (3) and winter (4) seasons. We parameterise this according to normal population levels found in honey bee colonies throughout the year [137].

Infection occurs via two pathways, either indirectly (represented by β) through cleaning or consuming contaminated material or stored food within the hive [122, 127–130] or, directly (represented by θ) through trophallaxis feeding, bee-to-bee contact or grooming [131, 132, 138]. We assume that the rate of indirect infection transmission β depends upon the amount of contamination present within the hive and the number of healthy bees, and the rate of direct transmission θ depends upon the number of healthy and infected bees. Seasonal mortality occurs at rate μ_i , parameterised according to the typical rate of mortality expected during each season [134]. Infection-based mortality α occurs as a result of infection after 8 days [139] and the infection can be treated with rate p , reverting infected individuals to healthy honey bees.

The within-hive contamination level Z proliferates at rate k according to the amount of uncontaminated environment available (with limited hive space) and the number of infected individuals, which we parameterise as the mean alive percentage spore viability [140]. The contamination is re-

moved at a rate d , which we parameterise as the mean dead percentage spore viability [140]. The model we study (Fig 3.1) is a 3-dimensional set of nonlinear ordinary differential equations (ODEs):

$$\frac{dX}{dt} = r(X + Y)\left(1 - \frac{X + Y}{M_i}\right) - \beta XZ - \theta XY - \mu_i X + pY \quad (3.1a)$$

$$\frac{dY}{dt} = \beta XZ + \theta XY - (\alpha + \mu_i + p)Y \quad (3.1b)$$

$$\frac{dZ}{dt} = kY(1 - Z) - dZ \quad (3.1c)$$

We parameterise system (3.1) using published data (Table 3.1) and calculate estimates for β and θ (Appendix B).

3.4 Results

The basic reproduction number R_0

We calculate the population growth rate ($\lambda = 0.026$) of system (3.1) from published data ([142] and Appendix B). We estimate the basic reproductive number of the infection in each season ($i = 1, 2, 3, 4$) as $R_{0spring}$, $R_{0summer}$, $R_{0autumn}$ and $R_{0winter}$ where

$$R_{0i} = \frac{M_i(\beta k + \theta d)(r - \mu_i)}{dr(p + \alpha_i + \mu_i)} \quad (3.2)$$

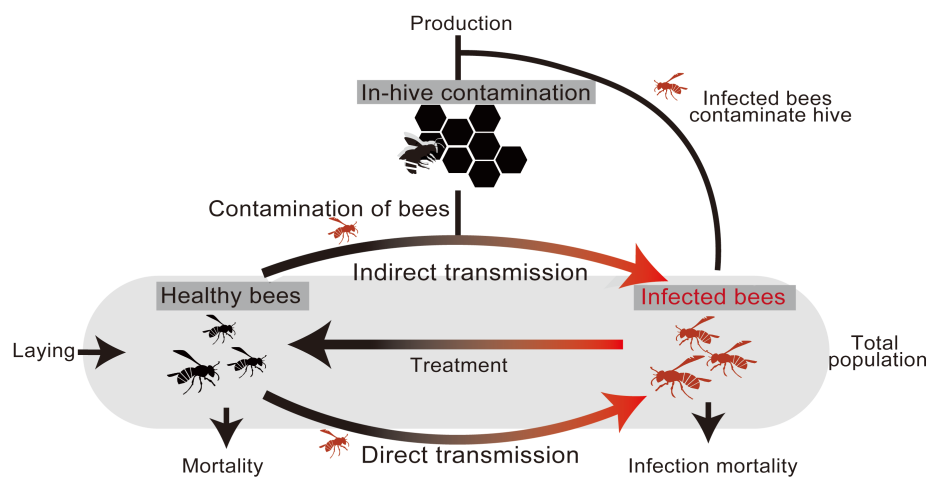


Figure 3.1: Outline of the honey bee disease dynamics model. The arrows represent the direction of flow between healthy and infected classes of honey bees within a hive. Bees can become infected either via direct or indirect transmission, the latter of which depends upon the level of in-hive contamination. Bees can revert to a healthy state if they are treated, and enter the system via a laying rate. Natural mortality and infection-based mortality is also taken into consideration.

Parameter	Description	Value					Source
		Spring	Summer	Autumn	Winter		
r	Colony growth rate	1/5	1/5	1/5	1/5	arbitrary	
M	Seasonal carrying capacity	1	13300/21800	8300/21800	6000/21800	[137, 141]	
β	Indirect transmission	variable	variable	variable	variable	determined from R_0 (Appendix B)	
θ	Direct transmission	variable	variable	variable	variable	determined from R_0 (Appendix B)	
μ	Seasonal mortality	1/44	1/25	1/44	1/190	[134]	
p	Treatment	≥ 0	≥ 0	≥ 0	≥ 0	variable	
α	Additional Mortality	1/8	1/8	1/8	1/8	[139]	
k	Mean % spore viability live	0.939	0.939	0.939	0.939	[140]	
d	Mean % spore viability dead	0.061	0.061	0.061	0.061	[140]	
λ	Malthusian growth rate	0.026	0.026	0.026	0.026	[142], (Appendix B)	

Table 3.1: Parameter values used in the honey bee disease dynamics model

We quantify the contributions to the chance of total disease outbreak R_0 from both only the indirect source R_I and the direct source R_D . This means that we can investigate the relationship between separate infection sources and their likely contributions to disease outbreak. A full derivation of the relationship between R_I , R_D and R_0 can be found in Appendix B, giving the following

$$R_I = \beta k X^* \Lambda_1 \Lambda_2 \quad (3.3)$$

$$R_D = \theta X^* \Lambda_1 \quad (3.4)$$

where $\Lambda_1 = \frac{1}{\alpha + \mu + p}$, $\Lambda_2 = \frac{1}{d}$, $X^* = \frac{M(r - \mu)}{r}$ and

$$R_0 = R_I + R_D \quad (3.5)$$

Therefore the total R_0 can be divided into relative contributions by R_I and R_D .

Treatment

From system (3.1) we determined the condition under which all infected individuals can be eradicated using treatment. The relationship between the basic reproductive number with (R_{0i}) and without treatment (R_{0i}^*) in each season ($i = 1, 2, 3, 4$) can be expressed as

$$R_{0i} = R_{0i}^* \frac{\alpha_i + \mu_i}{p + \alpha_i + \mu_i} \quad (3.6)$$

We determined the critical value of treatment which will eradicate all infection in a given season as

$$p_i^* = (\alpha_i + \mu_i)(R_{0i}^* - 1) \quad (3.7)$$

If p is larger than the critical value then the outbreak is prohibited. Fig 3.2 shows this critical value of treatment p_i^* for all seasons and percent contribution to R_0 by R_I . Treatment is required in spring for a wider range of indirect contributions to R_0 ($\geq 30\%$). There is a smaller range where treatment can stop the infection in summer ($\geq 60\%$), autumn ($\geq 80\%$) and winter ($\geq 90\%$).

Seasonal R_0

We use parameters and data from the literature (Table 3.1) to calculate an estimate for the basic reproductive number in summer:

$$1.18 \leq R_{0summer} \leq 1.68 \quad (3.8)$$

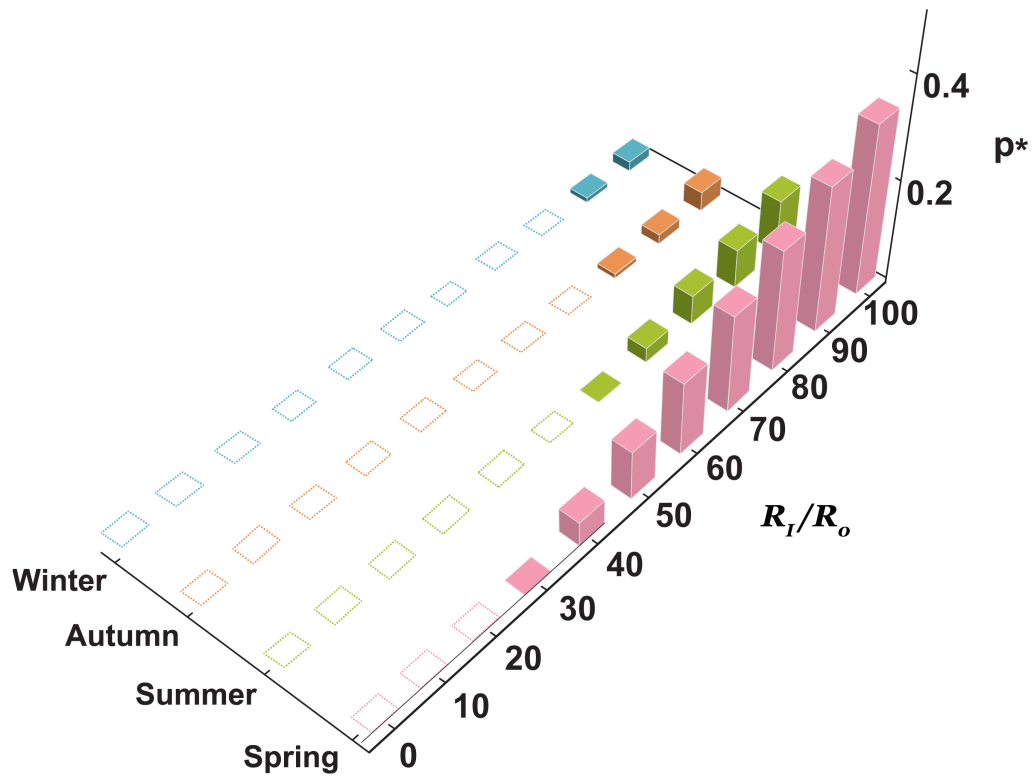


Figure 3.2: Simulations of the model showing the critical treatment (p^*) required to remove the infection in the 4 different seasons. The contribution by the indirect source of transmission R_I to the total measure of disease outbreak R_0 is expressed by $\frac{R_I}{R_0}$. Treatment is required in spring for a wider range of indirect transmission contributions to R_0 . Parameters taken from Table 3.1.

We take $R_{0summer} = R_{0max} = 1.68$ and rescale equation (3.2) to calculate the maximum basic reproductive number for each season (Appendix B).

$$R_{0spring} = 3.40$$

$$R_{0summer} = 1.68$$

$$R_{0autumn} = 1.30$$

$$R_{0winter} = 1.17$$

We quantify the contributions to disease outbreak from both only the indirect source R_I and only the direct source R_D (Appendix B). The total percent contribution by indirect transmission can be expressed as $\frac{R_I}{R_0}$, where the size of β and θ depend upon the ratio of R_I and R_D as derived in Appendix B.

For each set of seasonal parameters, we plot the total percent contribution of indirect transmission and the corresponding breakdown of both R_I and R_D (Fig. 3.3). In spring conditions R_0 is the largest of all the seasonal simulations giving a wide range of conditions for which both R_I and R_D are above 1 (30% - 70%). Hence either direct or indirect transmission can individually cause infection to spread to the entire population in this region. However, for other seasons there are no regions where both R_I and R_D are individually greater than 1.

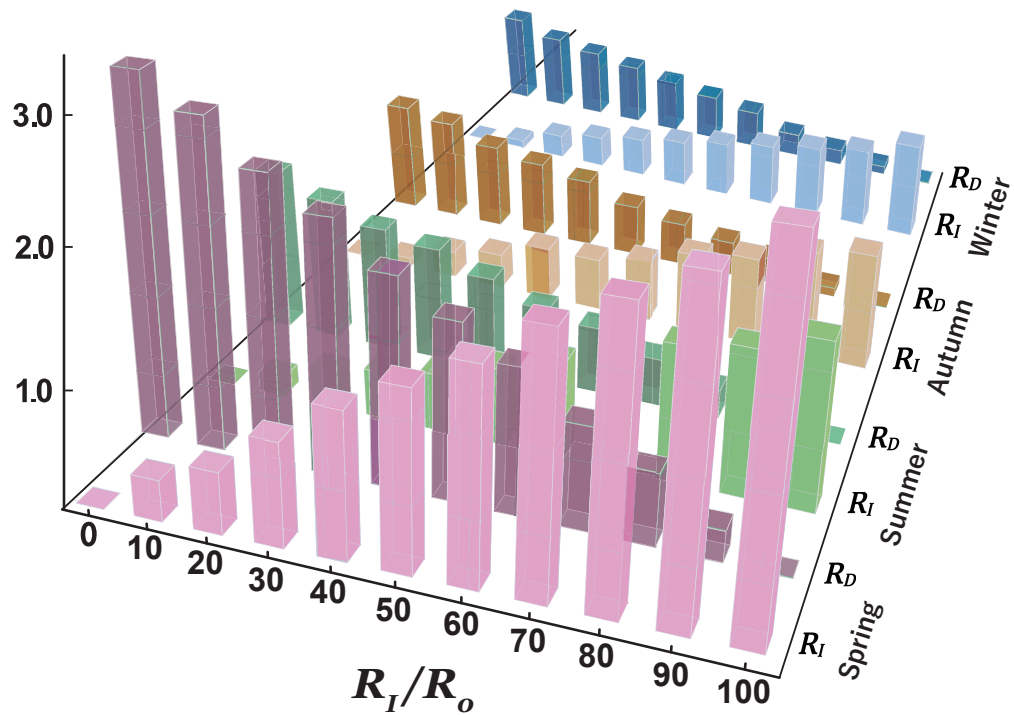


Figure 3.3: The calculated contributions to the total chance of disease outbreak R_0 by indirect transmission R_I and direct transmission R_D in each season. These values are calculated for a range of total percent contribution by indirect transmission $\frac{R_I}{R_0}$ and show that spring conditions provide a wider range of conditions for which both R_I and R_D are above 1 (30% - 70%). In spring conditions either direct or indirect transmission can individually cause an outbreak in infection, but for other seasons there is no such overlap where R_D and R_I are greater than 1. Parameters taken from Table 3.1.

Synergistic routes of transmission

Fig. 3.4 shows the population under baseline healthy dynamics, and infection and contamination levels, for 30%, 50% and 70% contributions by indirect R_I . For the total percentage infected honey bees, the prevalence expected by adding up the values for indirect and direct transmission is always lower than the combined simulated values (Fig. 3.4 B-D), representing a synergistic interaction within the infection dynamics of system (3.1). In all seasons aside from spring, the expected values of contamination are lower than the simulated values (Fig. 3.4 B-D) also representing a synergistic interaction within system (3.1).

3.5 Discussion

We predict that infection risk is greatest in the spring, at the start of the colony life cycle, and that it is easier to eradicate infection in the autumn or winter seasons. We show how the combination of two routes of transmission can synergistically increase infection and contamination levels in a honey bee hive. Disease outbreak is possible for singular routes of transmission, but multiple routes of transmission increase the likelihood of infection. Honey bees live in densely crowded populations, providing advantageous conditions for disease transmission through high contact rates [143]. Therefore, it is intuitive that an additional transmission route should

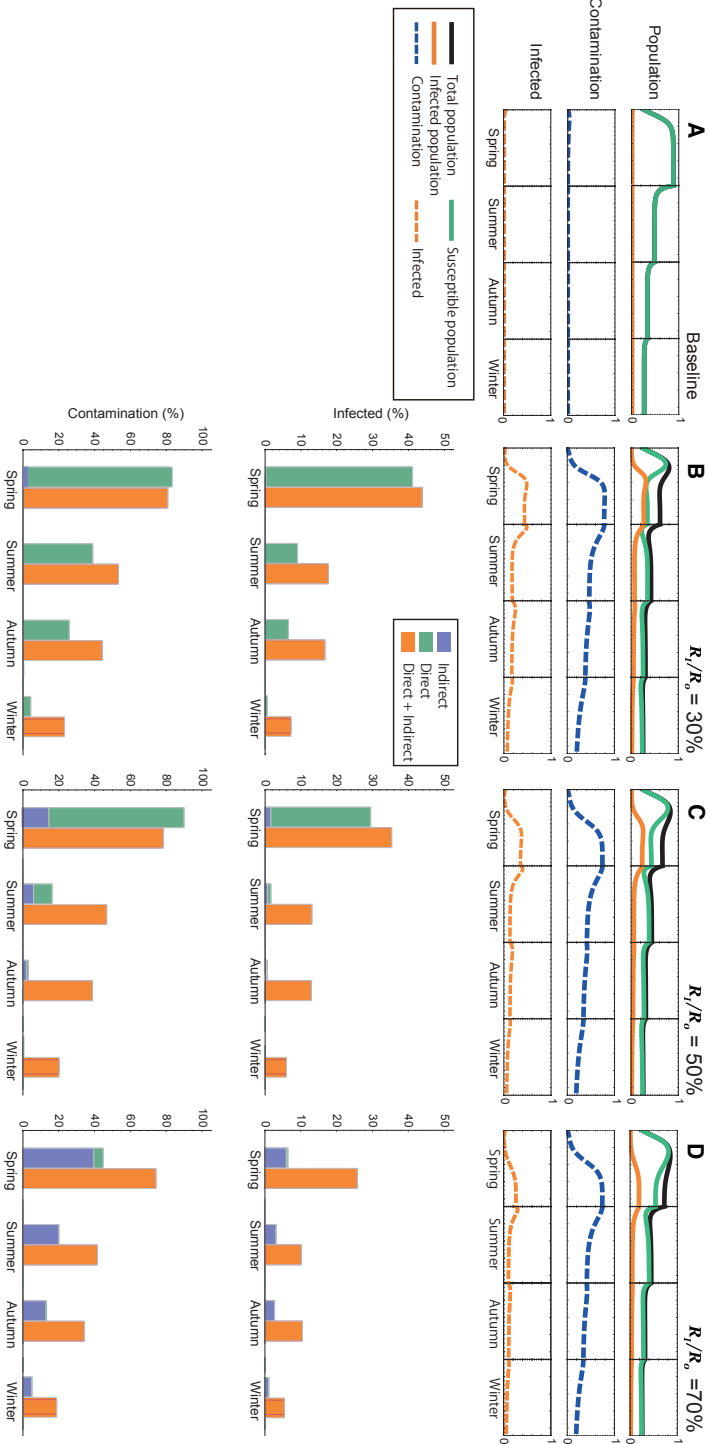


Figure 3.4: Simulations of the model for a range of R_I and R_D . (A) Baseline dynamics of the model under no infection and contamination (B) Dynamics under $R_I/R_0 = 30\%$ and resulting breakdown of % infected and % contamination for both direct (green bars) and indirect transmission (blue bars), and the combined synergistic effect (orange bars). (C) The dynamics of the model under $R_I/R_0 = 50\%$. (D) The dynamics of the model under $R_I/R_0 = 70\%$. The expected % infected for both routes is always lower than the simulation of the model representing a synergistic interaction in all seasons. For % contamination, there is synergy in all seasons but for spring. Parameters taken from Table 3.1.

result in a greater risk of outbreak of the disease. Our theory suggests that multiple routes of transmission could be crucial in understanding wider honey bee population decline. While the effects of multiple routes of transmission on epidemics are well studied [144], this work applies these ideas to honey bee losses, and indeed we suggest that multiple routes of transmission could be crucial in understanding honey bee population decline.

Throughout this study, we use *Nosema* disease as the motivating example for the model. However there is suggestive evidence [145] that many infections can be transmitted directly through feeding [143, 146, 147] and contact [148, 149]. In addition these viruses may be transmitted indirectly through faeces [150–152] or through the *Varroa destructor* vector [146, 153]. Thus, we argue that synergy in infection and contamination are not limited to the multiple routes of *Nosema* disease studied here, but is applicable to any honey bee infection with more than one transmission route. Therefore, we suggest that future work should carefully examine how these multiple routes of transmission affect disease spread in a honey bee colony, particularly for deformed wing virus (DWV), black queen cell virus (BQCV), acute bee paralysis virus (ABPV) and chronic bee paralysis virus (CBPV).

Alongside viruses, exposure to pesticide can result in residue contamination within the comb [81], providing an additional source of stress on the hive. In the current study we considered the effects of multiple routes of transmission of *Nosema* disease, however an additional stressor such as

pesticide exposure has the potential to enhance one of the routes of transmission. We therefore suggest future work could extend our current model framework to include more than one stressor, such as the buildup of pesticide residue alongside infection. Understanding this complex interaction between multiple stressors within the hive could shed new light upon honey bee colony losses.

While *Nosema* can be devastating to honey bee health, there are several practices which can be implemented to reduce infection. Our model suggests that this can be achieved by minimising one transmission route. This could occur through equipment management or sterilisation of the hive [154]. For example, inactivating the contaminated spores through heating the hive bodies and undrawn comb has been shown to reduce infection [154], explained in our model as minimising the fecal-oral route of transmission. An additional management practice is to provide the bees with nutrient supplementation [154], thus minimising the oral-oral route and subsequent total infection. Chemical treatments such as fumagillin [154] could also minimise the oral-oral route. Treating the remaining infected bees during the autumn and winter seasons could result in the complete eradication of spore contamination, and a healthy hive in the following spring.

This study provides an initial assessment of how multiple routes of transmission can synergistically increase infection and contamination and

thus contribute to honey bee mortality and decline. We hope that the framework presented in this paper can stimulate further empirical and theoretical studies focussing on multiple routes of transmission within a honey bee hive.

Chapter 4

Interactions between immunotoxicants and parasite stress: implications for host health

This chapter has previously been published as RD Booton, R Yamaguchi, JAR Marshall, DZ Childs, and Y Iwasa. Interactions between immunotoxicants and parasite stress: implications for host health. *J. Theor. Biol.*, 445:120–127, 2018. As author of this Elsevier article, I retain the right to include it in a thesis or dissertation, provided it is not published commercially. Permission is not required, but I reference the Journal of Theoretical Biology as the original source. The full published version is available on Science Direct.

4.1 Abstract

Many organisms face a wide variety of biotic and abiotic stressors which reduce individual survival, interacting to further reduce fitness. Here we studied the effects of two such interacting stressors: immunotoxicant exposure and parasite infection. We model the dynamics of a within-host infection and the associated immune response of an individual. We consider both the indirect sublethal effects on immunosuppression and the direct effects on health and mortality of individuals exposed to toxicants. We demonstrate that sublethal exposure to toxicants can promote infection through the suppression of the immune system. This happens through the depletion of the immune response which causes rapid proliferation in parasite load. We predict that the within-host parasite density is maximised by an intermediate toxicant exposure, rather than continuing to increase with toxicant exposure. In addition, high toxicant exposure can alter cellular regulation and cause the breakdown of normal healthy tissue, from which we infer higher mortality risk of the host. We classify this breakdown into three phases of increasing toxicant stress, and demonstrate the range of conditions under which toxicant exposure causes failure at the within-host level. These phases are determined by the relationship between the immunity status, overall cellular health and the level of toxicant exposure. We discuss the implications of our model in the context of individual bee

health. Our model provides an assessment of how pesticide stress and infection interact to cause the breakdown of the within-host dynamics of individual bees.

4.2 Introduction

During their lifetime, organisms are exposed to a wide range of chemical, physical and biological stressors, which can be defined as anthropogenic (e.g. toxicant exposure, pollutants) or natural (e.g. pathogens, parasites). Recently, there has been increasing interest in multiple stress approaches, examining the potential for stressors to interact [5]. Understanding the mechanisms behind these interactions is important for quantifying the true impacts of individual anthropogenic stress on organisms [155].

Pesticides are an important class of anthropogenic toxicant stress, with the use of pesticides continuing to increase globally [8–10]. Pesticides are crucially important to crop productivity, preserving around one-fifth of total crop yield contributing to food security [156] but concerns about detrimental side-effects [157, 158] have forced policy makers to restrict the application of some pesticides [159]. Non-target organisms frequently encounter these pesticides [9], with concentrations able to build up throughout food sources and within various life-stages of the organism [15, 160–164].

Toxicants such as pesticides can cause lethality [13–17], but more of-

ten have other sublethal effects such as impairments on foraging [165–168], feeding [169], learning [18, 19], memory [19, 170] and fecundity [171–173]. Exposure during early life can have both lethal and sublethal effects later appearing during adulthood [174, 175]. These environmental contaminants can interact in combination with other natural stressors. For example, combinations of toxicant exposure with parasite infections can increase individual mortality [176, 177], increase the initial pathogen load [82, 178] and increase the impact on reproduction and survival [179]. Toxicant-pathogen interactions have been observed in many types of organisms such as insects, snails, water fleas, frogs, salamanders, fish and mussels (see review by Holmstrup et al. [5]). In addition to toxicants causing direct lethality, they can also cause damage to individual immune defence. Individual organisms defend themselves against various infections via a suite of immune responses, and these can be damaged or inhibited through toxicant exposure [180]. For example, pesticides have been shown to reduce the total hemocyte abundance in insects [181, 182], the nodulation initiation [181, 183], the encapsulation response [182, 184] and antiviral defences [185].

Of particular recent concern are the widespread losses to global wild and managed bee populations [10, 186, 187], because of their importance to global food security and biodiversity [47, 120]. The Western honey bee (*Apis mellifera* L.) is widely recognised as the most important com-

mercial insect pollinator [49, 188, 189], but a single cause for their population decline has yet to be identified. There is agreement that these losses may have their origins within multiple stressors interacting with each other [54, 75, 76, 190]. Possible candidates include neonicotinoid pesticides [19, 22, 161], mites [71, 191], viruses [61, 64, 192] and microsporidia infections [68, 132].

In this study, we examine the mechanism by which immunotoxicants interact with the within-host cellular and immunological dynamics of a host to increase parasite load. We formulate the conditions under which sublethal toxicant exposure intensifies the infection levels within a host. This observed interaction between multiple stressors is currently poorly understood from an immunological perspective [193], while a rich body of theoretical research exists to describe the within-host dynamics of infectious diseases (see review by Mideo et al. [40]). We focus our study on the general ecotoxicological applications of the theoretical model, in the case of any immunotoxicant interacting with any parasite infection. We do this by formulating a system of nonlinear ordinary differential equations (ODEs) to investigate the consequences of immunosuppression by a toxicant and the effect this has on within-host infection. We first consider a toxicant-free environment to examine the conditions under which the infection can spread. We then consider the interaction between the infection and both lethal and sublethal exposure to toxicants and examine the out-

come on within-host dynamics. We also consider the case of aggressive direct lethality of toxicants on the production of new tissue cells.

4.3 Methods

The immune response of any individual relies upon the interdependent defence of physical, humoral and cellular responses, denoted in our model by a generalised immune function Z . Nowak and May [33] proposed a general model to describe the interaction between a cellular immune response and a replicating virus, in the setting of self-regulating cytotoxic T lymphocytes (CTLs) targeting infected cells. The model they present is simple but captures the fundamental biological processes governing the immune response to foreign antigens, and following this framework we denote within-host cell density as X . We denote the total parasite/pathogen density as Y . The total number of cells within the model represents a general susceptible subset of tissue cells. As a motivating example, our model can be thought of describing the midgut epithelial cells of the honey bee X under a *Nosema ceranae* infection Y [123] with associated immune response Z , although we also propose that our model can be thought of describing any interaction between any immunotoxicant and associated parasite or pathogen in a general host.

We assume that toxicant exposure reduces the functionality of the im-

immune system c rather than killing off individual immune cells. We make this assumption in order to simplify the analysis, however this also captures the inhibition and damage that toxicant exposure can have on the various functions associated with the immune response [180–185, 194–196]. This means that the linear function $-hQ$ can be thought of as inhibiting the immune functionality c . Toxicants are also lethally toxic to individuals at high enough exposure levels [13, 14, 16, 17], and we assume that rather than killing individual cells, the toxicant damages the vital functionality of the host, expressed through the parameter λ . We model both the direct/acute lethality (denoted by parameter r) and indirect sublethal immunotoxicity (denoted by parameter h) effects of toxicant exposure Q . For simplicity, we assume fast dynamics of virus replication compared to the replication of other within-host cells or immunity resulting in the formulation of the model (Fig. 4.1) as a 3-compartmental set of nonlinear ODEs;

$$\frac{dX}{dt} = \lambda - \beta YX - dX - rQ \quad (4.1a)$$

$$\frac{dY}{dt} = \beta YX - aY - pYZ \quad (4.1b)$$

$$\frac{dZ}{dt} = c - bZ - hQ \quad (4.1c)$$

with $c - hQ > 0$ and $\lambda - rQ > 0$. When $Z = 0$ (the immune response is depleted), we remove equation (4.1c) from system (4.1) and the system be-

comes the two dimensional system of equations (4.1a) and (4.1b*) without the immune response term $-pYZ$;

$$\frac{dX}{dt} = \lambda - \beta YX - dX - rQ \tag{4.1a}$$

$$\frac{dY}{dt} = \beta YX - aY \tag{4.1b*}$$

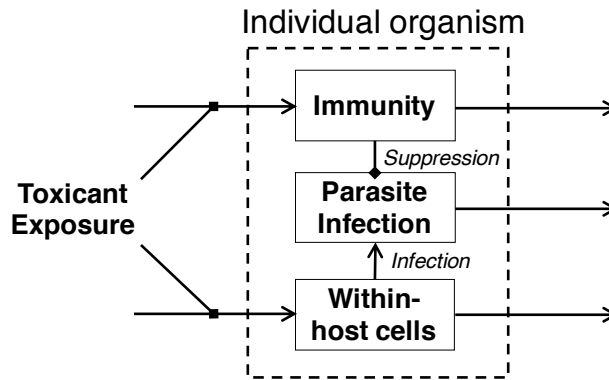


Figure 4.1: The modelling framework we use to model the interaction between toxicant exposure and parasite infection in an individual. Block arrows represent suppression. We model toxicant exposure as a suppressive effect on immunity and within-host cells.

We assume that within-host cells are produced at rate λ , and die at per-capita rate d . Parasites are created at rate β via a linear mass action, and are removed at per-capita rate a . The immune response Z is activated upon encountering parasites Y and the removal of parasites occurs at rate p . Although in reality, functions involved in immunity are not activated on the instance of meeting the parasite, but there is a complicated intermediary chain between processes which eventually result in the removal of parasites [197]. For simplicity, we assume that this process can be summarised by

our function pYZ . We assume that the immune dynamics Z are decoupled from those of within-host and parasite density. This represents the simplest possible assumption and various extensions to this assumption are possible. Immunity is therefore produced at rate c , and is removed at per-capita rate b .

Within our model we infer the mortality risk of the host through the status of the within-host cells X . Individual mortality risk is high when the number of within-host cells X are small, so that there is a negative correlation between the mortality of the host and the cell density. This condition enables us to think about the mortality risk of an individual analogous to a highly infected within-host tissue (e.g. parasite infection within the gut of a honey bee).

Our system of equations (4.1) were analysed using standard stability methods from dynamical systems theory and solved numerically with Wolfram Mathematica version number *10.0.2.0*, using parameters taken from Table 4.1. We performed a full parameter dependence analysis which demonstrated the same universal behaviours of the model which enabled us to choose arbitrary parameter sets.

Parameter	Symbol	Value
production of within-host cells	λ	0.1
rate of parasite infection	β	0.01
death of within-host cells	d	0.01
direct lethal effect of toxicant	r	0.1
toxicant exposure	Q	[0, 1.5]
death rate of parasites	a	0.01
immune suppression	p	0.009
production of immunity	c	0.1
removal of immunity	b	0.02
indirect sublethal effect of toxicant	h	0.3

Table 4.1: Parameter values used in the within-host stress model

4.4 Results

In the following section we consider the baseline case of parasite infection in a toxicant-free environment before analysing our within-host system under the addition of a toxicant. We then consider the absence of direct lethal effects of toxicants before presenting the case of an aggressive toxicant.

Toxicant-free model

Initially we examine system (4.1) under the condition of the absence of toxicant exposure (denoted by subscript A). Two possible outcomes are possible. First the infection is removed entirely by the immune system, in which case the total within-host cells and total immunity each reach a

constant level at the disease free equilibrium (DFE):

$$(X_A^{DFE}, Y_A^{DFE}, Z_A^{DFE}) = \left(\frac{\lambda}{d}, 0, \frac{c}{b} \right) \quad (4.2a)$$

where $\frac{\lambda}{d}$ and $\frac{c}{b}$ represent the ratio of total production to total removal of both within-host cells and immunity in the absence of toxicant respectively. Secondly the model predicts that an individual can become infected with parasites ($Y > 0$) under the following endemic equilibrium (EE):

$$(X_A^{EE}, Y_A^{EE}, Z_A^{EE}) = \left(\frac{ab + cp}{\beta b}, -\frac{d}{\beta} + \frac{b\lambda}{ab + cp}, \frac{c}{b} \right) \quad (4.2b)$$

This shows that it is possible for an individual bee to sustain a partial parasite infection without the addition of any toxicant in our model. The expression $\frac{ab+cp}{\beta b} = \frac{a}{\beta} + \frac{cp}{\beta b}$ represents the reduction in within-host cells.

Toxicant-Parasite model

Next we consider system (4.1) under the condition of an infection and toxicant exposure (denoted by subscript B). In this case the model predicts two possible outcomes. First, the parasite infection is removed either by immune suppression or by the direct effects of the toxicant on the production of within-host cells represented by the DFE:

$$(X_B^{DFE}, Y_B^{DFE}, Z_B^{DFE}) = \left(\frac{\lambda - rQ}{d}, 0, \frac{c - hQ}{b} \right) \quad (4.2c)$$

so that the addition of any toxicant reduces the total within-host cells by $\frac{rQ}{d}$ and reduces the immune function by $\frac{hQ}{b}$. Secondly the model predicts an infected individual under toxicant exposure represented by the EE:

$$(X_B^{EE}, Y_B^{EE}, Z_B^{EE}) = \left(\frac{ab + cp - hpQ}{\beta b}, \frac{-abd - cdp + dhpQ - bQr\beta + \beta b\lambda}{\beta ab + cp\beta - hpQ\beta}, \frac{c - hQ}{b} \right) \quad (4.2d)$$

In this case, the parasite density grows rapidly as a result of the toxicant suppressing the immune system. The introduction of the toxicant reduces both within-host cells and immunity in both an infection-free and infected individual, but an initial parasite infection is required for an infection to grow. The effect of toxicant exposure on the net change of within-host cells, parasite density and immunity within the individual is summarised in Table 4.2.

	No parasite infection	Initial parasite infection
Within-host cells X	reduced by $\frac{rQ}{d}$	reduced by $\frac{hpQ}{b\beta}$
Parasites Y	no change	increased by $\frac{bQ(hp\lambda - abr - cpr)}{(ab + cp)(ab + p(c - hQ))}$
Immunity Z	reduced by $\frac{rQ}{d}$	reduced by $\frac{hQ}{b}$

Table 4.2: The net change of immunity, within-host cells and parasites after the introduction of toxicant, compared to the no-toxicant model, for both the absence of parasite infection ($Y = 0$) and initial ($Y > 0$) parasite infection load.

Next we assume that the indirect (sublethal) effects of toxicant exposure on immunosuppression are more prominent than the direct (lethal) depletion of within-host cells. With an initial infection $Y > 0$ we define this as

occurring when the immune status of an individual is destroyed before the infection is removed or when

$$Z = 0 \quad \text{before} \quad Y = 0 \quad (4.3)$$

We summarise the behaviour of the model under this condition (Fig. 4.2) into 3 distinct phases which describe the mechanism underlying the interaction between toxicant exposure and infection at the within-host level of the organism, and the parameter dependence of infection and immunity at equilibrium. Note that the total number of cells within an individual organism is not constant. This is because both parasite and within-host cells are removed by either the toxicant exposure or infection and new cells are produced. The following dynamical phases are determined by the stability and feasibility analysis of the model (Appendix C):

Phase I $0 \leq Q < \frac{c}{h} = Q_0^*$

The model predicts that the initial state of an immune response is able to counter any infection. However, as the toxicant load is increased, the immune system is gradually depleted. Through a weakened immune suppression, this enables the parasite density to increase.

Phase II $Q_0^* = \frac{c}{h} \leq Q < \frac{\beta\lambda - ad}{r\beta} = Q_1^*$

The second phase begins at the point of maximum infection and where the immune system has been completely inhibited. The increase in toxicant stress gradually depletes the parasite density while the within-host cells remain constant.

Phase III $Q_1^* = \frac{\beta\lambda - ad}{r\beta} \leq Q < \frac{\lambda}{r}$

In phase three, the immune system has been destroyed and the parasite infection is no longer present leaving only a small fraction of within-host cells. Finally, the lethality of the toxicant causes the mortality of the individual bee and production of new cells ceases when $\lambda - rQ$ becomes zero which occurs at $Q = \frac{\lambda}{r}$.

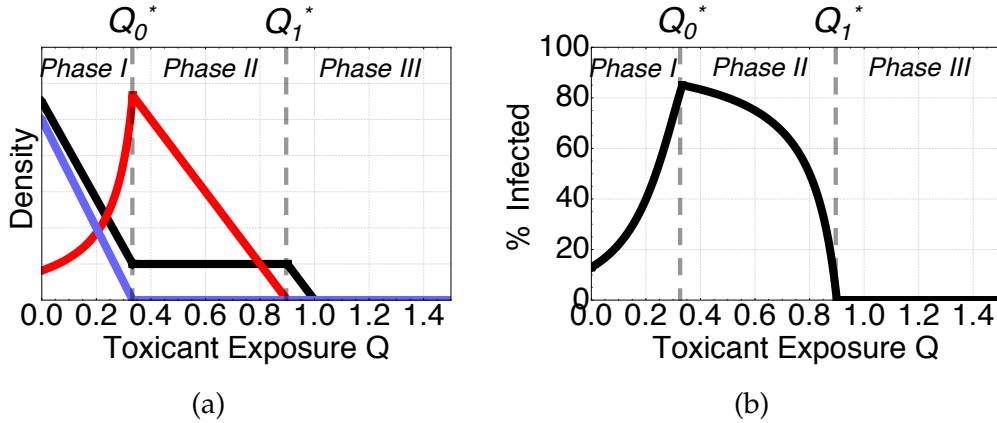


Figure 4.2: The mechanism of parasite infection under increasing toxicant exposure, for both immunosuppressive and lethal effects of toxicant with all parameters taken from Table 4.1. This shows the parameter dependence of immunity, parasite density and within-host cells at equilibrium within the dynamics of our model. In (a) the total densities of immune function (blue), parasite load (red) and within-host cells (black) change as an individual is subject to higher toxicant loads, according to the three phases of the model. In (b) the total % parasite infection (black) increases as the toxicant load is increased, before decreasing to 0 at Q_1^* .

Thus we have calculated the conditions under which the within-host dynamics change according to the level of toxicant exposure. Further additional analysis can be found in Appendix C. By understanding the relationship between the parameters in the model and toxicant stress, we can make some biological interpretations. We predict that the ratio of the production of immunity to the amount of immunotoxicity ($Q_0^* = \frac{c}{h}$) determines the point at which the infection load is at a maximum. The expression $\frac{c}{h}$ can be thought of as an indicator of immune status, and the point at which the toxicant stress becomes equal ($Q = Q_0^*$) represents the complete inhibition of the immune system. The expression $Q_1^* = \frac{\beta\lambda - ad}{r\beta} = \frac{\lambda}{r} - \frac{ad}{r\beta}$ represents the point at which the ratio of cell production to lethal toxicant mortality (indi-

cator of within-host cell status) compares to the ratio of the loss of cells to the toxicant cell depletion multiplied by the transmission of the infection. Therefore this condition represents the status of within-host dynamics and can be thought of as an indicator of health. When $Q = Q_1^*$, the infection has been removed but the overall health status is very low, from which we infer a higher mortality risk of the host. Therefore we have conditions describing how toxicant exposure relates to that of the immune status Q_0^* and overall health Q_1^* of the organism.

Our model predicts that a small amount of toxicant can cause the outbreak of an otherwise controlled infection. A healthy immune response can suppress the parasite infection to a very low level (Fig. 4.3a), but a small amount of toxicant can cause the status of both infection-free and infected individuals to decline rapidly (Fig. 4.3b).

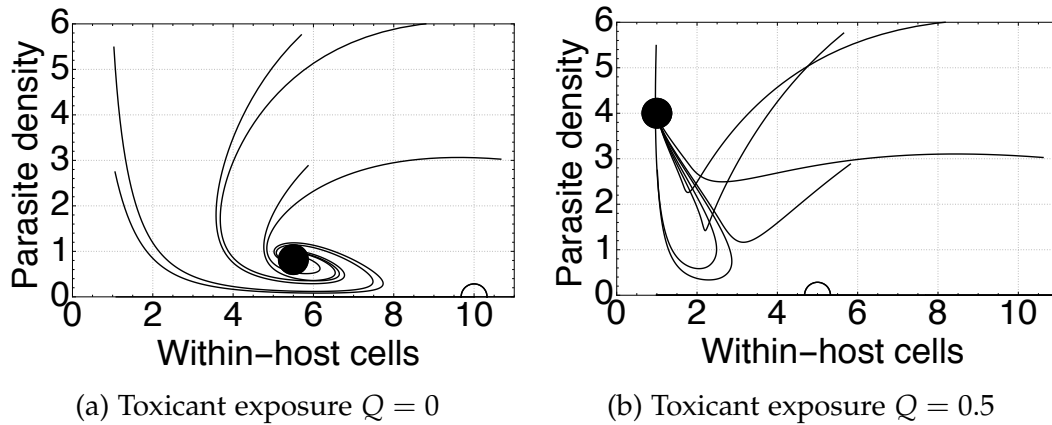


Figure 4.3: The convergence of the total density of within-host cells and parasites under no toxicant exposure (a) $Q = 0$, and small amounts of toxicant exposure (b) $Q = 0.5$. All other parameters are taken from Table 4.1. Black dots show the stable endemic equilibrium, white dots show the unstable disease-free equilibria and lines show the convergence from initial conditions. We assume an initial immune response ($Z = 10$) and an initial amount of within-host cells ($X > 0$), and either zero or positive parasite density ($Y \geq 0$).

Absence of toxicant lethality ($r = 0$)

In this case, we consider the absence of a direct lethal toxicant effect, therefore assuming that toxicant exposure only impairs the immune system and does not cause direct mortality. This changes the mechanism by which organisms become infected under increasing toxicant exposure. As before the immune system is inhibited leaving the organism vulnerable to attack by parasites. However after reaching a maximum infected threshold, the health status of the individual remains constant regardless of the amount of toxicant exposure (Fig. 4.4a). The individual remains highly infected (Fig. 4.4b) and an increasing exposure to the toxicant no longer causes

further damage to organism health status.

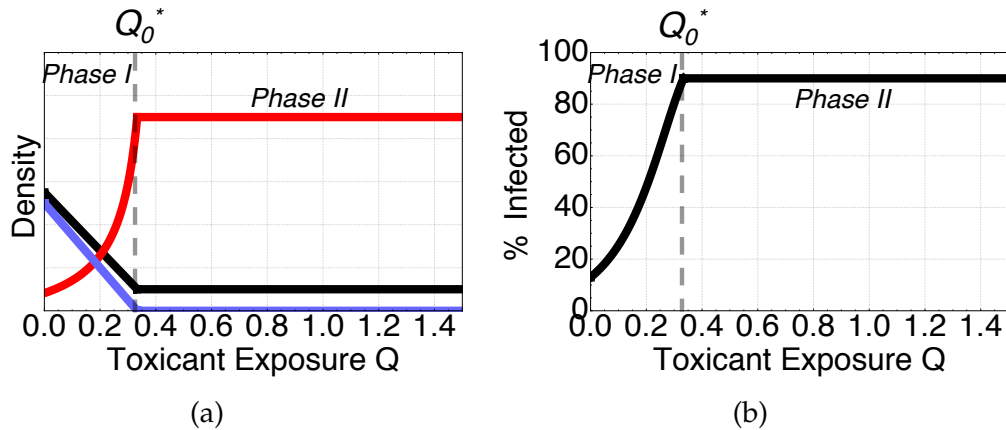


Figure 4.4: The mechanism of parasite infection under increasing toxicant exposure, for only the immunosuppressive toxicant effect. Parameters taken from Table 4.1, but with direct toxicant effect $r = 0$. In (a), the total density of immune function (blue), parasite load (red) and within-host cells (black) change as an individual is subject to higher toxicant loads, but now only within 2 phases. In (b), the total % parasite infection (black) increases as the toxicant load is increased, before remaining at equilibrium.

Aggressive toxicant lethality (large r)

It is worth noting that condition (4.3) is necessary to explore the interaction between toxicant immunosuppression and the immune system. If this were not the case, for example if the parameter r becomes large we would see a situation where the toxicant acts too aggressively upon the host and causes the parasite infection to be killed off (similar to phase II under the original assumption) and following this the within-host cells are destroyed. The immune system remains intact as the direct effect of the toxicant on production of within-host cells is greater than the immune effect. We again see three distinct phases as we increase the toxicant from low levels to high (Fig

4.5a). However now the toxicant exposure is more prominent and reduces both parasite and within-host cells, stopping the infection from spreading quickly (Fig. 4.5b). In this situation we also see a somewhat contradictory phase 3 in which the host has neither parasite or within-host cells but a small amount of immunity. This result demonstrates the necessity of our original condition.

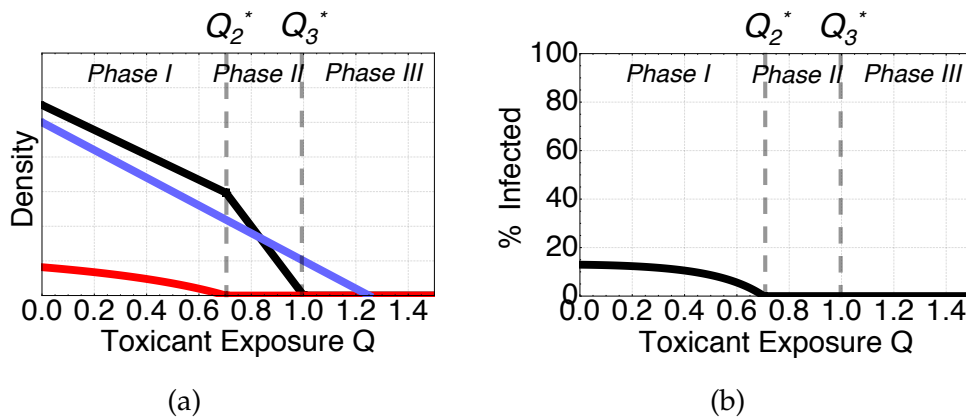


Figure 4.5: The mechanism of parasite infection under increasing toxicant exposure with aggressive direct mortality. Parameters taken from Table 4.1, but with indirect toxicant effect $h = 0.08$. In (a), the total density of immune function (blue), parasite load (red) and within-host cells (black) change as an individual bee is subject to higher toxicant loads, according to 3 phases. In (b), the total % parasite infection (black) decreases as the toxicant load is increased. The phases are determined by new critical levels of toxicant Q_2^* and Q_3^* .

The three distinct qualitative behaviours (maximised infection at intermediate toxicant, absence of toxicant lethality, and aggressive toxicant lethality) of the model are summarised in Fig. 4.6. This figure shows that the ratio between the parameters r and h determine the relationship between toxicant exposure and infection within a host. If r is too high, then

the parasite is inhibited before the immune system. However, if h is sufficiently high then the parasite is maximised at an intermediate toxicant exposure. The small region around $r = 0$ results in the parasite remaining at high density regardless of higher toxicant exposure. Additional examples of individual pairwise combinations of both immunosuppressive and lethal effects can be found in the appendix for both equilibria phase status (Appendix: Fig. C1) and total percentage parasite infection (Appendix: Fig. C2).

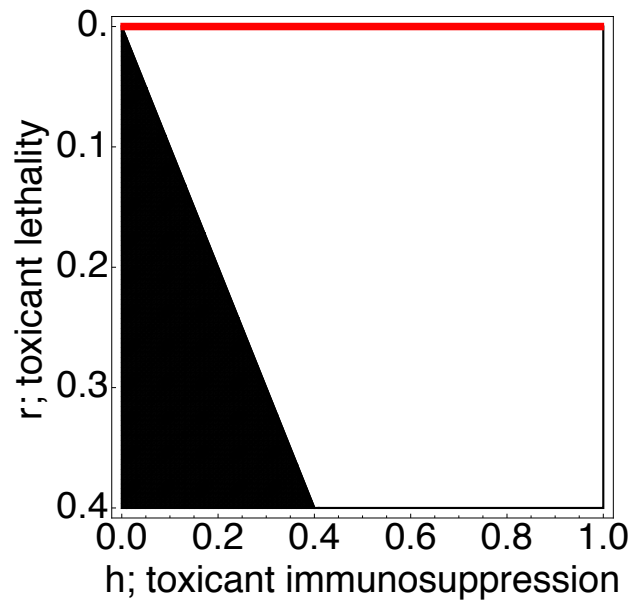


Figure 4.6: The qualitative behaviour of the model within $r - h$ lethal-immunosuppressive toxicant space. Parameters taken from Table 4.1, for a range of r and h . The white region represents the case of maximised parasite infection at intermediate toxicant exposure. The red region ($r = 0$) represents the toxicant-free parasite equilibrium. The black region represents the aggressive toxicant effect of the model.

4.5 Discussion

We have shown that interactions between general anthropogenic stress in the form of an immunotoxicant and parasites can promote within-host infection and reduce health status. This interaction is entirely dependent upon the phase of toxicant exposure. The immune response of the host can be divided into three such phases of increasing toxicant load; phase I, II and III (Fig. 4.2). In the first phase, sublethal doses of the toxicant damage the immune system. This results in suppression of the immune system and hence the individual organism becomes highly infected. In the second phase, intermediate exposure to the toxicant reduces the total density of parasites. In the third phase, the extremely high exposure to the toxicant leads to the loss of within-host cells and eventual mortality of the host.

Through disentangling the individual effects of both lethal and sublethal toxicant exposure, we were able to establish the role of each within the breakdown of within-host dynamics. Indirect (sublethal) suppression of the immune system causes rapid proliferation of parasites within the host (Fig. 4.3), while direct (lethal) mortality causes both parasites and within-host cells to die. However without the direct effect of the toxicant on the production of new cells, the host remains highly infective (Fig 4.4). We also predict that an extremely small toxicant exposure can cause the proliferation of a previously manageable infection. These results suggest

that the ratio between both lethal and immunosuppressive toxicant effects are important in determining the subsequent interaction with parasite infections. Our model suggests when assessing both sublethal and lethal toxicant effects, it is important to consider that higher lethal doses (LD50) could remove the parasite infection from the host and that there exists a range of intermediate sublethal exposure under which we predict that the parasite will proliferate.

The findings we present in this study shed new light on the poorly understood mechanism by which toxicants seem to interact with infection to increase mortality risk [193]. In the context of the recent losses to global bee populations [10, 186, 187], the joint immunotoxicant-infection interaction studied here is one example of the recent hypothesis that widespread native and managed bee losses may be multi-factorial [54, 75, 76, 190]. Joint pesticide-infection interactions have been shown to increase mortality risk within bees [176, 177]; for example, *Nosema ceranae* infections and thiacloprid, a neonicotinoid pesticide act jointly to increase individual mortality [178]. The findings we present in this paper propose one explanation of how interactions between these toxicants and infection occur at the within-host level. We show that these sublethal effects of anthropogenic stress are potentially more damaging to individual health, aggravating parasitic stress. This is in direct agreement to the positive correlation between low level (field condition) neonicotinoid treatment and increases in parasite and

viral infestations in bees [198, 199]. Infections within individual honey bees can be significantly increased by different levels of low or high sublethal pesticides [82]. Indeed, honey bees with undetectable levels of neonicotinoid imidacloprid which are reared in sublethal conditions still have increased infection levels [82]. This suggests that even extremely small sublethal exposure to pesticide can result in outbreaks of infection. We show that increasing the pesticide exposure by a small amount ($Q > 0$) can result in a transition from a manageable parasite density level to a highly infected individual.

Our results rely upon condition (4.3) which ensures that the immune response is destroyed before the within-host cells. This condition is crucial to ensuring reasonable behaviour of the model, and it should be noted that the reverse assumption predicts the presence of immunity even after both infected and within-host cells are dead (Fig 4.5a). We highlight this limitation of our theoretical work but argue that condition (4.3) is valid since the direct lethality of toxicants only occur at high doses [14] and various immunosuppressive effects occur from toxicants [180], thus suggesting that toxicants have a greater impact on suppressing the immune system. Within our model, we made assumptions about the way in which toxicant exposure acts upon the host. An alternative assumption could frame this exposure as acting through a density dependence upon immunity and within-host cells. We reproduced Fig 4.2 using the same parameters and

this assumption also yields the result that parasite density is maximised at an intermediate toxicant exposure (Appendix: Fig. C3). The qualitative behaviour of the parasite is unchanged by this density dependent assumption.

The framework provided in this study focuses on the failure of the immune system of an individual organism. However individuals interact within populations causing infection to spread to other susceptible individuals, and these populations have associated interdependent immune defences at both the within-host and between-host level. For example, social immunity involves many behavioural and population-level mechanisms such as social fever, a mechanism by which individuals increase the temperature of the surrounding environment in order to kill parasites [200], guarding, where patrolling guards prevent infected individuals from interacting with healthy individuals [201], hygienic cleaning behavioural traits, by which the population remove diseased or dead individuals [202] and storing antimicrobial food [203]. Hence the main limitation of our framework is that we may have only considered one half of both interdependent within and between-host immunities. Coupling population immunity models in the context of an epidemic alongside our individual immunity framework could further explain the interactions between toxicants and infection at both the individual and population level. Further theoretical work incorporating these multi-level dynamics could address the gap in

understanding bee decline as interacting stressors in similar ways to other models of colony collapse disorder [1, 96, 204].

This work highlights the need for further studies which focus on interactions between various stressors at the within-host level. Our theoretical study presents a starting position to think about these interactions at the within-host level in the context of the immune system of an individual organism. While our model has an inherently simple structure, the addition of the toxicant function can lead to complicated dynamics that are consistent with empirical observations. This framework can stimulate further empirical and theoretical studies which focus on the interaction between toxicant exposure, infection and the immune system at both the social group and individual level.

Chapter 5

**How do toxicants affect
epidemiological dynamics?**

5.1 Abstract

Populations are formed of their constituent interacting individuals, each with their own respective within-host biological processes. Infection not only spreads within the host organism but also spreads between individuals. Here we study a multilevel model which links the within-host statuses of immunity and parasite density to population epidemiology under sub-lethal and lethal toxicant exposure. We analyse this nested model in order to better understand how toxicants impact the spread of disease within populations. We demonstrate that outbreak of infection within a population is completely determined by the level of toxicant exposure, and that it is maximised by intermediate toxicant dosage. We classify the population epidemiology into 5 phases of toxicant exposure and calculate the conditions under which disease will spread, showing that there exists a threshold toxicant level under which epidemics will not occur. In general, higher toxicant load results in either extinction of the population or outbreak of infection. The within-host statuses of the individual host also determine the outcome of the epidemic at the population level. We discuss applications of our model in the context of disease ecology, predicting that increased exposure to toxicants could result in greater risk of epidemics. We predict that reducing toxicant exposure below our predicted safe threshold could contribute to controlling population level disease and infection.

5.2 Introduction

The spread of infectious disease within populations occurs at various scales of organisation. Population-scale processes are determined by the interacting individuals within such populations, each with their own respective individual within-host biological processes. Between-host epidemiological dynamics are determined primarily by host demography and transmission [205], while transmission is determined by the level of disease in infected individuals within the population [40]. Furthermore, the dynamics of diseased individuals are entirely dependent on their corresponding within-host parasite load and host defence mechanisms [40]. Infectious diseases such as host-parasite interactions depend upon two processes; both the immunological host-parasite interaction and the subsequent population level epidemiology [41].

Individual organisms are exposed to a wide variety of stressors. These stressors can be broadly defined as either abiotic (anthropogenic or climatic) or biotic (parasites or predation). These stressors either act alone, or in combination which can result in a higher than expected overall effect when synergistic interactions occur between them [5]. One such anthropogenic stressor is toxicant exposure; chemicals released into the environment which damage or have other detrimental effects on the host. Examples of such chemical stressors include pesticides in freshwater systems

[7], neonicotinoid insecticides in honey bee colonies [10], various environmental pollutants in rotifers [206] and *Daphnia* [207] and polychlorinated dibenzo-p-dioxins (PCDDs), biphenyls (PCBs) and dibenzofurans (PCDFs) in animals and humans [208]. Indeed, toxicants affect a wide range of non-target species, including birds, mammals [11], aquatic species [12], and insects [9].

In general, toxicants have lethal effects [13–17, 209], where the direct chronic lethality of toxicant exposure occurs at high doses [13, 16, 17]. Toxicants often have other effects on behaviour, learning, feeding, memory and fecundity [18, 19, 169, 173, 210, 211]. Individuals exposed to toxicants can face other stressors such as parasite infections which, when combined can cause further damage to the host. For example, the combination of parasite infection and toxicant exposure can increase the initial parasite load [82, 178], increase virulence [179] and increase mortality [176, 177] in the host. These interactions between toxicants and parasites are observed in a multitude of organisms [5]. In addition to the effects of toxicants on the functionality of the host, toxicants also sublethally damage or inhibit the individual immune response of the host [180]. There are a wide range of immunosuppressive effects which occur as a result of sublethal or field realistic levels of toxicant exposure [180, 182, 212–214]. Throughout this manuscript we will focus on these two effects of toxicant damage to the host: lethal exposure reducing the functionality of the host and sublethal

exposure causing a reduction in the functionality of the host immune response.

The individual impacts of stressors on host level processes are well studied, but the subsequent impact on higher scales of organisation such as populations are often not fully understood [20]. Toxicant research tends to focus either on the molecular, physiological or cellular levels, or on merely observing population decline, with the causal link between scales (within-host and population) rarely investigated [20]. For example, lethal and sub-lethal thresholds of toxicants are determined through experiments with individuals, leading to uncertainty as to what consequence this has for the population level [21]. Furthermore, interactions between multiple stressors lead to effects which are not predictable from understanding the individual effects of each stressor [179]. For example, the chemical stressor cadmium, in combination with other abiotic stressors can affect the population growth rate and life-history parameters of *Daphnia magna* [215]. Uncertainty in quantifying toxic effects can be explained through their interaction with other stressors at the individual level, which in turn alter the population dynamics [215]. In another study with *Daphnia magna*, pesticide exposure has been shown to enhance the virulence of endoparasites [179].

Many mathematical models either consider the within-host dynamics independent of the population [2], the epidemiological population dynamics independent of the within-host parasite dynamics [33, 125], or model

stressors as general population level processes [1, 58, 96]. Bridging multi-scale biological processes can be achieved using nested (also called embedded) mathematical models [39, 40]. Nested approaches embed models of within-host dynamics into the epidemiological population scale. This allows epidemiological parameters such as the basic reproduction number R_0 to be determined by the dynamics of within-host parameters such as parasite load, immune status and cellular health. This approach is particularly useful when the effects of within-host processes on determining population epidemiology are unknown [40], and as such, parameter relationships can be determined from the subsequent analysis of the nested model, providing important biological mechanistic predictions [39, 41–45]. For example, the model by Bhattacharya and Martcheva [23] relates the immune response of a species infected by a pathogen to population epidemiological parameters, using a nested within- and between-host approach. This study however focusses on ecological competition between species, rather than additional sources of stressors such as toxicants.

To date, little work addresses the interface between population epidemiology and toxicant stress [22, 23]. In this study, we examine how toxicants impact the spread of disease within populations, and how the subsequent epidemiology is formed from their respective within- and between-host processes. We introduce and analyse a nested model linking epidemiological between-host processes to those of a previously studied within-host

model [2]. This previous model examined interacting within-host processes: host immunity, host parasite load and host cellular health, and the effects of sublethal and lethal toxicant exposure. This previous study by Booton et al. [2] showed that within-host parasite density is maximised by intermediate doses of toxicant exposure, but they did not consider the subsequent effects of their results on population level epidemiology. Here, we investigate the change in the basic reproduction number of the epidemic as the toxicant load is increased from zero to lethal exposure (causing host mortality) and classify the resulting epidemiology into five distinct phases of infection. These phases are determined by the interplay between both within-host and between-host dynamics and processes.

5.3 Methods

Here we consider two scales of biological organisation, both the within-host immuno-infection dynamics and between-host population dynamics. We assume that the within-host dynamics are fast relative to a slower population level timescale, a commonly used method for linking multi-level scales [40, 43, 44]. Therefore each individual has equal average status of infection at the within-host level, dependent upon the individual's sub-class of infection (susceptible or infected). This significantly reduces the complexity of such nested models, and allows a substitution of within-host steady state

values into the between-host system. The separation of time scales through slow-fast dynamics is justified through assuming that each individual belongs to a sub-group of infection, which we characterise below as either susceptible or infected.

Within-host model

We use the simple modelling framework provided in Booton et al. [2] to describe the within-host infection dynamics under toxicant exposure in an individual. X , Y and Z represent the total within-host cells, parasite density and immune function, respectively. The total within-host cells X represent the uninfected cells within the host and Y represents the total number of parasite-infected cells as a measure of parasite density. Here the term uninfected implies that these cells could be potentially infected by a parasite. To simplify the analysis significantly we use a non-dimensionalised version of the original model published in Booton et al. [2]. The full derivation of this model can be found in Appendix D, and this model has the same qualitative dynamics, but with fewer parameters.

$$\frac{dX}{dt} = (1 - \xi_1 Q) - X(\phi + Y) \quad (5.1a)$$

$$\frac{dY}{dt} = Y(\epsilon X - \gamma - \omega Z) \quad (5.1b)$$

$$\frac{dZ}{dt} = (1 - \xi_2 Q) - Z \quad (5.1c)$$

Toxicant exposure Q both reduces the functionality of the immune system at rate $\tilde{\zeta}_2$ (sublethal) relative to the production of immunity and damages the functionality of the host at rate $\tilde{\zeta}_1$ (lethal) relative to the production of new cells. This linear relationship is the simplest possible assumption regarding the effects of the toxicant on the host, and other such assumptions (such as density-dependence) reproduce similar qualitative results to the model presented here [2]. The non-dimensionalisation process scaled the remaining parameters relative to the removal of immunity: ϕ sets the rate at which healthy cells are removed from the system, ϵ represents transmission of parasites and production of cells, γ sets the death rate of the parasites, and ω represents the immune suppression and production of immunity (all relative to the removal of immunity). Details on within-host parameter relationships and their substitutions can be found in Appendix D.

This model assumes to begin with that $1 - \tilde{\zeta}_1 Q > 0$ and $1 - \tilde{\zeta}_2 Q > 0$. At the point when $Z = 0$, equation (5.1c) is removed and the model becomes the system of equations (5.1a) and (5.1b) without the term $-\omega YZ$ (as $Z = 0$). In general throughout this paper we assume $\tilde{\zeta}_2 > \tilde{\zeta}_1$, which ensures sensible behaviour of the model. If the alternative assumption $\tilde{\zeta}_2 < \tilde{\zeta}_1$ holds true, the model predicts a healthy immune function even after the parasite and healthy cells are dead (representing host mortality). However in the main text we focus on the case $\tilde{\zeta}_2 > \tilde{\zeta}_1$ and argue that this

case is biologically valid since the direct lethality of toxicants generally occur at higher doses [13, 16, 17], and various types of immunosuppressive damage occur at sublethal or field realistic levels of toxicant [180, 182, 212]. Hence the assumption $\zeta_2 > \zeta_1$ ensures that the relative effect of sublethal damage is stronger than that of the lethal toxicant damage at lower doses. Similarly, after $Y = 0$, the model becomes equation (5.1a) but without the term $-XY$. The assumption that $Z = 0$ before $Y = 0$ ensures that we can investigate both the sublethal immunosuppressive effect and direct lethality of the toxicant before the death of the host at higher levels of Q .

We define X' to be the equilibrium state of within-host cells in an uninfected individual in the absence of infection, X^* to be the equilibrium state of within-host cells in an infected individual, and Y^* to be the equilibrium state of parasite density in an infected individual, given by the expressions (derivations of which can be found in Appendix D):

$$X' = \begin{cases} \frac{1-\zeta_1 Q}{\phi}, & \text{if } 1 - \zeta_2 Q > 0 \\ 0, & \text{otherwise} \end{cases} \quad (5.2a)$$

$$X^* = \begin{cases} \frac{\gamma - \zeta_2 Q \omega + \omega}{\epsilon}, & \text{if } 1 - \zeta_2 Q > 0 \\ \frac{\gamma}{\epsilon}, & \text{if } 1 - \zeta_2 Q \leq 0 \text{ \& } Y^* > 0 \\ X', & \text{if } 1 - \zeta_2 Q \leq 0 \text{ \& } Y^* = 0 \end{cases} \quad (5.2b)$$

$$Y^* = \begin{cases} \frac{\epsilon - \zeta_1 Q \epsilon}{\gamma - \zeta_2 Q \omega + \omega} - \phi, & \text{if } 1 - \zeta_2 Q > 0 \\ \frac{-\gamma \phi - \zeta_1 \epsilon + \epsilon}{\gamma}, & \text{if } 1 - \zeta_2 Q \leq 0 \text{ \& } \frac{-\gamma \phi - \zeta_1 \epsilon + \epsilon}{\gamma} > 0 \\ 0, & \frac{-\gamma \phi - \zeta_1 \epsilon + \epsilon}{\gamma} \leq 0 \end{cases} \quad (5.2c)$$

Between-host model

The dynamics of an infected population follow those of a simple susceptible - infected (S-I) model framework. Each individual can be classified into either healthy susceptible S or infected I and therefore the total population N is represented by $S + I$. We assume that new individuals enter the population at rate Λ . Transmission from a healthy susceptible individual to an infected individual occurs at rate θ proportional to the equilibrium status of within-host infection Y^* . We assume that the per capita mortality function u is the same for each class with rates $\frac{u}{1+kX}$ and $\frac{u}{1+kX^*}$ for uninfected and infected individuals respectively, where k sets the strength of the mortality function with respect to the numbers of within-host cells. This ensures that cell depletion at the within-host level causes mortality at the level of the individual hosts, where the mortality function increases as the cell count decreases, up to a maximum value of u . This also ensures that the death rate of an infected individual is inversely proportional to the equilibrium state of the within-host cells under parasitisation.

The coupled within-host and population level model is a two dimensional system of non-linear ordinary differential equations (ODEs):

$$\frac{dS}{dt} = \Lambda - \theta SIY^* - \frac{u}{1 + kX'} S \quad (5.3a)$$

$$\frac{dI}{dt} = \theta SIY^* - \frac{u}{1 + kX^*} I \quad (5.3b)$$

The model was analysed using standard methods from dynamical systems theory and were numerically solved with Wolfram Mathematica version number *10.0.2.0*. The algebraic equilibria were found using the Mathematica function *Solve* and the numeric equilibria by *NDSolve*. We chose a parameter set (Table 5.1) which highlights the typical qualitative behaviour of the model and we examine how this behaviour is modified by changing parameters around this standard set. The parameter set we chose is one such set which highlights the qualitative behaviour of the model.

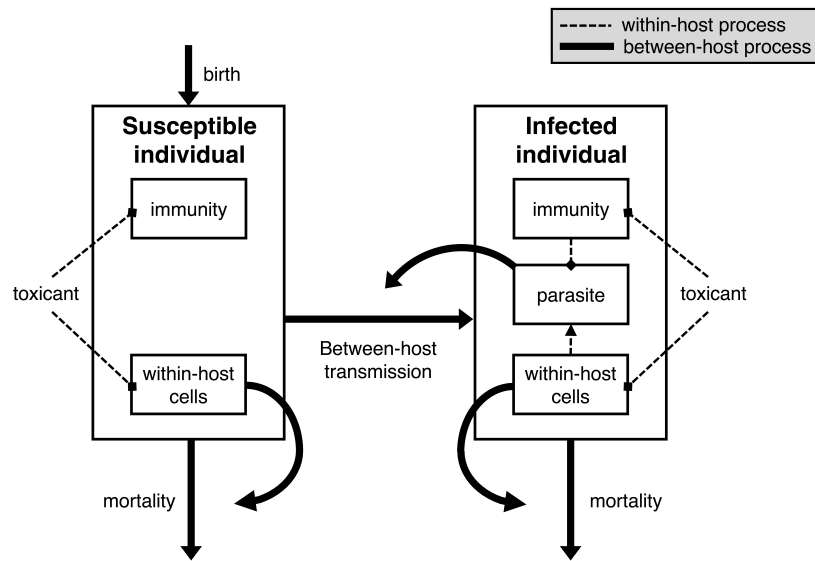


Figure 5.1: The outline of the multilevel model. Bold lines show the between-host processes and dashed show the within-host processes. Individuals can either be classified as susceptible or infected. Infection spreads between hosts dependent upon the within-host parasite density. The toxicant impacts immune function and the general functionality of the host. New individuals enter the system via birth and leave via death which is dependent upon the individual within-host cellular health status.

Parameter/ variable description	Symbol	Value
Within-host		
total within-host uninfected cells	X	
parasite density	Y	
immune function	Z	
lethal toxicant effect relative to production of new cells	ξ_1	0.5
sublethal toxicant effect relative to production of immunity	ξ_2	2
mortality of cells relative to removal of immunity	ϕ	0.4166
mortality of parasite relative to removal of immunity	γ	0.2
within-host transmission and production of cells relative to removal of immunity	ϵ	0.5
suppression and production of immunity relative to removal of immunity	ω	1
Between-host		
susceptible individuals	S	
infected individuals	I	
birth rate	Λ	0.01
between-host transmission rate	θ	0.01
mortality rate	u	0.01
relative effect of host mortality	k	1

Table 5.1: The between and within-host parameters used in the analysis and simulations of the model.

5.4 Results

States of the population system

System (5.3) has two solutions; the endemic equilibria (EE) and the disease free equilibria (DFE).

$$(S^{DFE}, I^{DFE}) = \left(\frac{\Lambda + k\Lambda X'}{u}, 0 \right) \quad (5.4a)$$

$$(S^{EE}, I^{EE}) = \left(\frac{u}{\theta Y^* + k\theta X^* Y^{*'}}, \frac{\Lambda + k\Lambda X^*}{u} - \frac{u}{\theta Y^* + k\theta Y^* X'} \right) \quad (5.4b)$$

Therefore system (5.3) either converges to the EE or DFE depending upon the basic reproduction number R_0 , calculated as

$$R_0 = \frac{\theta\Lambda Y^*(1 + kX')(1 + kX^*)}{u^2} \quad (5.5)$$

This tells us the threshold at which infection will spread throughout the population causing an epidemic ($R_0 > 1$). Increasing between-host transmission θ or population birth rate Λ increases the chance of outbreak. Increasing the density dependent mortality u decreases the chance of outbreak. We predict that infection can spread through a population when the parasite load Y^* exceeds the critical threshold

$$Y^* > \frac{u^2}{\theta\Lambda(1 + kX')(1 + kX^*)} \quad (5.6)$$

When the toxicant Q is not present in the system, we expect $R_0 = 1$ when $\phi \geq 0$, $\epsilon \geq 0$, $\gamma > 0$, $\omega \geq 0$, $\Lambda > 0$, $u > 0$, $\theta \geq 0$ and $k \geq 0$ and

$$0 < \phi < \frac{\epsilon}{\gamma + \omega} \quad (5.7a)$$

$$\theta + \frac{u^2\epsilon\phi(\gamma + \omega)}{\Lambda(k + \phi)(\phi(\gamma + \omega) - \epsilon)(k(\gamma + \omega) + \epsilon)} = 0 \quad (5.7b)$$

When the toxicant is at a critical level where immunity is depleted at

$Q = \frac{1}{\xi_2}$, we expect $R_0 = 1$ when $\phi > 0$, $\epsilon > 0$, $\gamma \geq 0$, $\omega \geq 0$, $\Lambda > 0$, $u > 0$, $\theta \geq 0$ and $k \geq 0$ and

$$0 \leq \xi_1 < \xi_2 \quad (5.8a)$$

$$0 < \gamma < \frac{\epsilon(\xi_2 - \xi_1)}{\xi_2\phi} \quad (5.8b)$$

$$\theta + \frac{\gamma\xi_2^2 u^2 \epsilon \phi}{\Lambda(\gamma k + \epsilon)(k(\xi_2 - \xi_1) + \xi_2\phi)(\gamma\xi_2\phi + \epsilon(\xi_1 - \xi_2))} = 0 \quad (5.8c)$$

When these conditions are met, the term $1 - \xi_2 Q$ is equal to 0, which corresponds to the point at which immunity is depleted $Z = 0$.

No feasible within or between-host disease model

Figure 5.2 shows the baseline dynamics of the model under the absence of within-host (and consequently between-host) infection. The lethality of the toxicant linearly kills off the population of individuals in phase 0. Even though immune function is reduced, there is no parasite present to exploit and infect the population. After a threshold value, all individual hosts are dead and the population is extinct (phase V). This figure represents the baseline dynamics of the model under increasing toxicity and no infection.

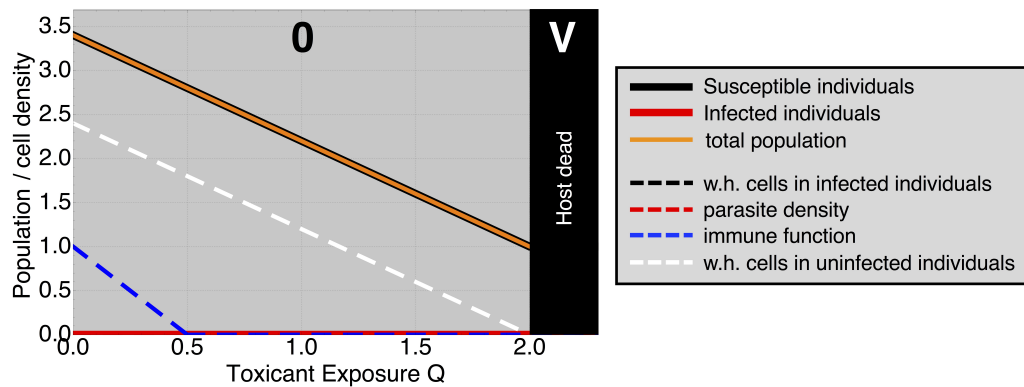


Figure 5.2: The baseline dynamics of the model without initial within-host infection. The absence of the within-host infection means that the infection cannot spread to the population level. Phase 0 corresponds to the region of no feasible infection and phase V corresponds to the death of all individuals within the population. Parameters as in Table 5.1, but with the initial parasite density $Y^* = 0$.

Dynamical phases of the population under increasing toxicant exposure

Figure 5.3 shows the predicted stage of the epidemic under increasing toxicant exposure according to the simulations of the model. In general, there are 5 separate phases present in the model, as defined below (outbreak is denoted by *).

Phase I: no population epidemic

For low exposure to toxicant, the basic reproduction number is low ($R_0 < 1$). This means that epidemics cannot occur at the population level. There is a very small within-host infection burden (Y^*) which increases as the

toxicant exposure increases. In this phase, the individual parasite burden is not large enough to cause between-host transmission and thus the population only declines a relatively small amount from the direct exposure to the toxicant.

Phase II^* : outbreak

Here, the toxicant level is increased beyond a critical threshold causing $R_0 > 1$ and outbreak at the population level. This threshold is determined by the relationship between the within-host immunity, parasite burden and healthy cell status, and the population rate of transmission (Eq. 5.5). This phase is characterised by a functioning but declining immune status, caused by the increasing toxicant exposure. Combined with a within-host parasite density reaching a peak at the end of phase II^* , we see an outbreak of population level infection, and healthy susceptibles reaching a minimum, while the total population decreases rapidly.

Phase III^* : disease reduced

Increasing the toxicant exposure further results in a complete depletion of the within-host immune status. The basic reproduction number of the infection begins to drop resulting in fewer infected cases and therefore an increase in healthy individuals. Infected individuals are killed off by the mortality induced by the epidemic. This higher level of toxicant exposure

causes the parasite density to drop below the minimum required for an infection to spread at the population level (determined by Eq. 5.6). This means that the total population is able to recover marginally due to the infection being removed.

Phase IV: disease controlled

At the start of phase IV, the population epidemic is over ($R_0 < 1$). As the toxicant exposure is increased again, the within-host parasite density decreases to 0. At these very high levels of exposure, the individuals are killed by the direct mortality inducing toxicant causing the population to decline once again.

Phase V: host dead

At extremely high levels of exposure the host is killed due to the lethality of the toxicant. All within-host functions are depleted. This results in the population reaching extinction.

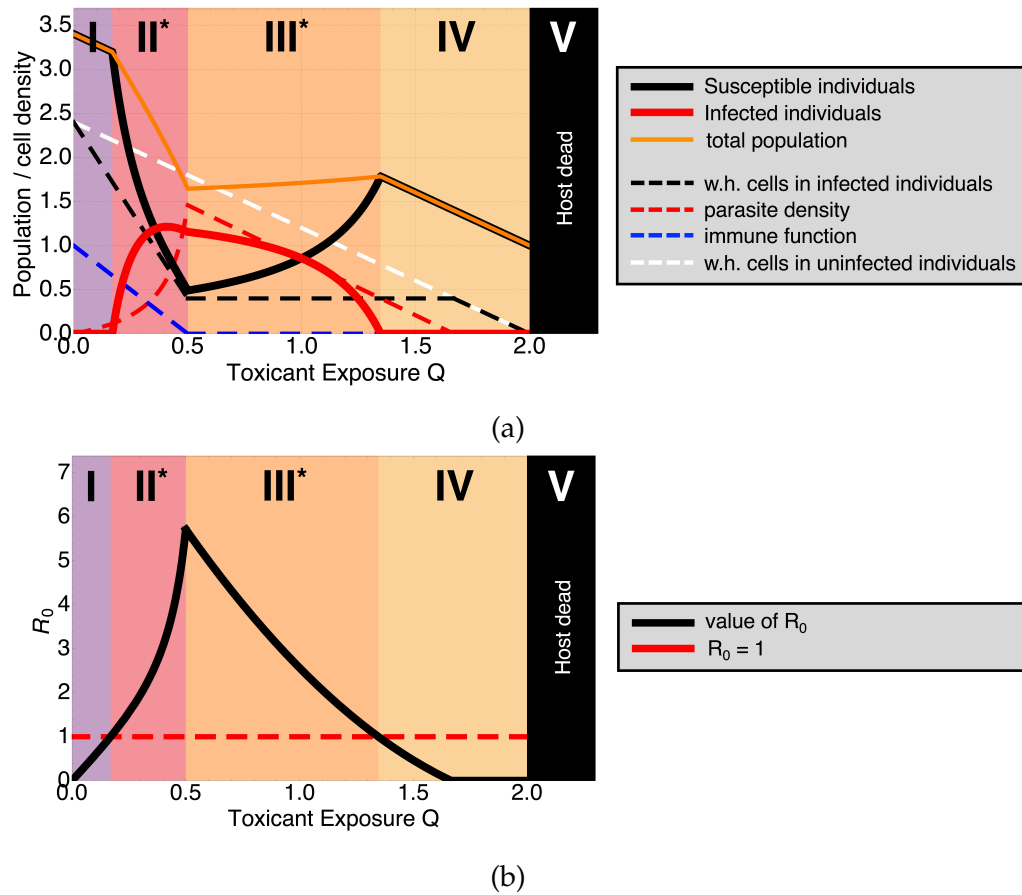


Figure 5.3: The predicted five phases of an infected population under increasing toxicant stress Q . Starred phases (II^* and III^*) represent the outbreak of infection where $R_0 > 1$. In (a) solid lines represent the population dynamics and dashed lines the within-host dynamics. In (b) the black line shows the value of R_0 and the dashed red line shows the threshold at which $R_0 = 1$ and above which outbreak will occur within the population. Parameters taken from Table 5.1.

Within-host parameter phase dependence

We outline the behaviour of the model for a wider range of parameters.

We do this to investigate how the tradeoffs between certain within- and between-host functions determine the subsequent population epidemic.

We define the phases as above, with phase 0 representing the region where

there is no feasible within-host or between-host disease.

Direct lethal effect ζ_1 and sublethal ζ_2 toxicant effect

Figure 5.4 shows the predicted phase of the population epidemic for 3 different levels of toxicant exposure, and for a range of lethal toxicant effect (relative to the production of new within-host cells) and sublethal toxicant effect (relative to the production of immunity). The white regions in Fig. 5.4 show the space in which the assumption $\zeta_2 < \zeta_1$ is broken. First, the absence of toxicant exposure ($Q = 0$) results in no such epidemic for any value of lethal and sublethal toxicant effect. Second, as the toxicant exposure is increased to an intermediate value ($Q=0.50$), outbreak (phase II^*) occurs when the toxicant has both sufficiently high lethal and high sublethal effect. Third, as the toxicant reaches high levels ($Q = 1.50$), the outcome of the outbreak can fall into any of the phases of epidemiology ($0 - V$), dependent upon the respective lethal and sublethal properties of the toxicant. Higher lethal and sublethal toxicant stress can result in the extinction of the population, whereas lower lethality and higher sublethal effects are required for outbreak (phases II^* and III^*).

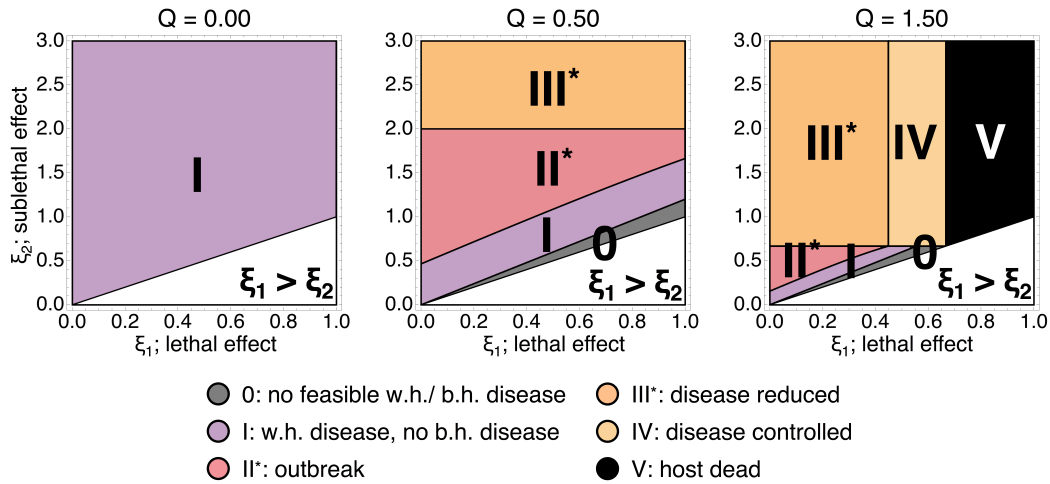


Figure 5.4: The predicted phase (0 – V) epidemiological outcome of the population level dynamics for 3 levels of toxicant exposure and varying direct lethal toxicant effect (relative to the production of new within-host cells) ξ_1 and sublethal effect (relative to the production of immunity) ξ_2 . Note that the white region represents the phase space under which the assumption $\xi_2 > \xi_1$ is no longer valid. Starred phases (II* and III*) represent the outbreak of infection within the population. For the absence of toxicant exposure $Q = 0$, outbreak cannot occur for any value of ξ_1 and ξ_2 . For intermediate $Q = 0.50$, outbreak occurs if the values of ξ_1 and ξ_2 are sufficiently large. For lethal $Q = 1.50$, any of the phases can occur dependent upon the choice of ξ_1 and ξ_2 . High values of ξ_1 and ξ_2 result in extinction of the population. Parameters as in Table 5.1, but for varying ξ_1 and ξ_2 as above.

Within-host transmission and production of cells (relative to removal of immunity) ϵ and between-host transmission θ

Figure 5.5 likewise shows the predicted phase for a range of different levels of ϵ and θ . In the absence of toxicant ($Q = 0$), outbreak can only occur (II*) if the within-host transmission and production of cells ϵ is sufficiently high. Otherwise, no epidemic can occur for any value of between-host transmission. Secondly as the toxicant is increased to an intermediate

value ($Q = 1.00$), the epidemic occurs (III^*) if both parameters are sufficiently large. Third, at extremely high levels of exposure ($Q = 2.00$), the population becomes extinct.

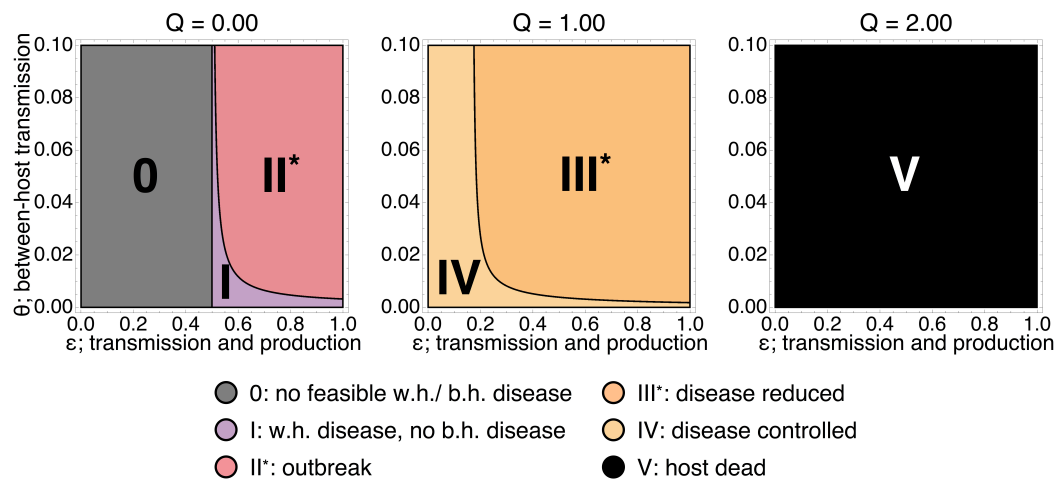


Figure 5.5: The dynamical phase (0 - V) for a range of within-host transmission and production of cells (relative to the removal of immunity) ϵ and between-host transmission θ . Starred phases (II^* and III^*) represent the outbreak of infection within the population. For $Q = 0$, outbreak will occur (II^*) if ϵ is sufficiently large, otherwise phase 0 will occur for any value of θ . For $Q = 1.00$, phase III^* occurs only if both ϵ and θ are large enough. For high $Q = 2.00$, population extinction occurs for any chosen values of ϵ and θ . Parameters as in Table 5.1, but for varying ϵ and θ .

Birth rate Λ and mortality rate u

Figure 5.6 shows the relationship between the between-host birth and death rates and the predicted stage of the epidemic. In the absence of toxicant exposure ($Q = 0$), there are 2 possible outcomes. A low death rate is required to see the outbreak of the disease. Otherwise between-host disease is not possible for any choice of Λ and u . Increasing the toxicant exposure to higher levels ($Q = 1.00$) results in a complete switch to either the

reduction or control of the disease. Finally, increasing the exposure to an extremely high level ($Q = 2.00$) results in host death and the extinction of the population.

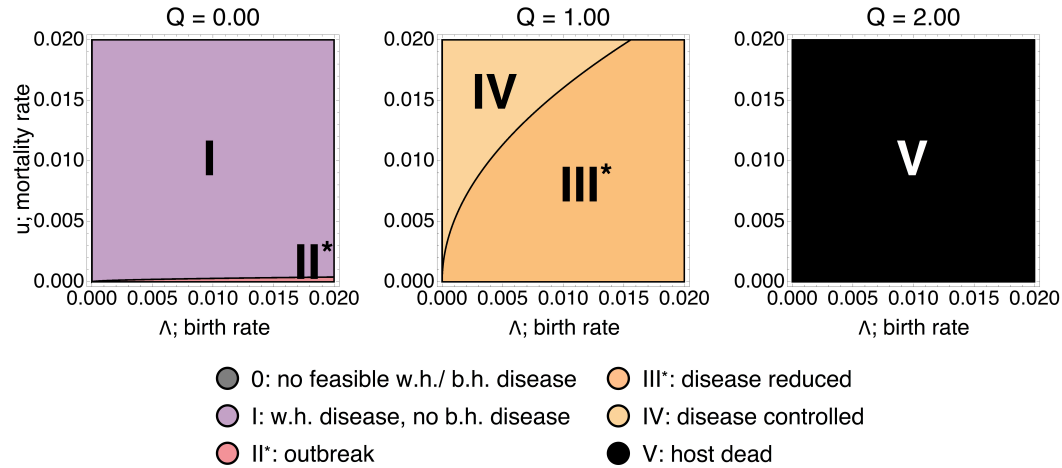


Figure 5.6: The predicted phase (0 - V) for a range of between-host birth rate Λ and between-host mortality u . Starred phases (II^* and III^*) represent the outbreak of infection within the population. For $Q = 0$, outbreak will occur (II^*) if u is sufficiently low. For $Q = 1.00$, either outbreak III^* occurs or phase IV occurs depending on the choice of Λ and u . For $Q = 2.00$, all hosts are dead and extinction of the population occurs. Parameters as in Table 5.1, but for varying transmission parameters Λ and u .

Absence of, and aggressive toxicant exposure

We explore the case of the absence of toxicant exposure ($\zeta_1 = 0$) in Fig. 5.7, and also the case of aggressive toxicant exposure (ζ_1 larger than ζ_2) in Fig. 5.8.

Setting the lethal toxicant exposure $\zeta_1 = 0$ (Fig. 5.7) results in similar phase based dynamics observed in Fig. 5.3. Under this condition, the first stages of the epidemic can be divided into phases I and II^* , qualita-

tively identical to those found in Fig. 5.3. However, after the host immune function is destroyed, a new phase III^*b occurs for any increasing value of toxicant. This results in a persistent epidemic caused by the lack of any lethal effects of the toxicant. In this case, the basic reproduction number remains constant for all further toxicant exposure. Therefore the low toxicant behaviour of the model is similar to the original, even after removing this lethal toxicant effect $\zeta_1 = 0$.

We set the lethal toxicant effect higher than the sublethal effect in Fig. 5.8. This is in order to examine the effect of reversing the assumption used throughout this paper ($\zeta_2 < \zeta_1$). We see that this alternative assumption predicts three phases of the epidemic which are broadly similar to those found in Fig. 5.3. The individual is highly infective to begin with and then the lethal toxicant effect begins to remove the within-host parasite density. After this, the population level infection is removed from the system, and the model returns back to phases IV and V seen in the original dynamical behaviour of the model.

Both of these figures highlight similar epidemiological phases of the model under different assumptions, and are sub-dynamics of the original dynamics found in Fig. 5.3.

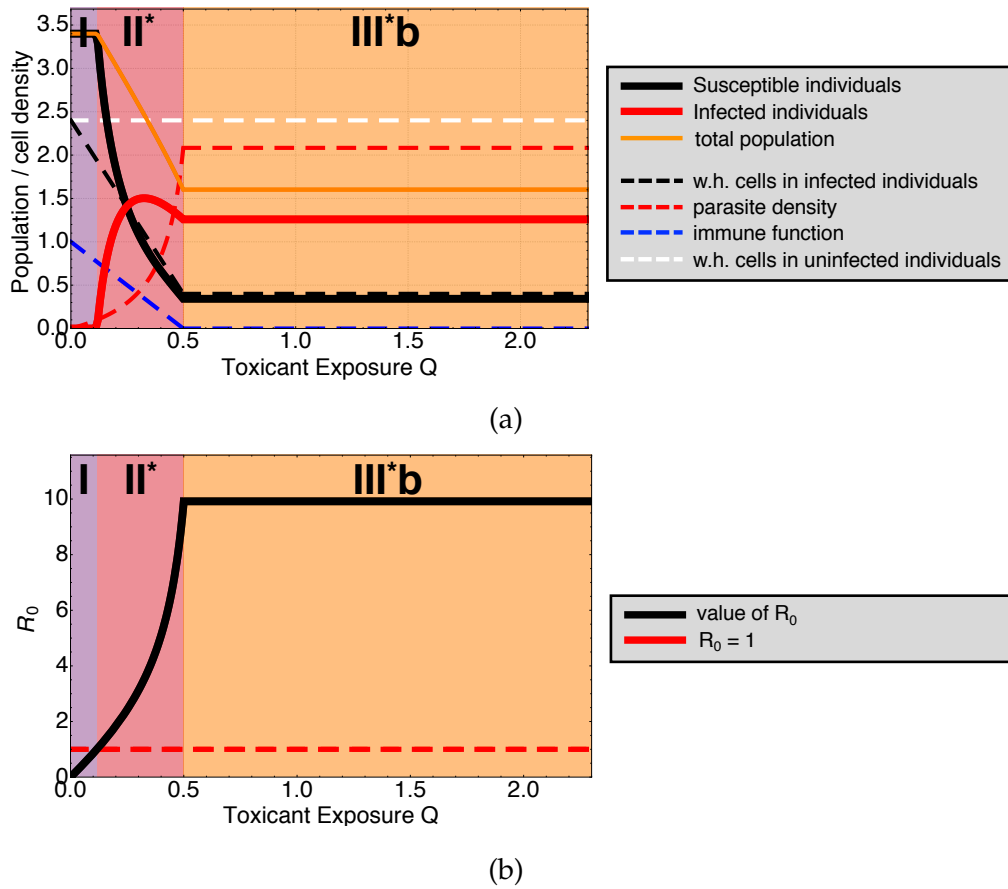


Figure 5.7: The predicted three phases of an infected population under increasing toxicant stress Q with no direct lethality of the toxicant $\zeta_1 = 0$. Starred phases (II^* and III^*b) represent the outbreak of infection where $R_0 > 1$. The individual remains highly infective in the absence of toxicant lethality. Parameters taken from Table 5.1 but with $\zeta_1 = 0$.

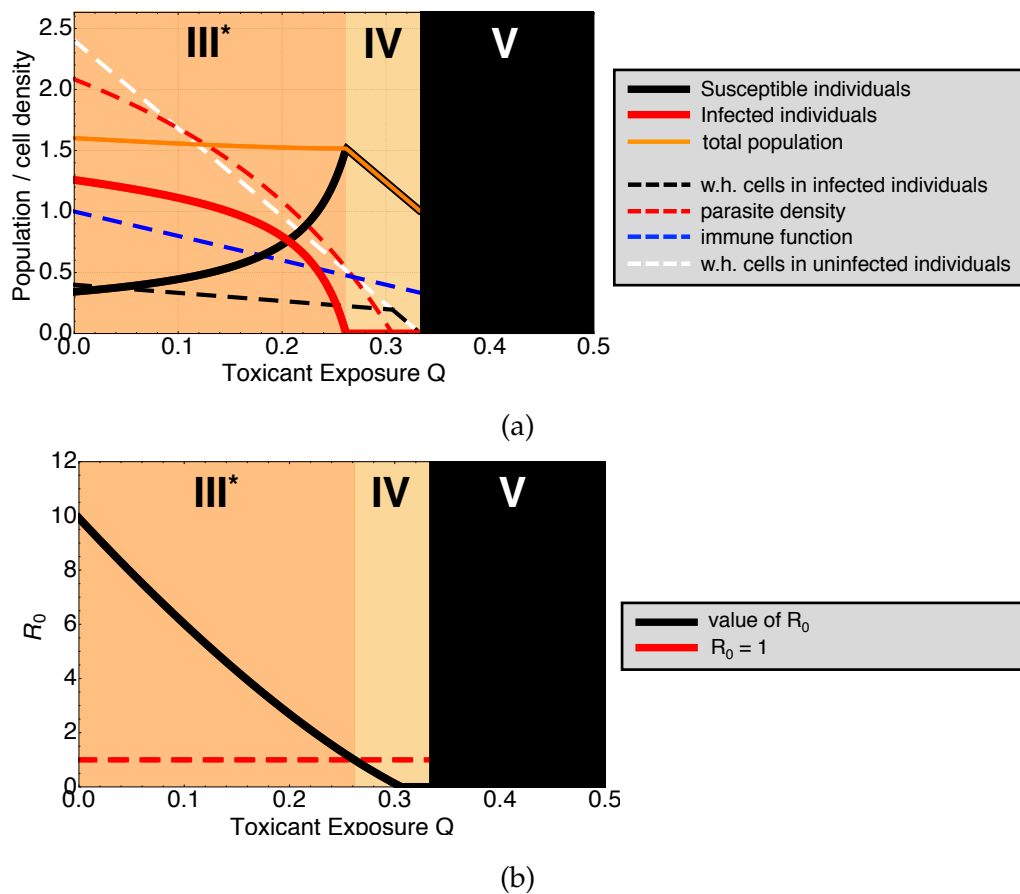


Figure 5.8: The predicted three phases of an infected population under increasing toxicant stress Q with a relatively aggressive lethal effect of the toxicant $\zeta_1 > \zeta_2$. Starred phase *III** represents the outbreak of infection where $R_0 > 1$. The individual is highly infective to begin with and then the aggressive toxicant effect removes the within-host parasite load which reduces the chance of infection at the population level. Parameters taken from Table 5.1 but $\zeta_1 = 3$, $\zeta_2 = 2$ and $\epsilon = 3$.

5.5 Discussion

We have studied and analysed a nested multi-level model of within and between-host processes to understand how toxicants impact epidemiological dynamics. A key finding is that population epidemics are dependent

upon the level of toxicant exposure. In general, infection prevalence is maximised by intermediate levels of toxicant. We classify this population epidemic into 5 phases showing that any outbreak is dependent on the toxicant's sublethal and lethal properties. Higher toxicant exposure results in either outbreak of infection or death of the population. In particular, the stress-mediated within-host statuses of immune function and parasite load also determine the outcome of the epidemic at the population level.

Importantly our model predicts that epidemics may not occur until reaching an intermediate threshold exposure of toxicant. At low levels of exposure, the parasite density is able to increase but between-host infection is equal to zero within the population until reaching a critical threshold (at the start of phase II^*). Sublethal toxicant exposure can have dramatic consequences for population epidemiology, causing widespread outbreak. These results support the body of work on synergistic interactions between environmental chemicals and natural stressors [5], and highlight the effects of toxicants on higher scales of organisation such as population dynamics, which are often not understood [20] or difficult to experimentally test [21].

Our model also predicts that population epidemics follow phase-based transitions dependent on the level of toxicant exposure. Within our model, 5 such phases are present. First, the parasite burden is too small within individuals to have any impact on the population level. Only when the parasite density crosses a minimum threshold (Eq. 5.6) do we see any pop-

ulation level impact. The immunosuppressive toxicant effect causes the parasite density to rapidly multiply and spread between individuals. Under increasing exposure, prevalence only subsides when the parasite is reduced by the lethal toxicant effect. The sublethal immunosuppressive effect of the toxicant only impacts the population if the toxicant exposure is low. Otherwise the lethality of the toxicant takes over and kills the host, causing extinction of the population. These complicated phase-based epidemics show that the effect of toxicant exposure upon population disease outbreak is non-linear. Interestingly, when considering the population density under increasing toxicant exposure we see a rapid decrease in the population in the early and late stages of this exposure. However, in phase *III**, we see a marginal increase in the density which represents population recovery. This is caused by a significant reduction in the epidemiological dynamics, and means that the healthy population is able to recover. This has implications for environmental assessors, where often the indicator of an ecosystem's healthy state is population density, rather than the individual clinical states of a system. Our results suggest that by only monitoring population density the underlying dynamics may go unnoticed, especially in the predicted mid-range toxicant phase *III**.

A further prediction the model makes is that tradeoffs between within- and between-host functions determine the subsequent population epidemiology (Fig. 5.4, Fig. 5.5 and Fig. 5.6). We show that outbreak will occur

when the individual sublethal toxicant effect is relatively higher than that of the lethal effect. Although we also predict that higher exposure to toxicants can result in any of the defined epidemiological phases. This suggests that population epidemiology can be completely determined by the relative sublethal and lethal properties of the toxicant. In addition, we also show that the sublethal toxicant effect determines whether the population will become extinct at high toxicant exposure. This further suggests that the individual properties of toxicants are important in determining outbreak. The tradeoff between different scales of transmission also determine these phase-based epidemics. In general, higher levels of both within- and between-host transmission result in outbreak. Another implication of these phase-based plots are that slight increases in parameters can result in sudden epidemiological switches. For example, the third panel in Fig. 5.4 shows all of the phases in our system. A slight increase in the sublethal effect ζ_2 at this high toxicant exposure $Q = 1.50$ can result in abrupt transitions between phase 0 or I to phase IV. These kind of transitions show that these phases of epidemiology are sensitive to slight perturbations in the effects of sublethal and lethal toxicant exposure. Introducing a new toxicant into a healthy population with only a slightly stronger sublethal effect on the host could cause a dramatic regime shift and ultimately high mortality rates (shift from phase I to phase IV).

The results in the main text of this paper depend entirely upon the rela-

tive sublethal and lethal effects of the toxicant, particularly on the assumption that $\zeta_2 > \zeta_1$. We focussed on this assumption for multiple reasons. If this assumption were reversed, the within-host model predicts unrealistically that the immune function will be present even after the host is dead. In Fig. 5.8 we show that under this reverse assumption, the results still fall into the phase based transitions seen under the normal assumption, and are sub-dynamics of the original phases shown in Fig 5.3. Another reason we focus on the case of $\zeta_2 > \zeta_1$ is because direct chronic lethality often occurs at higher doses of toxicant [13, 16, 17] and immunosuppressive damage occurs at various levels of lower dose toxicant exposure [180, 182, 212]. Therefore we argue that focussing on the case in which host mortality occurs at higher toxicant exposure and immunosuppressive damage occurs at lower, sublethal levels is biologically realistic.

These results have a number of applications, one such application being motivated by the impacts that toxicants have on a wide range non-target species [7, 9–12, 206–208]. For example, the recent and widespread losses in worldwide bee populations [10] are thought to be caused by multifactorial synergistic stressors [54, 75, 76, 176, 190]. Within this setting, this work fills a previously identified research gap [22] by outlining the complicated relationship between toxicant stress and population epidemics. In general, increased exposure to toxicants should result in more colony epidemics and therefore greater population losses. Intermediate exposure to toxicants

could result in dramatic decreases in overall colony health. Reducing the sublethal toxicant exposure below the predicted safe phase *I* threshold (to ensure $R_0 < 1$ in Eq. 5.5) ensures that no colony epidemic can occur. These results highlight the nonlinear relationship between pesticide exposure and population epidemiology. Indeed, the very general nature of this model means that these results may be applied to any disease ecology system exposed to toxicants.

The framework presented in this study focusses on linking two scales of biological organisation under toxicant stress. This toxicant stress affects the within-host dynamics in two ways, acting as an indirect immunosuppressant and directly impacting the vital functionality of individual health. However, we did not explicitly model the population-level toxicant effects. For example, pesticide exposure has been shown to impair foraging behaviour in bees, and increase forager mortality leading to reductions in brood production and overall colony success [165]. Investigating this additional route of stress within our framework would further clarify the role of toxicants in population-level processes. A further improvement to the model could investigate the role of social immunity, a process by which populations prevent infection from spreading. Social insects are known to perform behavioural traits such as removing diseased or dead individuals [202], preventing others from interacting with infected individuals [201], and collectively raising the temperature of the surrounding environment

through a process known as social fever [200], all in order to prevent further infection. Incorporating these social mechanisms into our nested multilevel modelling framework could shed new light on the way that populations use innate and social immunity to combat disease.

In summary, this work takes a multifactorial approach to model infection at the population level which can be divided into 5 phases dependent upon the level of toxicant stress. We predict that infection within populations is maximised by intermediate toxicant exposure, and that there exists a toxicant threshold below which individual parasite density is controlled and outbreak does not occur. The modelling framework used here presents a starting position to think about how within-host functions such as immunity and parasite density determine population level effects. This work highlights the need for experimental studies which focus on measuring epidemiological traits of populations under increasing toxicant exposure.

Chapter 6

Discussion

In this chapter we summarise the main findings of this thesis and discuss extensions and applications of these studies.

6.1 Summary

The objective of this thesis was to examine the effects of stressors on various ecological systems. We have found many results which are novel within the fields of stress ecology and eco-epidemiology, particularly in the context of honey bee colonies. We summarise the main findings of this thesis as:

- Sublethal stressors can cause the sudden collapse in populations of an important ecological species. Around a critical level of increasing stress, the presence of a saddle-node bifurcation causes irreversible consequences for populations of honey bee colonies (Chapter 2).

- Increasing levels of stress can be counteracted by regulatory functions of the individual species. For example, higher birth rates and altering the balance of age-structured division of labour can counteract the effects of stress (Chapter 2).
- Disease stressors acting through multiple routes of infection synergistically increase the levels of infection and contamination as compared to those diseases with only one route of transmission (Chapter 3).
- The interactions between multiple stressors are completely dependent upon the relative levels of each, and this relationship can be non-linear. For example, an interaction between toxicant and parasite is maximised by an intermediate level of toxicant, rather than simply linearly increasing. This occurs at both the within-host and between-host level (Chapters 4 and 5).
- The stress response of an organism can be divided into three phases dependent upon the level of increasing sublethal and lethal stressor exposure. These phases are also determined by the relationship between the within-host processes and the stressor (Chapter 4).
- Within a multi-stressor environment, the outbreak of infections at the population level are determined by the exposure to other abiotic stressors. There is a threshold exposure of stressor exposure under which epidemics will not occur (Chapter 5).

- The within-host statuses of individuals also determine the outcome of epidemics at the population level. The combination of within- and between-host dynamics result in five-phases of population epidemiology. These phases are determined by the balance of within- and between-host parameters and the exposure to stressors (Chapter 5).

6.2 Future work

There are many possible extensions to the modelling frameworks presented within this thesis. There are also various results contained here which have direct implications for future experimental work. We suggest various streams of research which could be conducted arising from the results contained within this thesis.

The bistability caused by sublethal stressors present in Chapter 2 opens up the possibility of using early warning signals (EWS) to track honey bee colony collapse and predict the period leading up to a critical transition. In recent years, the field of EWS has been used to understand the underlying dynamics of ecological systems and predict critical threshold tipping points of dynamical systems [216]. If increasing sublethal stress can cause these sudden collapses of honey bee colonies (Chapter 2), then we should be able to forecast and prevent such collapses from occurring by using EWS methods. However, in order to track these EWS, we need high-resolution

data from both before and after the critical transition (colony collapse), to avoid potential false negatives and confirm that the EWS framework is indeed predicting colony collapse accurately. As to this date, no such dataset exists, although some track continuous hive weight data [217], which could be used as a measure of overall colony function and therefore used to track EWS. We suggest that an empirical dataset of various honey bee colony functions (weight of the hive, temperature, brood/food storage) is collected. This data needs to be temporal, high-resolution and crucially needs to monitor those dynamics of a normal hive in comparison to that of a colony undergoing colony collapse disorder or other sudden changes in dynamical behaviour. The potential implications of such a dataset combined with the applications of EWS and our model framework are wide-spanning and may prove valuable to honey bee conservation. For example, real-time tracking data combined with a EWS toolbox interface could provide apiculturists with updates about the health of their colonies and potential warnings of imminent collapse.

We made several simplifications in Chapter 2 in order to divide the honey bee hive into distinct compartments, appropriate for modelling. However, we only divided the population into two: the within-hive adults and forager classes. While these two distinct classes capture the difference between mortality rates and behaviour in foragers and within-hive adult bees [89], the hive is actually intricately divided into many such classes

[83]. For example, dedicated bees will clean and feed the inner hive and receiver honey bees receive, pack and store nectar [112]. Including the dynamics of more classes of honey bee could help understand how these additional regulatory processes are affected by stress, and how they contribute to overall colony dynamics.

Within this thesis we mostly did not consider the effects of seasonality, instead only concentrating on this aspect in Chapter 3. It has been shown that honey bee health depends upon the season [74, 111, 134] and honey bee population levels normally fluctuate with the time of year [137]. We suggest extending the framework provided in Chapter 2 to include seasonal effects on important regulatory functions of the hive, in order to examine how this determines overall colony health and the presence of sudden critical transitions. We also suggest extending the frameworks provided in Chapters 4 and 5 to include seasonal effects, particularly to investigate the effects this has on both the within- and between-host epidemiology. The results from Chapter 3 and other modelling studies including honey bee seasonality [94, 99] highlight the importance of including such seasonal effects within theoretical work.

Within Chapter 4 and 5 we made assumptions about the way in which toxicant stress affects the host organism, namely that it reduces the functionality of the immune system (see [180–185, 194–196]) and is lethally toxic at high enough exposure, damaging vital functions of the host rather than

killing individual cells (see [13, 14, 16, 17]). An alternative assumption is entirely possible based upon toxicant acting through a density-dependence on immunity and direct cell damage. We briefly touch upon this assumption in Appendix C, which yields similar results (Figure C3) to the original model contained within Chapter 4. Although the within-host parasite dynamics are relatively unchanged by this density dependence assumption, the effects that this could have on the population level are unknown. We suggest that further work should apply these within-host density dependent stressor assumptions within a population level framework in order to clarify that we obtain the same phase-based epidemiology found in Chapter 5.

Another important biological mechanism that we did not consider in this thesis is social immunity. The process of social immunity is crucial in defending organisms such as eusocial insects against infection. Social insects remove dead or diseased conspecifics [202] which removes a potential source of infection [201], and perform other behavioural traits such as increasing the internal temperature of the environment to kill parasites [200]. Chapters 4 and 5 only include strict innate within-host immunity, but we suggest incorporating the effects of social immunity into this framework, due to the central role it plays within immune defence mechanisms particularly in social insect colonies [218]. The role of social immunity relative to direct innate immunity in combatting infection within populations

is unknown, especially when combined with a multi-stressors framework. Future work should incorporate both aspects of immunity and their implications for population dynamics and epidemiology.

Bibliography

- [1] RD Booton, Y Iwasa, JAR Marshall, and DZ Childs. Stress-mediated Allee effects can cause the sudden collapse of honey bee colonies. *J. Theor. Biol.*, 420:213–219, 2017.
- [2] RD Booton, R Yamaguchi, JAR Marshall, DZ Childs, and Y Iwasa. Interactions between immunotoxicants and parasite stress: implications for host health. *J. Theor. Biol.*, 445:120–127, 2018.
- [3] NMV Straalen. Peer reviewed: ecotoxicology becomes stress ecology. *Environ. Sci. Technol.*, 37(17):324A–330A, 2003.
- [4] A Sih, AM Bell, and JL Kerby. Two stressors are far deadlier than one. *Trends Ecol. Evol.*, 19(6):274–276, 2004.
- [5] M Holmstrup, AM Bindsbøl, GJ Oostingh, A Duschl, V Scheil, HR Köhler, S Loureiro, AMVM Soares, ALG Ferreira, C Kienle, A Gerhardt, R Laskowski, PE Kramarz, M Bayley, C Svendsen, and DJ Spurgeon. Interactions between effects of environmental chemicals and natural stressors: a review. *Sci. Total Environ.*, 408(18):3746–3762, 2010.
- [6] R Truhaut. Ecotoxicology: Objectives, principles and perspectives. *Ecotoxicol. Environ. Saf.*, 1(2):151–173, 1977.

- [7] R Relyea and J Hoverman. Assessing the ecology in ecotoxicology: A review and synthesis in freshwater systems. *Ecol. Lett.*, 9(10):1157–1171, 2006.
- [8] A Elbert, M Haas, B Springer, W Thielert, and R Nauen. Applied aspects of neonicotinoid uses in crop protection. *Pest Manag. Sci.*, 64:1099–1105, 2008.
- [9] LW Pisa, V Amaral-Rogers, LP Belzunces, JM Bonmatin, CA Downs, D Goulson, DP Kreuzweiser, C Krupke, M Liess, M McField, CA Morrissey, DA Noome, J Settele, N Simon-Delso, JD Stark, JP Van der Sluijs, H Van Dyck, and M Wiemers. Effects of neonicotinoids and fipronil on non-target invertebrates. *Environ. Sci. Pollut. Res.*, 22:68–102, 2015.
- [10] D Goulson, E Nicholls, C Botías, and EL Rotheray. Bee declines driven by combined stress from parasites, pesticides, and lack of flowers. *Science*, 347:1255957, 2015.
- [11] CT Eason, EC Murphy, GRG Wright, and EB Spurr. Assessment of risks of brodifacoum to non-target birds and mammals in New Zealand. *Ecotoxicology*, 11(1):35–48, 2002.
- [12] GL Phipps and GW Holcombe. A method for aquatic multiple species toxicant testing: Acute toxicity of 10 chemicals to 5 vertebrates and 2 invertebrates. *Environ. Pollut. A*, 38(2):141–157, 1985.
- [13] S Suchail, D Guez, and LP Belzunces. Discrepancy between acute and chronic toxicity induced by imidacloprid and its metabolites in *Apis mellifera*. *Environ. Toxicol. Chem.*, 20(11):2482–2486, 2001.
- [14] T Iwasa, N Motoyama, JT Ambrose, and RM Roe. Mechanism for the differential toxicity of neonicotinoid insecticides in the honey bee, *Apis mellifera*. *Crop Prot.*, 23:371–378, 2004.

- [15] T Blacqui re, G Smaghe, CA Van Gestel, and V Mommaerts. Neonicotinoids in bees: a review on concentrations, side-effects and risk assessment. *Ecotoxicology*, 21(4):973–992, 2012.
- [16] H Pan, Y Liu, B Liu, Y Lu, X Xu, X Qian, K Wu, and N Desneux. Lethal and sublethal effects of cycloxaprid, a novel cis-nitromethylene neonicotinoid insecticide, on the mirid bug *Apolygus lucorum*. *J. Pest. Sci.*, 87(4):731–738, 2014.
- [17] R Wang, W Zhang, W Che, C Qu, F Li, N Desneux, and C Luo. Lethal and sublethal effects of cyantraniliprole, a new anthranilic diamide insecticide, on *Bemisia tabaci* (Hemiptera: Aleyrodidae) MED. *Crop Prot.*, 91:108–113, 2017.
- [18] A Decourtye, E Lacassie, and MH Pham-Del gue. Learning performances of honeybees (*Apis mellifera* L) are differentially affected by imidacloprid according to the season. *Pest Manag. Sci.*, 59:269–278, 2003.
- [19] SM Williamson and GA Wright. Exposure to multiple cholinergic pesticides impairs olfactory learning and memory in honeybees. *J. Exp. Biol.*, 216:1799–1807, 2013.
- [20] HR Kohler and R Triebskorn. Wildlife ecotoxicology of pesticides: can we track effects to the population level and beyond? *Science*, 341:759–765, 2013.
- [21] A Gergs, A Zenker, V Grimm, and TG Preuss. Chemical and natural stressors combined: from cryptic effects to population extinction. *Sci. Rep.*, 3:2036, 2013.
- [22] O Lundin, M Rundl f, HG Smith, I Fries, and R Bommarco. Neonicotinoid insecticides and their impacts on bees: A systematic review of research approaches and identification of knowledge gaps. *PLOS ONE*, 10:e0136928, 2015.
- [23] S Bhattacharya and M Martcheva. An immuno-eco-epidemiological model of competition. *J. Biol. Dyn.*, 10(1):314–341, 2016.

- [24] BJ Brosi, KS Delaplaine, M Boots, and JC de Roode. Ecological and evolutionary approaches to managing honey bee disease. *Nat Ecol Evol*, 1(9):1250–1262, 2017.
- [25] BC Sheldon and S Verhulst. Ecological immunology: Costly parasite defences and trade-offs in evolutionary ecology. *Trends in Ecology and Evolution*, 11(8):317–321, 1996.
- [26] CL Folt, YC Chen, MV Moore, and J Burnaford. Synergism and antagonism among multiple stressors. *Limnol. Oceanogr.*, 44(3):864–877, 1999.
- [27] A Coors and L De Meester. Synergistic, antagonistic and additive effects of multiple stressors: Predation threat, parasitism and pesticide exposure in *Daphnia magna*. *J. Appl. Ecol.*, 45(6):1820–1828, 2008.
- [28] WO Kermack and AG McKendrick. A contribution to the mathematical theory of epidemics. *Proc. Royal Soc. A*, 115(772):700–721, 1927.
- [29] F. Brauer and C. Castillo-Chavez. *Mathematical models in population biology and epidemiology*, volume 40. Springer, New York, 2012.
- [30] RM Anderson and RM May. Population biology of infectious diseases: Part I. *Nature*, 280(5721):361–367, 1979.
- [31] RM May and RM Anderson. Population biology of infectious diseases: Part II. *Nature*, 280(5722):455–461, 1979.
- [32] HW Hethcote. The mathematics of infectious diseases. *SIAM Review*, 42(4):599–653, 2000.
- [33] M Nowak and RM May. *Virus dynamics: mathematical principles of immunology and virology: mathematical principles of immunology and virology*. Oxford Univ. Press, UK, 2000.

- [34] AS Perelson. Modelling viral and immune system dynamics. *Nat. Rev. Immunol.*, 2(1):28–36, 2002.
- [35] MA Nowak and CRM Bangham. Population dynamics of immune responses to persistent viruses. *Science*, 272(5258):74–79, 1996.
- [36] GI Marchuk, RV Petrov, AA Romanyukha, and GA Bocharov. Mathematical model of antiviral immune response. I. Data analysis, generalized picture construction and parameters evaluation for hepatitis B. *J. Theor. Biol.*, 151(1):1–40, 1991.
- [37] GA Bocharov and AA Romanyukha. Mathematical model of antiviral immune response III. Influenza A virus infection. *J. Theor. Biol.*, 167(4):323–360, 1994.
- [38] F Nazzi, SP Brown, D Annoscia, F Del Piccolo, G Di Prisco, P Varricchio, GD Vedova, F Cattonaro, E Caprio, and F Pennacchio. Synergistic parasite-pathogen interactions mediated by host immunity can drive the collapse of honeybee colonies. *PLOS Pathog.*, 8(6):e1002735, 2012.
- [39] M Gilchrist and A Sasaki. Modeling host-parasite coevolution: a nested approach based on mechanistic models. *J. Theor. Biol.*, 218(3):289–308, 2002.
- [40] N Mideo, S Alizon, and T Day. Linking within- and between-host dynamics in the evolutionary epidemiology of infectious diseases. *Trends Ecol. Evol.*, 23(9):511–517, 2008.
- [41] Z Feng, J Velasco-Hernandez, B Tapia-Santos, and MCA Leite. A model for coupling within-host and between-host dynamics in an infectious disease. *Nonlinear Dyn.*, 68(3):401–411, 2012.
- [42] S Alizon and M van Baalen. Emergence of a convex trade-off between transmission and virulence. *Am. Nat.*, 165(6):E155–E167, 2005.

- [43] MA Gilchrist and D Coombs. Evolution of virulence: Interdependence, constraints, and selection using nested models. *Theor. Popul. Biol.*, 69(2):145–153, 2006.
- [44] Z Feng, J Velasco-Hernandez, and B Tapia-Santos. A mathematical model for coupling within-host and between-host dynamics in an environmentally-driven infectious disease. *Math. Biosci.*, 241(1):49–55, 2013.
- [45] Z Feng, X Cen, Y Zhao, and J Velasco-Hernandez. Coupled within-host and between-host dynamics and evolution of virulence. *Math. Biosci.*, 270:204–212, 2015.
- [46] KV Lee, N Steinhauer, K Rennich, ME Wilson, DR Tarpy, DM Caron, R Rose, KS Delaplane, K Baylis, EJ Lengerich, J Pettis, JA Skinner, JT Wilkes, R Sagili, and D VanEngelsdorp. A national survey of managed honey bee 2013-2014 annual colony losses in the USA. *Apidologie*, 46(3):292–305, 2015.
- [47] AM Klein, BE Vaissière, JH Cane, I Steffan-Dewenter, SA Cunningham, C Kremen, and T Tscharntke. Importance of pollinators in changing landscapes for world crops. *Proc. R. Soc. Lond., B, Biol. Sci.*, 274(1608):303–313, 2007.
- [48] B Dainat, JD Evans, YP Chen, L Gauthier, and P Neumann. Predictive markers of honey bee colony collapse. *PLOS ONE*, 7(2):e32151, 2012.
- [49] N Gallai, JM Salles, J Settele, and BE Vaissière. Economic valuation of the vulnerability of world agriculture confronted with pollinator decline. *Ecol. Econ.*, 68:810–821, 2009.
- [50] RM Goodwin, HM Cox, MA Taylor, LJ Evans, and HM McBrydie. Number of honey bee visits required to fully pollinate white clover (*Trifolium repens*) seed crops in Canterbury, New Zealand. *New Zeal. J. Crop. Hort.*, 39(1):7–19, 2011.
- [51] RR Rucker, WN Thurman, and M Burgett. Honey bee pollination markets and the internalization of reciprocal benefits. *Am. J. Agric. Econ.*, 94(4):956–977, 2012.

- [52] G Allen-Wardell, P Bernhardt, R Bitner, A Burquez, S Buchmann, and J Cane. The potential consequences of pollinator declines on the conservation of biodiversity and stability of food crop yields. *Conserv. Biol.*, 12(1):8–17, 1998.
- [53] JC Biesmeijer, SPM Roberts, and M Reemer. Parallel declines in pollinators and insect-pollinated plants in Britain and the Netherlands. *Science*, 313(5785):351–354, 2006.
- [54] SG Potts, JC Biesmeijer, and C Kremen. Global pollinator declines: trends, impacts and drivers. *Trends Ecol. Evol.*, 25:345–353, 2010.
- [55] LA Burkle, JC Marlin, and TM Knight. Plant-pollinator interactions over 120 years: loss of species, co-occurrence, and function. *Science*, 339(6127):1611–1615, 2013.
- [56] D VanEngelsdorp, D Cox Foster, and M Frazier. Fall-dwindle disease: Investigations into the causes of sudden and alarming colony losses experienced by beekeepers in the fall of 2006. Preliminary report: First revision. *Pennsylvania Department of Agriculture*, 2006.
- [57] D VanEngelsdorp, J Hayes Jr., RM Underwood, D Caron, and J Pettis. A survey of managed honey bee colony losses in the USA, fall 2009 to winter 2010. *J. Apic. Res.*, 50(1):1–10, 2011.
- [58] M Henry, M Beguin, F Requier, and O Rollin. A common pesticide decreases foraging success and survival in honey bees. *Science*, 336(6079):348–350, 2012.
- [59] PL Dai, Q Wang, JH Sun, and F Liu. Effects of sublethal concentrations of bifenthrin and deltamethrin on fecundity, growth, and development of the honeybee *Apis mellifera ligustica*. *Environ. Toxicol. Chem.*, 29(3):644–649, 2010.
- [60] A Decourtye and J Devillers. Comparative sublethal toxicity of nine pesticides on

- olfactory learning performances of the honeybee *Apis mellifera*. *Arch. Environ. Contam. Toxicol.*, 48(2):242–250, 2005.
- [61] AC Highfield, A El Nagar, LCM Mackinder, LMLJ Noël, MJ Hall, SJ Martin, and DC Schroeder. Deformed wing virus implicated in overwintering honeybee colony losses. *Appl. Environ. Microbiol.*, 75(22):7212–7220, 2009.
- [62] JJ Bromenshenk, CB Henderson, CH Wick, MF Stanford, AW Zulich, RE Jabbour, SV Deshpande, PE McCubbin, RA Seccomb, PM Welch, T Williams, DR Firth, E Skowronski, MM Lehmann, SL Bilimoria, J Gress, KW Wanner, and RA Cramer. Iridovirus and microsporidian linked to honey bee colony decline. *PLOS ONE*, 5(10):e13181, 2010.
- [63] C Runckel, ML Flenniken, JC Engel, JG Ruby, D Ganem, R Andino, and JL DeRisi. Temporal analysis of the honey bee microbiome reveals four novel viruses and seasonal prevalence of known viruses, *Nosema*, and *Crithidia*. *PLOS ONE*, 6(6):e20656, 2011.
- [64] J Moore, A Jironkin, D Chandler, N Burroughs, DJ Evans, and EV Ryabov. Recombinants between Deformed wing virus and *Varroa destructor* virus-1 may prevail in *Varroa destructor*-infested honeybee colonies. *J. Gen. Virol.*, 92(1):156–161, 2011.
- [65] KA Aronstein and KD Murray. Chalkbrood disease in honey bees. *J. Invertebr. Pathol.*, 103:S20–S29, 2010.
- [66] I Fries. *Nosema ceranae* in European honey bees (*Apis mellifera*). *Journal of Invertebrate Pathology*, 103:S73–S79, 2010.
- [67] RJ Paxton. Does infection by *Nosema ceranae* cause "Colony Collapse Disorder" in honey bees (*Apis mellifera*). *J. Apic. Res.*, 49(1):80–84, 2010.

- [68] M Higes and A Meana. *Nosema ceranae* (Microsporidia), a controversial 21st century honey bee pathogen. *Environ. Microbiol. Rep.*, 5(1):17–29, 2013.
- [69] JD Evans and RS Schwarz. Bees brought to their knees: microbes affecting honey bee health. *Trends Microbiol.*, 19(12):614–620, 2011.
- [70] F Eischen. Overwintering performance of honey bee colonies heavily infested with *Acarapis woodi*. *Apidologie*, 18(4):293–304, 1987.
- [71] D Sammataro, U Gerson, and G Needham. Parasitic mites of honey bees: life history, implications, and impact. *Annu. Rev. Entomol.*, 45(1):519–548, 2000.
- [72] SF Pernal and RW Currie. The influence of pollen quality on foraging behavior in honeybees (*Apis mellifera* L.). *Behav. Ecol. Sociobiol.*, 51(1):53–68, 2001.
- [73] C Alaux, F Ducloz, D Crauser, and Y Le Conte. Diet effects on honeybee immunocompetence. *Biol. Lett.*, 6:562–565, 2010.
- [74] HR Mattila and GW Otis. Dwindling pollen resources trigger the transition to broodless populations of long-lived honeybees each autumn. *Ecol. Entomol.*, 32(5):496–505, 2007.
- [75] FLW Ratnieks and NL Carreck. Clarity on honey bee collapse? *Science*, 327(5962):152–153, 2010.
- [76] AJ Vanbergen. Threats to an ecosystem service: pressures on pollinators. *Front. Ecol. Environ.*, 11(5):251–259, 2013.
- [77] RM Francis, SL Nielsen, and P Kryger. *Varroa*-virus interaction in collapsing honey bee colonies. *PLOS ONE*, 8(3):e57540, 2013.
- [78] ED Pilling and PC Jepson. Synergism between EBI fungicides and a pyrethroid insecticide in the honeybee (*Apis mellifera*). *Pestic. Sci.*, 39(4):293–297, 1993.

- [79] RM Johnson, HS Pollock, and MR Berenbaum. Synergistic interactions between in-hive miticides in *Apis mellifera*. *J. Econ. Entomol.*, 102(2):474–479, 2009.
- [80] RM Johnson, L Dahlgren, BD Siegfried, and MD Ellis. Acaricide, fungicide and drug interactions in honey bees (*Apis mellifera*). *PLOS ONE*, 8(1):e54092, 2013.
- [81] JY Wu, CM Anelli, and WS Sheppard. Sub-lethal effects of pesticide residues in brood comb on worker honey bee (*Apis mellifera*) development and longevity. *PLOS ONE*, 6(2):e14720, 2011.
- [82] JS Pettis, J Johnson, and G Dively. Pesticide exposure in honey bees results in increased levels of the gut pathogen *Nosema*. *Naturwissenschaften*, 99(2):153–158, 2012.
- [83] GE Robinson. Regulation of division of labor in insect societies. *Annu. Rev. Entomol.*, 37(1):637–665, 1992.
- [84] PK Visscher. The honey bee way of death: necrophoric behaviour in *Apis mellifera* colonies. *Animal Behav.*, 31(4):1070–1076, 1983.
- [85] M Winston. *The biology of the honey bee*. Harvard University Press, 1991.
- [86] NH Fefferman and PT Starks. A modeling approach to swarming in honey bees (*Apis mellifera*). *Insectes Soc.*, 53(1):37–45, 2006.
- [87] BR Johnson. Organization of work in the honeybee: a compromise between division of labour and behavioural flexibility. *Proc. R. Soc. Lond., B, Biol. Sci.*, 270(1511):147–152, 2003.
- [88] ZY Huang and GE Robinson. Regulation of honey bee division of labor by colony age demography. *Behav. Ecol. Sociobiol.*, 39(3):147–158, 1996.

- [89] TD Seeley. *The wisdom of the hive: the social physiology of honey bee colonies*. Harvard University Press, 1995.
- [90] A Neukirch. Dependence of the life span of the honeybee (*Apis mellifica*) upon flight performance and energy consumption. *J. Comp. Physiol. A*, 146(1):35–40, 1982.
- [91] PK Visscher and R Dukas. Survivorship of foraging honey bees. *Insectes Soc.*, 44(1):1–5, 1997.
- [92] DS Khoury, MR Myerscough, and AB Barron. A quantitative model of honey bee colony population dynamics. *PLOS ONE*, 6(4):e18491, 2011.
- [93] DS Khoury, AB Barron, and MR Myerscough. Modelling food and population dynamics in honey bee colonies. *PLOS ONE*, 8(5):e59084, 2013.
- [94] S Russell, AB Barron, and D Harris. Dynamic modelling of honey bee (*Apis mellifera*) colony growth and failure. *Ecol. Model.*, 265:158–169, 2013.
- [95] B Dennis and WP Kemp. How hives collapse: Allee effects, ecological resilience, and the honey bee. *PLOS ONE*, 11(2):e0150055, 2016.
- [96] J Bryden, RJ Gill, RAA Mitton, NE Raine, and VAA Jansen. Chronic sublethal stress causes bee colony failure. *Ecol. Lett.*, 16(12):1463–1469, 2013.
- [97] C Kribs-Zaleta and C Mitchell. Modeling colony collapse disorder in honeybees as a contagion. *Math. Biosci. Eng.*, 11(6):1275–1294, 2014.
- [98] EO Jatulan, JF Rabajante, CGB Banaay, AC Fajardo, and EC Jose. A mathematical model of intra-colony spread of American foulbrood in European honeybees (*Apis mellifera* L.). *PLOS ONE*, 10(12):e0143805, 2015.

- [99] V Ratti, PG Kevan, and HJ Eberl. A mathematical model of the honeybee-Varroa destructor-acute Bee paralysis virus system with seasonal effects. *Bull. Math. Bio.*, 77(8):1493–1520, 2015.
- [100] C Lu, KM Warchol, and RA Callahan. In situ replication of honey bee colony collapse disorder. *Bull. Insectology*, 65(1):99–106, 2012.
- [101] JP Staveley, SA Law, A Fairbrother, and CA Menzie. A causal analysis of observed declines in managed honey bees (*Apis mellifera*). *Hum. Ecol. Risk Assess.*, 20(2):566–591, 2014.
- [102] L Bortolotti, R Montanari, J Marcelino, P Medrzycki, S Maini, and C Porrini. Effects of sub-lethal imidacloprid doses on the homing rate and foraging activity of honey bees. *Bull. Insectology*, 56(1):63–67, 2003.
- [103] D VanEngelsdorp, JD Evans, C Saegerman, C Mullin, E Haubruge, BK Nguyen, M Frazier, J Frazier, D Cox-Foster, Y Chen, R Underwood, DR Tarpy, and JS Pettis. Colony collapse disorder: a descriptive study. *PLOS ONE*, 4(8):e6481, 2009.
- [104] MD Allen and EP Jeffree. The influence of stored pollen and of colony size on the brood rearing of honeybees. *Ann. Appl. Biol.*, 44(4):649–656, 1956.
- [105] JR Harbo. Effect of population size on brood production, worker survival and honey gain in colonies of honeybees. *J. Apic. Res.*, 25(1):22–29, 1986.
- [106] D Cramp. *A practical manual of beekeeping*. Spring Hill, 2008.
- [107] SE Fahrback and GE Robinson. Juvenile hormone, behavioral maturation, and brain structure in the honey bee. *Dev. Neurosci.*, 18(1-2):102–114, 1996.
- [108] SM Shehata, GF Townsend, and Shuel RW. Seasonal physiological changes in queen and worker honeybees. *J. Apic. Res.*, 20(2):69–78, 1981.

- [109] JA Kefuss. The influence of photoperiod on the flight activity of honeybees. *J. Apic. Res.*, 17(3):137–151, 1978.
- [110] EC Yang, YC Chuang, YL Chen, and LH Chang. Abnormal foraging behavior induced by sublethal dosage of imidacloprid in the honey bee (Hymenoptera: Apidae). *J. Econ. Entomol.*, 101(6):1743–1748, 2008.
- [111] T D Seeley. *Honeybee ecology: a study of adaptation in social life*. Princeton University Press, 1985.
- [112] FLW Ratnieks and C Anderson. Task partitioning in social insects. *Insectes Soc.*, 46(2):95–108, 1999.
- [113] TD Seeley, S Kühnholz, and A Weidenmüller. The honey bee’s tremble dance stimulates additional bees to function as nectar receivers. *Behav. Ecol. Sociobiol.*, 39(6):419–427, 1996.
- [114] JG Venegas, T Winkler, G Musch, MF Vidal Melo, D Layfield, N Tgavalekos, AJ Fischman, RJ Callahan, G Bellani, and RS Harris. Self-organized patchiness in asthma as a prelude to catastrophic shifts. *Nature*, 434(7034):777–782, 2005.
- [115] B Litt, R Esteller, J Echaz, M D’Alessandro, R Shor, T Henry, P Pennell, C Epstein, R Bakay, M Dichter, and G Vachtsevanos. Epileptic seizures may begin hours in advance of clinical onset: a report of five patients. *Neuron*, 30(1):51–64, 2001.
- [116] PE McSharry, LA Smith, and L Tarassenko. Prediction of epileptic seizures: are nonlinear methods relevant? *Nat. Med.*, 9(3):241–242, 2003.
- [117] RM May, SA Levin, and G Sugihara. Complex systems: ecology for bankers. *Nature*, 451(7181):893–895, 2008.

- [118] M Scheffer, S Carpenter, JA Foley, C Folke, and B Walker. Catastrophic shifts in ecosystems. *Nature*, 413(6856):591–6, 2001.
- [119] C Folke, S Carpenter, B Walker, M Scheffer, T Elmqvist, L Gunderson, and CS Holling. Regime shifts, resilience, and biodiversity in ecosystem management. *Annu. Rev. Ecol. Evol. Syst.*, 35(1):557–581, 2004.
- [120] J Bascompte, P Jordano, and JM Olesen. Asymmetric coevolutionary networks facilitate biodiversity maintenance. *Science*, 312(5772):431–433, 2006.
- [121] KM Smith, EH Loh, MK Rostal, CM Zambrana-Torrel, L Mendiola, and P Daszak. Pathogens, pests, and economics: drivers of honey bee colony declines and losses. *EcoHealth*, 10(4):434–445, 2013.
- [122] M Higes, R Martín-Hernández, and A Meana. *Nosema ceranae* in Europe: an emergent type C nosemosis. *Apidologie*, 41(3):375–392, 2010.
- [123] Y Chen, JD Evans, IB Smith, and JS Pettis. *Nosema ceranae* is a long-present and wide-spread microsporidian infecton of the European honey bee (*Apis mellifera*) in the United States. *J. Invertebr. Pathol.*, 97(2):186–188, 2008.
- [124] I Fries, G Ekbohm, and E Villumstad. *Nosema apis*, sampling techniques and honey yield. *J. Apic. Res.*, 23(2):102–105, 1984.
- [125] RM Anderson and RM May. *Infectious diseases of humans: dynamics and control*. Oxford Univ. Press, Oxford, 1992.
- [126] TD Seeley and SA Kolmes. Age polyethism for hive duties in honey bees - illusion or reality? *Ethology*, 87(3-4):284–297, 1991.
- [127] WF Huang and LF Solter. Comparative development and tissue tropism in *Nosema apis* and *Nosema ceranae*. *J. Invertebr. Pathol.*, 113(1):35–41, 2013.

- [128] L Bailey. The epidemiology and control of Nosema disease of the honeybee. *Ann. Appl. Biol.*, 43(3):379–389, 1955.
- [129] DM Eiri, G Suwannapong, M Endler, and JC Nieh. Nosema ceranae can infect honey bee larvae and reduces subsequent adult longevity. *PLOS ONE*, 10(5):e0126330, 2015.
- [130] M Higes, R Martín-Hernández, E Garrido-Bailón, P García-Palencia, and A Meana. Detection of infective Nosema ceranae (Microsporidia) spores in corbicular pollen of forager honeybees. *J. Invertebr. Pathol.*, 97(97):76–78, 2008.
- [131] ML Smith. The honey bee parasite nosema ceranae: Transmissible via food exchange? *PLOS ONE*, 7(8):e43319, 2012.
- [132] M Higes, R Martín-Hernández, E Garrido-Bailón, AV González-Porto, P García-Palencia, A Meana, MJ del Nozal, R Mayo, and JL Bernal. Honeybee colony collapse due to Nosema ceranae in professional apiaries. *Environ. Microbiol. Rep.*, 1(2):110–113, 2009.
- [133] MI Betti, LM Wahl, and M Zamir. Effects of infection on honey bee population dynamics: a model. *PLOS ONE*, 9(10):e110237, 2014.
- [134] DJT Sumpter and SJ Martin. The dynamics of virus epidemics in Varroa-infested honey bee colonies. *J. Anim. Ecol.*, 73(1):51–63, 2004.
- [135] V Ratti, PG Kevan, and HJ Eberl. A mathematical model for population dynamics in honeybee colonies infested with Varroa destructor and the Acute bee paralysis virus. *Can. Appl. Math. Q.*, pages 1–27, 2012.
- [136] SJ Martin. The role of varroa and viral pathogens in the collapse of honeybee colonies: a modelling approach. *J. Appl. Ecol.*, 38(5):1082–1093, 2001.

- [137] ML Winston. *The Biology of the Honeybee*. Harvard Univ. Press, 1991.
- [138] L Bourgeois, L Beaman, B Holloway, and TE Rinderer. External and internal detection of *Nosema ceranae* on honey bees using real-time PCR. *J. Invertebr. Pathol.*, 109(3):323–325, 2012.
- [139] M Higes, P García-Palencia, R Martín-Hernández, and A Meana. Experimental infection of *Apis mellifera* honeybees with *Nosema ceranae* (Microsporidia). *J. Invertebr. Pathol.*, 94(3):211–217, 2007.
- [140] S Fenoy, C Rueda, M Higes, R Martín-Hernández, and C Del Aguila. High-level resistance of *Nosema ceranae*, a parasite of the honeybee, to temperature and desiccation. *Appl. Environ. Microbiol.*, 75(21):6886–6889, 2009.
- [141] A Rohatgi. "WebPlotDigitizer", 2011.
- [142] M Higes, R Martín-Hernández, C Botías, EG Bailón, AV González-Porto, L Barrios, MJ Del Nozal, JL Bernal, JJ Jiménez, PG Palencia, and A Meana. How natural infection by *Nosema ceranae* causes honeybee colony collapse. *Environ. Microbiol.*, 10(10):2659–2669, 2008.
- [143] Y Chen, J Evans, and M Feldlaufer. Horizontal and vertical transmission of viruses in the honey bee, *Apis mellifera*. *J. Invertebr. Pathol.*, 92(3):152–159, 2006.
- [144] IZ Kiss, DM Green, and RR Kao. The effect of contact heterogeneity and multiple routes of transmission on final epidemic size. *Math. Biosci.*, 203(1):124–136, 2006.
- [145] R Manley, M Boots, and L Wilfert. Emerging viral disease risk to pollinating insects: ecological, evolutionary and anthropogenic factors. *J. Appl. Ecol.*, 52(2):331–340, 2015.

- [146] M Shen, L Cui, N Ostiguy, and D Cox-Foster. Intricate transmission routes and interactions between picorna-like viruses (Kashmir bee virus and Sacbrood virus) with the honeybee host and the parasitic varroa mite. *J. Gen. Virol.*, 86(8):2281–2289, 2005.
- [147] R Singh, AL Levitt, EG Rajotte, EC Holmes, N Ostiguy, D VanEngelsdorp, WI Lipkin, CW Depamphilis, AL Toth, and DL Cox-Foster. RNA viruses in hymenopteran pollinators: Evidence of inter-taxa virus transmission via pollen and potential impact on non-*Apis* hymenopteran species. *PLOS ONE*, 5(12):e14357, 2010.
- [148] L Bailey, AJ Gibbs, and RD Woods. Two viruses from adult honey bees (*Apis mellifera* Linnaeus). *Virology*, 21(3):390–395, 1963.
- [149] L Bailey, BV Ball, and JN Perry. Honeybee paralysis: its natural spread and its diminished incidence in England and Wales. *J. Apic. Res.*, 22(3):191–195, 1983.
- [150] YP Chen, JS Pettis, A Collins, and MF Feldlaufer. Prevalence and transmission of honeybee viruses. *Appl. Environ. Microbiol.*, 72(1):606–611, 2006.
- [151] ACF Hung. PCR detection of Kashmir bee virus in honey bee excreta. *J. Apic. Res.*, 39(3-4):103–106, 2000.
- [152] M Ribière, P Lallemand, AL Iscache, F Schurr, O Celle, P Blanchard, V Olivier, and JP Faucon. Spread of infectious chronic bee paralysis virus by honeybee (*Apis mellifera* L.) feces. *Appl. Environ. Microbiol.*, 73(23):7711–7716, 2007.
- [153] PL Bowen-Walker, SJ Martin, and A Gunn. The transmission of Deformed wing virus between honeybees (*Apis mellifera* L.) by the ectoparasitic mite varroa jacobsoni Oud. *J. Invertebr. Pathol.*, 73(1):101–6, 1999.
- [154] HL Holt and CM Grozinger. Approaches and challenges to managing *Nosema*

- (microspora: Nosematidae) parasites in honey bee (hymenoptera: Apidae) colonies. *J. Econ. Entomol.*, 109(4):1487–1503, 2016.
- [155] M Jansen, R Stoks, A Coors, W van Doorslaer, and L de Meester. Collateral damage: rapid exposure-induced evolution of pesticide resistance leads to increased susceptibility to parasites. *Evolution*, 65(9):2681–2691, 2011.
- [156] EC Oerke and HW Dehne. Safeguarding production - losses in major crops and the role of crop protection. *Crop Prot.*, 23(4):275–285, 2004.
- [157] European Food Safety Authority. Conclusion on the peer review of the pesticide risk assessment for bees for Clothianidin. *EFSA Journal*, 11:1–58, 2013.
- [158] European Food Safety Authority. Conclusion on the peer review of the pesticide risk assessment for bees for the active substance imidacloprid. *EFSA Journal*, 11:1–55, 2013.
- [159] M Gross. EU ban puts spotlight on complex effects of neonicotinoids. *Curr. Biol.*, 23(11):R462–R464, 2013.
- [160] CH Krupke, JD Holland, EY Long, and BD Eitzer. Planting of neonicotinoid-treated maize poses risks for honey bees and other non-target organisms over a wide area without consistent crop yield benefit. *J. Appl. Ecol.*, 54(5):1449–1458, 2017.
- [161] H. Charles J. Godfray, Tjeerd Blacquière, Linda M. Field, Rosemary S. Hails, Simon G. Potts, Nigel E. Raine, Adam J. Vanbergen, Angela R. McLean, H. Charles J. Godfray, Tjeerd Blacquie, Simon G. Potts, Nigel E. Raine, Adam J. Vanbergen, and Angela R. McLean. A restatement of recent advances in the natural science evidence base concerning neonicotinoid insecticides and insect pollinators. *Proc. R. Soc. Lond., B, Biol. Sci.*, 282:20151821, 2015.

- [162] JL Bernal, E Garrido-Bailón, MJ Del Nozal, AV González-Porto, R Martín-Hernández, JC Diego, JJ Jiménez, JL Bernal, and M Higes. Overview of pesticide residues in stored pollen and their potential effect on bee colony (*Apis mellifera*) losses in Spain. *J. Econ. Entomol.*, 103(6):1964–1971, 2010.
- [163] D Goulson. An overview of the environmental risks posed by neonicotinoid insecticides. *J. Appl. Ecol.*, 50(4):977–987, 2013.
- [164] C Botías, A David, J Horwood, A Abdul-Sada, E Nicholls, E Hill, and D Goulson. Neonicotinoid residues in wildflowers, a potential route of chronic exposure for bees. *Environ. Sci. Technol.*, 49(21):12731–12740, 2015.
- [165] RJ Gill, O Ramos-Rodriguez, and NE Raine. Combined pesticide exposure severely affects individual-and colony-level traits in bees. *Nature*, 491(7422):105–108, 2012.
- [166] RJ Gill and NE Raine. Chronic impairment of bumblebee natural foraging behaviour induced by sublethal pesticide exposure. *Funct. Ecol.*, 28(6):1459–1471, 2014.
- [167] H Feltham, K Park, and D Goulson. Field realistic doses of pesticide imidacloprid reduce bumblebee pollen foraging efficiency. *Ecotoxicology*, 23(3):317–323, 2014.
- [168] DA Stanley, AL Russell, SJ Morrison, C Rogers, and NE Raine. Investigating the impacts of field-realistic exposure to a neonicotinoid pesticide on bumblebee foraging, homing ability and colony growth. *J. Appl. Ecol.*, 53(5):1440–1449, 2016.
- [169] P Han, CY Niu, CL Lei, JJ Cui, and N Desneux. Quantification of toxins in a Cry1Ac + CpTI cotton cultivar and its potential effects on the honey bee *Apis mellifera* L. *Ecotoxicology*, 19(8):1452–1459, 2010.
- [170] A Decourtye, C Armengaud, M Renou, J Devillers, S Cluzeau, M Gauthier, and MH Pham-Delègue. Imidacloprid impairs memory and brain metabolism in the honeybee (*Apis mellifera* L.). *Pestic. Biochem. Physiol.*, 78(2):83–92, 2004.

- [171] PR Whitehorn, S O'Connor, FL Wackers, and D Goulson. Neonicotinoid pesticide reduces bumble bee colony growth and queen production. *Science*, 336:351–352, 2012.
- [172] M Rundlöf, GKS Andersson, R Bommarco, I Fries, V Hederström, L Herbertsson, O Jonsson, BK Klatt, TR Pedersen, J Yourstone, and HG Smith. Seed coating with a neonicotinoid insecticide negatively affects wild bees. *Nature*, 521(7550):77–80, 2015.
- [173] GR Williams, A Troxler, G Retschnig, K Roth, O Yañez, D Shutler, P Neumann, and L Gauthier. Neonicotinoid pesticides severely affect honey bee queens. *Sci. Rep.*, 5:14621, 2015.
- [174] EC Yang, HC Chang, WY Wu, and YW Chen. Impaired olfactory associative behavior of honeybee workers due to contamination of imidacloprid in the larval stage. *PLOS ONE*, 7(11):e49472, 2012.
- [175] K Tan, W Chen, S Dong, X Liu, Y Wang, and JC Nieh. A neonicotinoid impairs olfactory learning in Asian honey bees (*Apis cerana*) exposed as larvae or as adults. *Sci. Rep.*, 5:10989, 2015.
- [176] C. Alaux, JL Brunet, C Dussaubat, F Mondet, S Tchamitchan, M Cousin, J Brillard, A Baldy, LP Belzunces, and Y Le Conte. Interactions between *Nosema* microspores and a neonicotinoid weaken honeybees (*Apis mellifera*). *Environ. Microbiol.*, 12(3):774–782, 2010.
- [177] C Vidau, M Diogon, J Aufauvre, and R Fontbonne. Exposure to sublethal doses of fipronil and thiacloprid highly increases mortality of honeybees previously infected by *Nosema ceranae*. *PLOS ONE*, 6:e21550, 2011.
- [178] V Doublet, M Labarussias, JR de Miranda, RF Moritz, and RJ Paxton. Bees under

- stress: Sublethal doses of a neonicotinoid pesticide and pathogens interact to elevate honey bee mortality across the life cycle. *Environ. Microbiol.*, 17(4):969–983, 2015.
- [179] A Coors, E Decaestecker, M Jansen, and L De Meester. Pesticide exposure strongly enhances parasite virulence in an invertebrate host model. *Oikos*, 117(12):1840–1846, 2008.
- [180] RR James and J Xu. Mechanisms by which pesticides affect insect immunity. *J. Invertebr. Pathol.*, 109(2):175–182, 2012.
- [181] P de Azambuja, ES Garcia, NA Ratcliffe, and JD Warthen. Immune-depression in *Rhodnius prolixus* induced by the growth inhibitor, azadirachtin. *J. Insect Physiol.*, 37(10):771–777, 1991.
- [182] A Brandt, A Gorenflo, R Siede, M Meixner, and R Büchler. The neonicotinoids thiacloprid, imidacloprid, and clothianidin affect the immunocompetence of honey bees (*Apis mellifera* L.). *J. Insect Physiol.*, 86:40–47, 2016.
- [183] A Zibae and AR Bandani. Effects of *Artemisia annua* L.(Asteracea) on the digestive enzymatic profiles and the cellular immune reactions of the Sunn pest, *Eurygaster integriceps* (Heteroptera: Scutellaridae), against *Beauveria bassiana*. *Bull. Entomol. Res.*, 100(2):185–196, 2010.
- [184] JM Delpuech, F Frey, and Y Carton. Action of insecticides on the cellular immune reaction of *Drosophila melanogaster* against the parasitoid *Leptopilina boulardi*. *Environ. Toxicol. Chem.*, 15(12):2267–2271, 1996.
- [185] G Di Prisco, V Cavaliere, D Annoscia, P Varricchio, E Caprio, F Nazzi, G Gargiulo, and F Pennacchio. Neonicotinoid clothianidin adversely affects insect immunity and promotes replication of a viral pathogen in honey bees. *Proc. Natl. Acad. Sci.*, 110(46):18466–18471, 2013.

- [186] R van der Zee, L Pisa, S Andonov, R Brodschneider, JD Charrière, R Chlebo, MF Coffey, K Crailsheim, B Dahle, A Gajda, A Gray, MM Drazic, M Higes, L Kauko, A Kence, M Kence, N Kezic, H Kiprijanovska, J Kralj, P Kristiansen, R Martin Hernandez, F Mutinelli, BK Nguyen, C Otten, A Özkirim, SF Pernal, M Peterson, G Ramsay, V Santrac, V Soroker, G Topolska, A Uzunov, F Vejsnæs, S Wei, and S Wilkins. Managed honey bee colony losses in Canada, China, Europe, Israel and Turkey, for the winters of 2008-9 and 2009-10. *J. Apic. Res.*, 51(1):100–114, 2012.
- [187] D VanEngelsdorp, D Caron, J Hayes, R Underwood, M Henson, K Rennich, A Spleen, M Andree, R Snyder, K Lee, K Roccasecca, M Wilson, J Wilkes, E Lengerich, and J Pettis. A national survey of managed honey bee 2010-11 winter colony losses in the USA: results from the Bee Informed Partnership. *J. Apic. Res.*, 51(1):115–124, 2012.
- [188] S Lautenbach, R Seppelt, J Liebscher, and CF Dormann. Spatial and temporal trends of global pollination benefit. *PLOS ONE*, 7(4):e35954, 2012.
- [189] MH Allsopp, WJ de Lange, and R Veldtman. Valuing insect pollination services with cost of replacement. *PLOS ONE*, 3(9):e3128, 2008.
- [190] P Neumann and NL Carreck. Honey bee colony losses. *J. Apic. Res.*, 49(1):1–6, 2010.
- [191] P Rosenkranz, P Aumeier, and B Ziegelmann. Biology and control of *Varroa destructor*. *J. Invertebr. Pathol.*, 103:S96–S119, 2010.
- [192] EV Ryabov, GR Wood, JM Fannon, JD Moore, JC Bull, D Chandler, A Mead, N Burroughs, and DJ Evans. A virulent strain of Deformed wing virus (DWV) of honeybees (*Apis mellifera*) prevails after *Varroa destructor*-mediated, or in vitro, transmission. *PLOS Pathog.*, 10(6):e1004230, 2014.

- [193] JE Cresswell, N Desneux, and D VanEngelsdorp. Dietary traces of neonicotinoid pesticides as a cause of population declines in honey bees: An evaluation by Hill's epidemiological criteria. *Pest Manag. Sci.*, 68(6):819–827, 2012.
- [194] HM Nasr, MEI Badawy, and EI Rabea. Toxicity and biochemical study of two insect growth regulators, buprofezin and pyriproxyfen, on cotton leafworm *Spodoptera littoralis*. *Pestic. Biochem. Physiol.*, 98(2):198–205, 2010.
- [195] Z Ma, X Han, J Feng, G Li, and X Zhang. Effects of terpinen-4-ol on four metabolic enzymes and polyphenol oxidase (PPO) in *Mythimna separata* Walker. *Agric. Sci. China.*, 7(6):726–730, 2008.
- [196] E Büyükgüzel. Evidence of oxidative and antioxidative responses by *Galleria mellonella* larvae to malathion. *J. Econ. Entomol.*, 102(1):152–159, 2009.
- [197] S Alizon and M van Baalen. Acute or chronic? Within-host models with immune dynamics, infection outcome, and parasite evolution. *Am. Nat.*, 172(6):E244–E256, 2008.
- [198] GP Dively, MS Embrey, A Kamel, DJ Hawthorne, and JS Pettis. Assessment of chronic sublethal effects of imidacloprid on honey bee colony health. *PLOS ONE*, 10(3):e0118748, 2015.
- [199] F Sánchez-Bayo, D Goulson, F Pennacchio, F Nazzi, K Goka, and N Desneux. Are bee diseases linked to pesticides? - A brief review. *Environ. Int.*, 89-90:7–11, 2016.
- [200] PT Starks, CA Blackie, and TD Seeley. Fever in honeybee colonies. *Naturwissenschaften*, 87(5):229–231, 2000.
- [201] KD Waddington and WC Rothenbuhler. Behaviour associated with hairless-black syndrome of adult honeybees. *J. Apic. Res.*, 15(1):35–41, 1976.

- [202] M Spivak and M Gilliam. Hygienic behaviour of honey bees and its application for control of brood diseases and Varroa. Part II. Studies on hygienic behaviour since the Rothenbuhler era. *Bee World*, 79(4):169–186, 1998.
- [203] RA Morse and K Flottum. *Honey bee pests, predators, and diseases*. A.I. Root Co., Medina, OH, 1997.
- [204] CJ Perry, E Søvik, MR Myerscough, and AB Barron. Rapid behavioral maturation accelerates failure of stressed honey bee colonies. *Proc. Natl. Acad. Sci.*, 112(1):3427–32, 2015.
- [205] B Grenfell and J Harwood. (Meta)population dynamics of infectious diseases. *Trends Ecol. Evol.*, 12(10):395–399, 1997.
- [206] TW Snell and CR Janssen. Rotifers in ecotoxicology: a review. *Hydrobiologia*, 313(1):231–247, 1995.
- [207] SV Buratini, E Bertoletti, and PA Zagatto. Evaluation of *Daphnia similis* as a test species in ecotoxicological assays. *Bull. Environ. Contam. Toxicol.*, 73(5):878–882, 2004.
- [208] M Van Den Berg, L Birnbaum, ATC Bosveld, B Brunström, P Cook, M Feeley, JP Giesy, A Hanberg, R Hasegawa, SW Kennedy, T Kubiak, JC Larsen, FXR Van Leeuwen, AKD Liem, C Nolt, RE Peterson, L Poellinger, S Safe, D Schrenk, D Tillitt, M Tysklind, M Younes, F Wærn, and T Zacharewski. Toxic equivalency factors (TEFs) for PCBs, PCDDs, PCDFs for humans and wildlife. *Environ. Health Perspect.*, 106(12):775–792, 1998.
- [209] TR Martin and DM Holdich. The acute lethal toxicity of heavy metals to peracarid crustaceans (with particular reference to fresh-water asellids and gammarids). *Water Res.*, 20(9):1137–1147, 1986.

- [210] RE Warner, KK Peterson, and L Borgman. Behavioural pathology in fish: a quantitative study of sublethal pesticide toxication. *J. Appl. Ecol.*, 3:223–247, 1966.
- [211] PE Davies, LSJ Cook, and D Goenarso. Sublethal responses to pesticides of several species of australian freshwater fish and crustaceans and rainbow trout. *Environ. Toxicol. Chem.*, 13(8):1341–1354, 1994.
- [212] NC Bols, JL Brubacher, RC Ganassin, and LEJ Lee. Ecotoxicology and innate immunity in fish. *Dev. Comp. Immunol.*, 25(8-9):853–873, 2001.
- [213] MK Gilbertson, GD Haffner, KG Drouillard, A Albert, and B Dixon. Immunosuppression in the northern leopard frog (*Rana pipiens*) induced by pesticide exposure. *Environ. Toxicol. Chem.*, 22(1):101–110, 2003.
- [214] R Mason. Immune Suppression by Neonicotinoid Insecticides at the Root of Global Wildlife Declines. *J. Environ. Immunol. Toxicol.*, 1(1):3–12, 2013.
- [215] EH Heugens, LT Tokkie, MH Kraak, AJ Hendriks, NM Van Straalen, and W Admiraal. Population growth of *Daphnia magna* under multiple stress conditions: joint effects of temperature, food, and cadmium. *Environ. Toxicol. Chem.*, 25(5):1399–1407, 2006.
- [216] M Scheffer, J Bascompte, WA Brock, V Brovkin, SR Carpenter, V Dakos, H Held, EH van Nes, M Rietkerk, and G Sugihara. Early-warning signals for critical transitions. *Nature*, 461(7260):53–59, 2009.
- [217] WG Meikle, BG Rector, Mercadier G, and N Holst. Within-day variation in continuous hive weight data as a measure of honey bee colony activity. *Apidologie*, 39(6):694–707, 2008.
- [218] S Cremer, SAO Armitage, and P Schmid-Hempel. Social immunity. *Curr. Biol.*, 17(16):R693–R702, 2007.

Appendix A

Appendix for Chapter 2

Linearisation Around The Zero Equilibrium

Clearly, $(H, F) = (0, 0)$ is an equilibrium of the system. We can perform a linearisation around the zero equilibrium to determine the stability of this fixed point. Let us define the following functions

$$\begin{aligned}g_1(H, F) &= \frac{dH}{dt} \\ &= L \frac{H + F}{\omega + H + F} - H \left(\alpha - \sigma \frac{F}{k + F + H} \right) - \frac{\mu H}{\phi + H + F} - \gamma(H + F)H \\ g_2(H, F) &= \frac{dF}{dt} \\ &= H \left(\alpha - \sigma \frac{F}{k + F + H} \right) - mF - \frac{\mu F}{\phi + H + F}\end{aligned}$$

Now, since $\exists (H^*, F^*)$, steady state of

$$\frac{dH}{dt} = \frac{dF}{dt} = 0$$

Then

$$\begin{aligned}\frac{dH^*}{dt} &= g_1(H^*, F^*) \\ \frac{dF^*}{dt} &= g_2(H^*, F^*)\end{aligned}$$

We can calculate the Jacobian matrix for (H^*, F^*) as

$$J = \begin{pmatrix} \left(\frac{dg_1}{dH}\right)_* & \left(\frac{dg_1}{dF}\right)_* \\ \left(\frac{dg_2}{dH}\right)_* & \left(\frac{dg_2}{dF}\right)_* \end{pmatrix}$$

$$\begin{aligned}\frac{dg_1}{dH} &= -\alpha - F\gamma - 2H\gamma + \frac{F^2\sigma}{(F+H+k)^2} + \frac{Fk\sigma}{(F+H+k)^2} + \\ &\quad \frac{H\mu}{(F+H+\phi)^2} - \frac{\mu}{F+H+\phi} - \frac{(F+H)L}{(F+H+\omega)^2} + \frac{L}{F+H+\omega} \\ \frac{dg_1}{dF} &= -H\gamma + \frac{H(H+k)\sigma}{(F+H+k)^2} + \frac{H\mu}{(F+H+\phi)^2} - \frac{(F+H)L}{(F+H+\omega)^2} + \frac{L}{F+H+\omega} \\ \frac{dg_2}{dH} &= \alpha - \frac{F(F+k)\sigma}{(F+H+k)^2} + \frac{F\mu}{(F+H+\phi)^2} \\ \frac{dg_2}{dF} &= -m - \frac{H(H+k)\sigma}{(F+H+k)^2} - \frac{\mu(H+\phi)}{(F+H+\phi)^2}\end{aligned}$$

Evaluating the Jacobian at the equilibrium point $(H_0^*, F_0^*) = (0, 0)$,

$$J^* = \begin{pmatrix} -\alpha - \frac{\mu}{\phi} + \frac{L}{\omega} & \frac{L}{\omega} \\ \alpha & -m - \frac{\mu}{\phi} \end{pmatrix}$$

Calculating the eigenvalues,

$$\lambda_1 = \frac{L\phi - 2\mu\omega - m\phi\omega - \alpha\phi\omega - \phi\sqrt{L^2 + 2Lm\omega + 2L\alpha\omega + m^2\omega^2 - 2m\alpha\omega^2 + \alpha^2\omega^2}}{2\phi\omega}$$

$$\lambda_2 = \frac{L\phi - 2\mu\omega - m\phi\omega - \alpha\phi\omega + \phi\sqrt{L^2 + 2Lm\omega + 2L\alpha\omega + m^2\omega^2 - 2m\alpha\omega^2 + \alpha^2\omega^2}}{2\phi\omega}$$

In order for the origin to be stable, we require all eigenvalues to be real and of negative sign. If we assume that all other parameters are nonzero, $\omega > 0, \alpha > 0, \phi > 0, L > 0, m > 0$ and that stress is also nonzero $\mu > 0$ then this happens either when (1)

$$0 < \omega < \frac{L(m + \alpha)}{m\alpha}$$

and when

$$\mu > \frac{L\phi + \omega \left(-\phi(m + \alpha) + \sqrt{\frac{\phi^2(L^2 + 2L\omega(m + \alpha) + (m - \alpha^2)\omega^2)}{\omega^2}} \right)}{2\omega}$$

or when (2),

$$\omega \geq \frac{L(m + \alpha)}{m\alpha}$$

So in order for the system to have a stable equilibrium at $(0,0)$, we require either (1) or (2) to hold true. If stress is present $\mu > 0$, then we have obtained the conditions for the stability of the origin.

Bifurcations of Critical Parameters

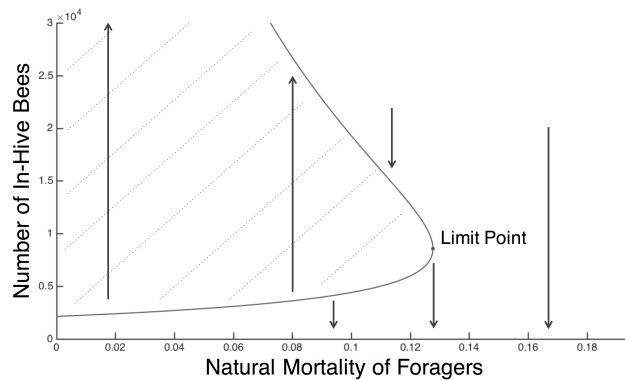


Figure A1: The saddle-node bifurcation through the parameter of natural mortality rate, m , with parameters taken from Table 2.1. The location of the limit point represents the critical death rate after which the total number of in-hive bees will become 0. For low initial values of in-hive bees, the colony can fail with no natural mortality present.

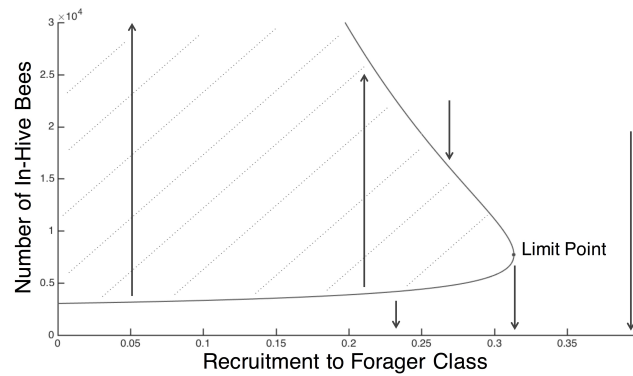


Figure A2: The saddle-node bifurcation through the parameter of recruitment α , with parameters taken from Table 2.1. The bifurcation is similar to the natural mortality bifurcation, with the limit point being approached from low parameter values. If recruitment is critically high, then the colony will fail.

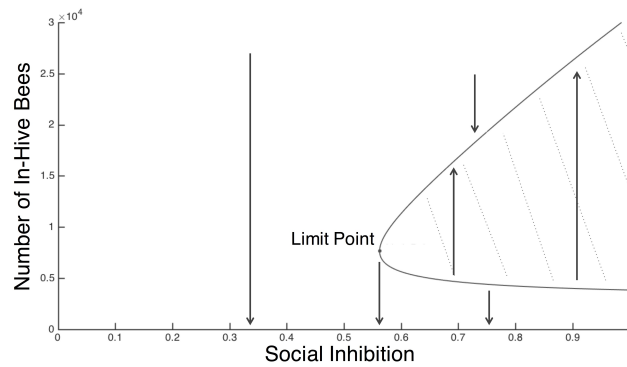


Figure A3: The reversed direction saddle-node bifurcation through the parameter of social inhibition σ , with parameters taken from Table 2.1. For high values of social inhibition task switching, the colony can sustain if the initial number of bees is greater than the critically low amount. If the social inhibition decreases below the limit point, then the colony will fail.

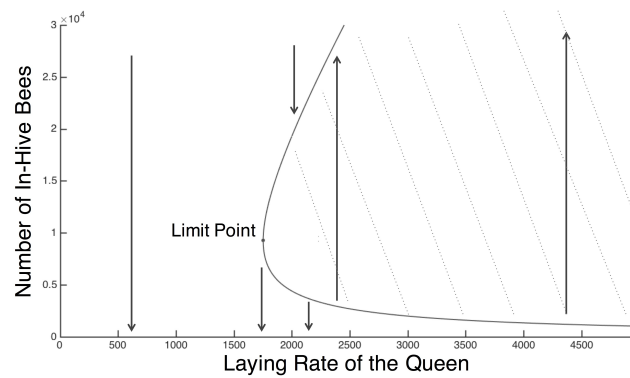


Figure A4: The reversed direction saddle-node bifurcation through the parameter of laying rate of the queen L , with parameters taken from Table 2.1. The bifurcation is similar to the bifurcation for social inhibition. If the queen lays more than the critically low value around the limit point, then the colony will sustain given that the initial number of bees is greater than the unstable branch.

Model Comparison

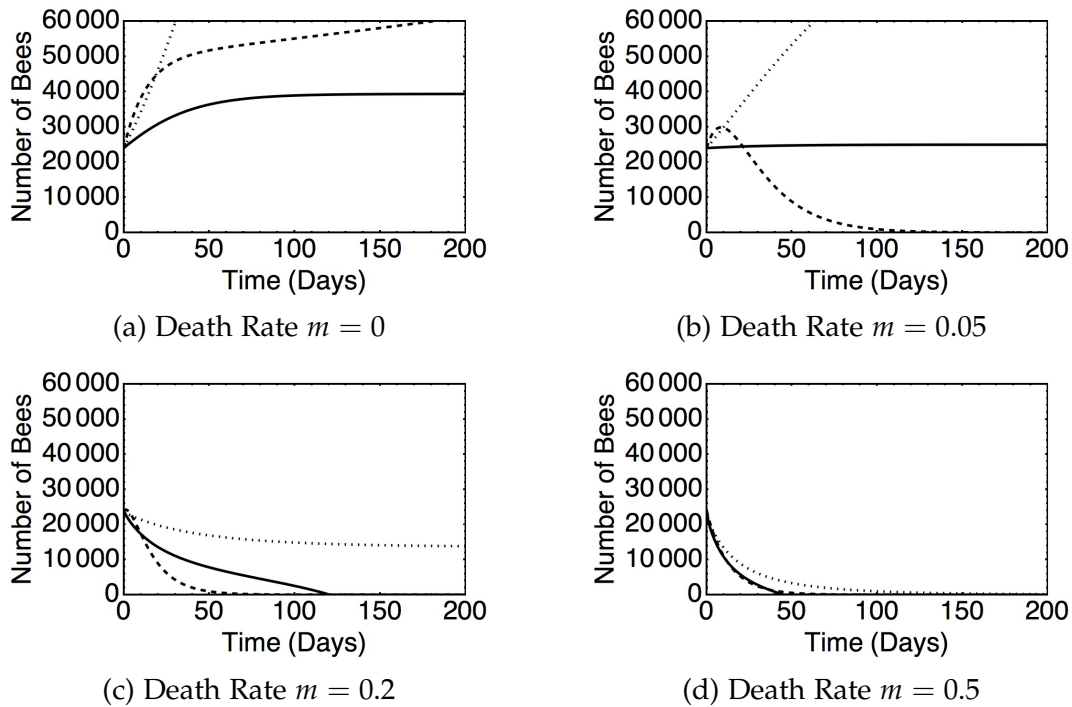
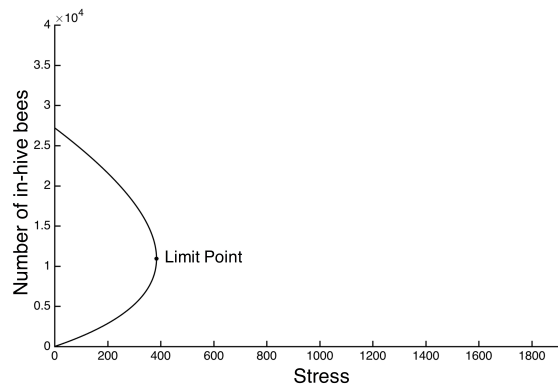
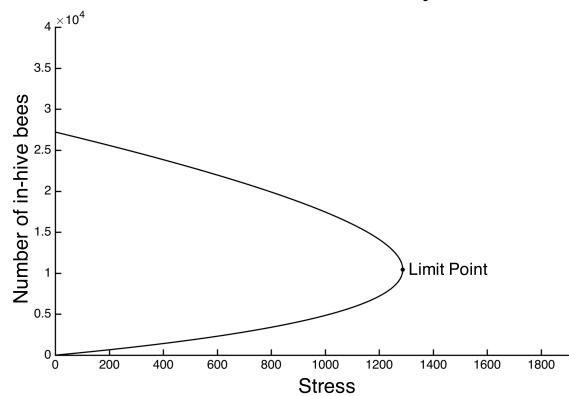


Figure A5: The comparison between our simulated model, and other author's models, with parameters taken from Table 2.1. The black curve represents our adjusted model including the limiting γ function. The dotted curve represents the Khoury et al. model [92] and dashed curve represents the Bryden et al. model [96]. As we increase each model through the death rate parameter, the sudden switch between indefinite growth and collapse exhibited by the Bryden model, and the very gradual decrease in the population exhibited by the Khoury model can be compared to the stabilisation of the population at low mortality and sudden collapse at higher mortality exhibited by our model.

The effect of stress on population dynamics



(a) Stress function only in-hive bees



(b) Stress function only forager bees

Figure A6: The bifurcation through stress when acting only on the in-hive population (a) and only on the forager population (b), with parameters taken from Table 2.1. In (a) we see similar dynamics to the original model, however in (b) the limit point occurs at a higher stress level. The same qualitative dynamics are present (saddle-node bifurcation) in both cases.

Appendix B

Appendix for Chapter 3

Calculating the Malthusian growth parameter λ

We use the online application WebPlotDigitizer to extract data from Figure 2A published in [142]. This gives us the initial growth rate of the infection in the summer. We summarise this extracted data in the following table

Time (days)	% infection
0	0
30	0
60	8.7
90	21.9
120	42.6
150	51.4
180	67.6
210	85.3
240	92.6
270	39.2

We can plot this data from the first initial infection using a log scale and fit an exponential model to the initial data points: $ae^{\lambda t} = 4.10e^{0.026t}$

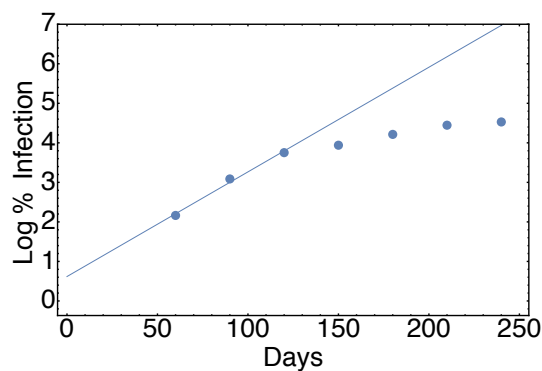


Figure B1

Therefore the Malthusian parameter for the initial growth rate is $\lambda = 0.026$.

R_0 in each season

At the disease free equilibrium

$$(X^*, Y^*, Z^*) = \left(\frac{M(r - \mu)}{r}, 0, 0 \right)$$

The original system of ODEs becomes

$$\begin{aligned} \frac{dX}{dt} &= \beta \frac{M(r - \mu)}{r} Z - \theta \frac{M(r - \mu)}{r} Y - (\alpha + \mu + p)Y \\ \frac{dZ}{dt} &= kY(1 - Z) - dZ \end{aligned}$$

Calculating the Jacobian for this model gives

$$J = \begin{pmatrix} -p - \alpha + M\theta - \frac{\mu(r + M\theta)}{r} & \frac{M\beta(r - \mu)}{r} \\ k(1 - Z) & -d - kY \end{pmatrix}$$

Evaluating at $(Y^*, Z^*) = (0, 0)$ gives

$$J = \begin{pmatrix} -p - \alpha + M\theta - \frac{\mu(r + M\theta)}{r} & \frac{M\beta(r - \mu)}{r} \\ k & -d \end{pmatrix}$$

Calculating the determinant and substituting X^* gives

$$J = \begin{vmatrix} \lambda + (\alpha + \mu + p) - \theta X^* & -\beta X^* \\ -k & \lambda + d \end{vmatrix} = 0$$

Then

$$(\lambda + (\alpha + \mu + p) - \theta X^*)(\lambda + d) - \beta k X^* = 0$$

Let $\Lambda_1 = \frac{1}{\alpha + \mu + p}$ and $\Lambda_2 = \frac{1}{d}$ so that

$$\begin{aligned} (\lambda + \frac{1}{\Lambda_1} - \theta X^*)(\lambda + \frac{1}{\Lambda_2}) - \beta k X^* &= 0 \\ (\lambda \Lambda_1 + 1 - \theta X^* \Lambda_1)(\lambda \Lambda_2 + 1) - \beta k X^* \Lambda_1 \Lambda_2 &= 0 \end{aligned}$$

R_0 in each season is expressed as

$$\begin{aligned} R_0 &= \frac{M_i(\beta k + \theta d)(r - \mu_i)}{dr(p + \alpha_i + \mu_i)} \\ &= \frac{X^*(\beta k + \theta d)}{d(p + \alpha_i + \mu_i)} \\ &= \frac{X^* \beta k}{d(p + \alpha_i + \mu_i)} + \frac{X^* \theta}{(p + \alpha_i + \mu_i)} \\ &= \beta k X^* \Lambda_1 \Lambda_2 + \theta X^* \Lambda_1 \\ &= R_I + R_D \end{aligned}$$

so that

$$R_I = \beta k X^* \Lambda_1 \Lambda_2$$

$$R_D = \theta X^* \Lambda_1$$

Combining we obtain the following relation between the Malthusian coefficient λ , the contribution to R_0 from the indirect transmission R_I and direct transmission R_D .

$$(\lambda \Lambda_1 + 1 - R_D)(\lambda \Lambda_2 + 1) = R_I$$

Therefore

$$R_{0min} = \lambda \Lambda_1 + 1 \leq R_0 \leq (\lambda \Lambda_1 + 1)(\lambda \Lambda_2 + 1) = R_{0max}$$

Rescaling from the definition of R_0 we can find R_0 for all seasons using the seasonal parameters, e.g.

$$\frac{R_{0summer}(\alpha + \mu_2)}{M_2(r - \mu_2)} = \frac{R_{0spring}(\alpha + \mu_1)}{M_1(r - \mu_1)}$$
$$R_{0spring} = \frac{R_{0summer} M_1(\alpha + \mu_2)(r - \mu_1)}{M_2(r - \mu_2)(\alpha + \mu_1)}$$

So that the maximum R_0 in each season is

$$R_{0spring} = 3.40$$

$$R_{0summer} = 1.68$$

$$R_{0autumn} = 1.30$$

$$R_{0winter} = 1.17$$

Estimating β and θ from the value of R_0

The size of β and θ depend upon the choice of R_I and R_D . With $R_0 = R_{0max}$

we derive the following values for β and θ .

$R_I : R_D$	β	θ
100:0	0.037	0
70:30	0.026	0.170
50:50	0.018	0.284
30:70	0.011	0.397
0:100	0	0.567

Appendix C

Appendix for Chapter 4

Stability Analysis around the DFE

We perform the stability analysis for the system under the assumption $Z = 0$ before $Y = 0$ (equation 4.3 in the main text).

Phase I $0 \leq Q < \frac{c}{h} = Q_0^*$

We analyse the system in the region $c - hQ > 0$ and $\lambda - rQ > 0$ (phase I).

This ensures that X, Y and Z exist. The system describing the dynamics of the host under toxicant exposure

$$\begin{aligned}\frac{dX}{dt} &= \lambda - \beta YX - dX - rQ \\ \frac{dY}{dt} &= \beta YX - aY - pYZ \\ \frac{dZ}{dt} &= c - bZ - hQ\end{aligned}$$

has equilibria

$$(X_B^{DFE}, Y_B^{DFE}, Z_B^{DFE}) = \left(\frac{\lambda - rQ}{d}, 0, \frac{c - hQ}{b} \right)$$

$$(X_B^{EE}, Y_B^{EE}, Z_B^{EE}) = \left(\frac{ab + cp - hpQ}{\beta b}, \frac{-abd - cdp + dhpQ - bQr\beta + \beta b\lambda}{\beta ab + cp\beta - hpQ\beta}, \frac{c - hQ}{b} \right)$$

The Jacobian matrix of the system is calculated as follows

$$J = \begin{pmatrix} -d - \beta Y & -\beta X & 0 \\ \beta Y & -a - pZ + \beta X & -pY \\ 0 & 0 & -b \end{pmatrix}$$

The Jacobian evaluated at the DFE is

$$J_{DFE} = \begin{pmatrix} -d & \beta \left(\frac{rQ - \lambda}{d} \right) & 0 \\ 0 & -a - p \left(\frac{c - hQ}{b} \right) + \beta \left(\frac{\lambda - rQ}{d} \right) & 0 \\ 0 & 0 & -b \end{pmatrix}$$

which has eigenvalues

$$-b$$

$$-d$$

$$-\frac{abd + cdp - dhpQ + bQr\beta - b\beta\lambda}{bd}$$

The system has a stable node at the DFE when all eigenvalues are real and

negative. Clearly $-b < 0$ and $-d < 0$, so the DFE is a stable node when

$$Q < \frac{abd + cdp - b\beta\lambda}{dhp - br\beta}$$

and a saddle (at least one of the eigenvalues is positive) when

$$Q > \frac{abd + cdp - b\beta\lambda}{dhp - br\beta}$$

Therefore $\frac{abd+cdp-b\beta\lambda}{dhp-br\beta}$ gives us the threshold toxicant exposure value at which a small density of parasite will cause outbreak within the host. In the parameter space explored in the manuscript the DFE is unstable for any value of Q in the phase I region $0 \leq Q < \frac{c}{h}$.

Phase II $Q_0^* = \frac{c}{h} \leq Q < \frac{\beta\lambda - ad}{r\beta} = Q_1^*$

In this region, the system becomes

$$\begin{aligned}\frac{dX}{dt} &= \lambda - \beta Y X - dX - rQ \\ \frac{dY}{dt} &= \beta Y X - aY\end{aligned}$$

with equilibria

$$\begin{aligned}(X_B^{DFE}, Y_B^{DFE}) &= \left(\frac{\lambda - rQ}{d}, 0 \right) \\ (X_B^{EE}, Y_B^{EE}) &= \left(\frac{a}{\beta'}, -\frac{ad + r\beta Q - \beta\lambda}{a\beta} \right)\end{aligned}$$

The Jacobian matrix is calculated as follows

$$J = \begin{pmatrix} -d - \beta Y & -\beta X \\ \beta Y & -a + \beta X \end{pmatrix}$$

The Jacobian evaluated at the DFE is

$$J_{DFE} = \begin{pmatrix} -d & -\beta\left(\frac{\lambda - rQ}{d}\right) \\ 0 & -a + \beta\left(\frac{\lambda - rQ}{d}\right) \end{pmatrix}$$

which has eigenvalues

$$\begin{aligned} & -d \\ & -a + \beta\left(\frac{\lambda - rQ}{d}\right) \end{aligned}$$

The system has a stable node at the DFE when all eigenvalues are real and negative. Clearly $-d < 0$, so the DFE is a stable node when

$$Q > \frac{\beta\lambda - ad}{r\beta}$$

and (unstable) saddle if eigenvalues are real and of opposite signs which occurs when

$$Q < \frac{\beta\lambda - ad}{r\beta}$$

which corresponds to the definition for Phase II ($Q < \frac{\beta\lambda - ad}{r\beta} = Q_1^*$). After this threshold toxicant exposure, the DFE becomes stable and hence the parasite is removed from the host.

Phase III $Q_1^* = \frac{\beta\lambda - ad}{r\beta} \leq Q < \frac{\lambda}{r}$

In this phase, the system becomes

$$\frac{dX}{dt} = \lambda - dX - rQ$$

with equilibria

$$X_B = \frac{\lambda - rQ}{d}$$

and corresponding eigenvalue $-d$ evaluated at the equilibrium. Since this is negative, the equilibrium is always stable for $d > 0$. At the point at which the equilibrium becomes 0, the host is dead and the equations are undefined for larger Q . This happens when the assumption $\lambda - rQ > 0$ is reversed.

To summarise, the EE equilibria is feasible until one of $c - hQ > 0$ and $\lambda - rQ > 0$ is broken. After phase I ($Q = \frac{c}{h} = Q_0^*$), then $Z = 0$, and the equilibria is expressed in terms of the two dimensional system X and Y . After which the EE equilibria is feasible until $Q = \frac{\beta\lambda - ad}{r\beta} = Q_1^*$, at which point $Y = 0$, so the system reverts to the one dimensional system of X , and

a stable DFE. This equilibria is feasible until $Q^* = \frac{\lambda}{r}$ after which all state values are equal to 0.

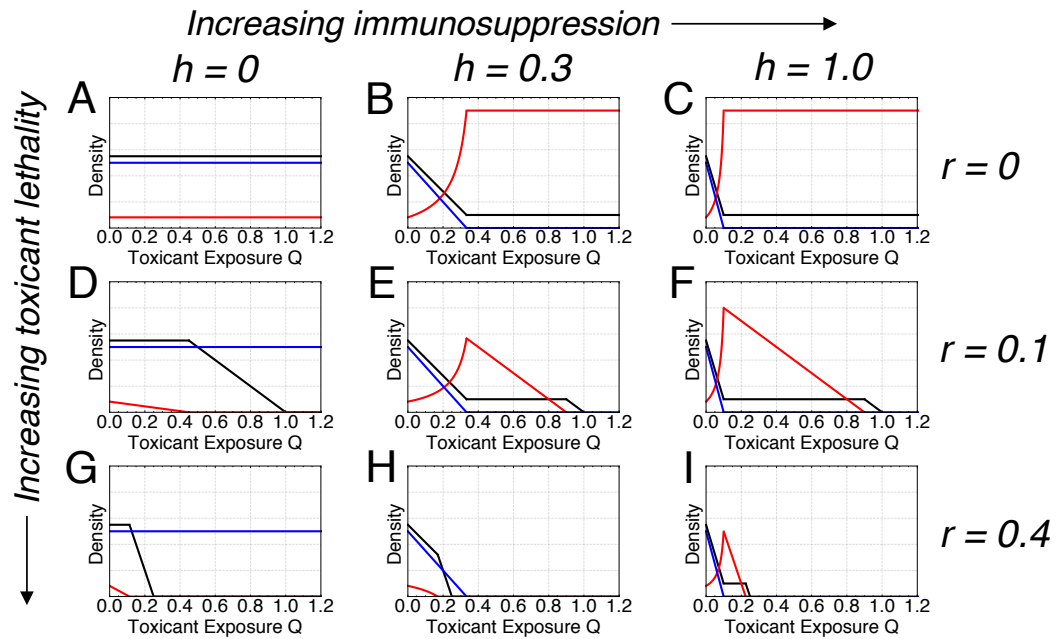


Figure C1: The mechanism of parasite infection under increasing toxicant exposure, for a pairwise range of both immunosuppressive ($h = 0, 0.3, 1.0$) and lethal ($r = 0, 0.1, 0.4$) effects of toxicant with all parameters taken from Table 4.2. This shows the parameter dependence of immunity, parasite density and within-host cells at equilibrium within the dynamics of our model. The total densities of immune function (blue), parasite load (red) and within-host cells (black) change as an individual is subject to higher toxicant loads, according to the phases of the model.

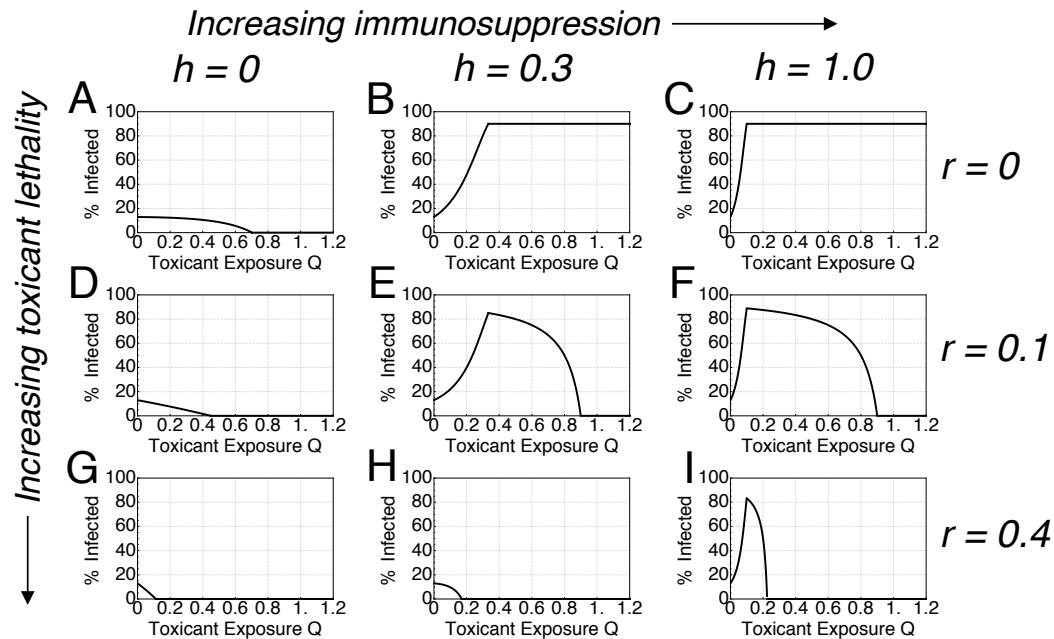


Figure C2: The mechanism of parasite infection under increasing toxicant exposure, for a pairwise range of both immunosuppressive ($h = 0, 0.3, 1.0$) and lethal ($r = 0, 0.1, 0.4$) effects of toxicant with all parameters taken from Table 4.2. This shows how the total % parasite infection (black) changes depending upon the combination of both immunosuppressive and lethal effects.

Density dependent assumption

System (4.1) assumes that toxicant exposure reduces the sources of within-host cells λ and immunity c . We explore the alternative assumption that toxicant load reduces the within-host cells and immune function dependent upon the density of both, respectively. In this case, system (4.1) be-

comes

$$\begin{aligned}\frac{dX}{dt} &= \lambda - \beta YX - dX - rQX \\ \frac{dY}{dt} &= \beta YX - aY - pYZ \\ \frac{dZ}{dt} &= c - bZ - hQZ\end{aligned}$$

We reproduce Fig. 4.2 from the main text in order to examine the equilibria under this new assumption with the same parameter set. Figure C3 shows the dynamical behaviour of the model under this assumption. We show that parasite load is still maximised at an intermediate toxicant exposure, and the removal of the parasite at high toxicant exposure.

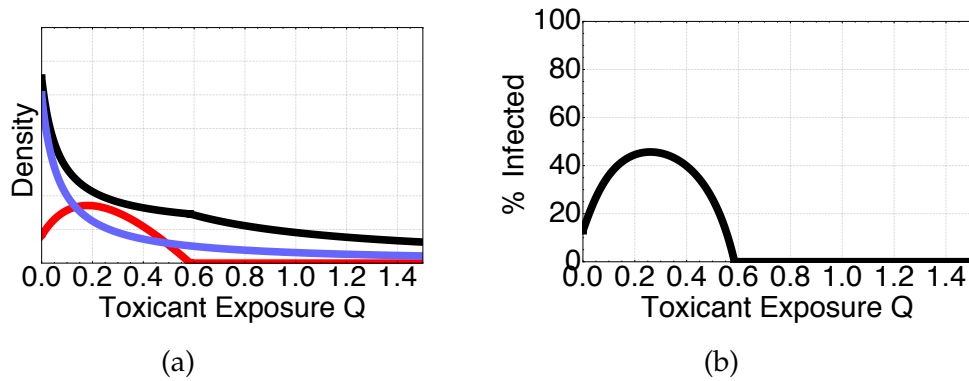


Figure C3: The mechanism of parasite infection under increasing toxicant exposure for density-dependent assumption. This shows the parameter dependence of immunity, parasite density and within-host cells at equilibrium within the dynamics of our model. In (a) the total densities of immune function (blue), parasite load (red) and within-host cells (black) change as an individual is subject to higher toxicant loads. In (b) the total % parasite infection (black) changes as the toxicant load is increased. Parameters as in Table 4.2.

Appendix D

Appendix for Chapter 5

Derivation of non-dimensional model

We use the simple modelling framework provided in Booton et al. [2] to describe the within-host infection dynamics under toxicant exposure in an individual. X , Y and Z represent the total within-host cells, parasite density and immune function, respectively. Toxicant exposure Q both reduces the functionality of the immune system at rate h (sublethal) and damages the functionality of the host at rate r (lethal). λ sets the rate of production for new healthy cells, β the rate of infection, d the death of healthy cells, a the death of parasites, p the immune suppression, c the production of immunity and b the removal of immunity. This model is given by the below equations

$$\frac{dX}{dt} = \lambda - \beta YX - dX - rQ$$

$$\frac{dY}{dt} = \beta YX - aY - pYZ$$

$$\frac{dZ}{dt} = c - bZ - hQ$$

In order to significantly reduce the analysis we non-dimensionalise this model. We write these differential equations in terms of the new variables:

$$\mathcal{X} = \hat{X}X, \mathcal{Y} = \hat{Y}Y, \mathcal{Z} = \hat{Z}Z \text{ and}$$

$$t = \hat{t}t$$

, where the quantities $\hat{X}, \hat{Y}, \hat{Z}$ and \hat{t} will be chosen later. By the chain rule,

$$\begin{aligned} \frac{d\mathcal{X}}{dt} &= \frac{\hat{X}}{\hat{t}} \frac{dX}{dt} \\ &= \frac{\lambda \hat{X}}{\hat{t}} - \frac{\beta \mathcal{X} \mathcal{Y}}{\hat{t} \hat{Y}} - \frac{d\mathcal{X}}{\hat{t}} - \frac{rQ \hat{X}}{\hat{t}} \end{aligned}$$

$$\begin{aligned} \frac{d\mathcal{Y}}{dt} &= \frac{\hat{Y}}{\hat{t}} \frac{dY}{dt} \\ &= \frac{\beta \mathcal{X} \mathcal{Y}}{\hat{t} \hat{X}} - \frac{a\mathcal{Y}}{\hat{t}} - \frac{p\mathcal{Y} \mathcal{Z}}{\hat{t} \hat{Z}} \end{aligned}$$

$$\begin{aligned} \frac{d\mathcal{Z}}{dt} &= \frac{\hat{Z}}{\hat{t}} \frac{dZ}{dt} \\ &= \frac{c\hat{Z}}{\hat{t}} - \frac{b\mathcal{Z}}{\hat{t}} - \frac{hQ\hat{Z}}{\hat{t}} \end{aligned}$$

Let $\hat{t} = b$, $\hat{X} = \frac{b}{\lambda}$, $\hat{Y} = \frac{b}{b}$, $\hat{Z} = \frac{\hat{t}}{c} = \frac{b}{c}$, $\tilde{\zeta}_1 = \frac{r}{\lambda}$, $\tilde{\zeta}_2 = \frac{h}{c}$, which gives

$$\begin{aligned}\frac{d\mathcal{X}}{dt} &= 1 - \mathcal{X}\mathcal{Y} - \frac{d}{b}\mathcal{X} - \xi_1 Q \\ \frac{d\mathcal{Y}}{dt} &= \frac{\beta\lambda}{b^2}\mathcal{X}\mathcal{Y} - \frac{a}{b}\mathcal{Y} - \frac{pc}{b^2}\mathcal{Y}\mathcal{Z} \\ \frac{d\mathcal{Z}}{dt} &= 1 - \mathcal{Z} - \xi_2 Q\end{aligned}$$

Then we let $\phi = \frac{d}{b}$, $\gamma = \frac{a}{b}$, $\epsilon = \frac{\beta\lambda}{b^2}$ and $\omega = \frac{pc}{b^2}$ which gives the final simplified set of equations

$$\begin{aligned}\frac{d\mathcal{X}}{dt} &= (1 - \xi_1 Q) - \mathcal{X}(\phi + \mathcal{Y}) \\ \frac{d\mathcal{Y}}{dt} &= \mathcal{Y}(\epsilon\mathcal{X} - \gamma - \omega\mathcal{Z}) \\ \frac{d\mathcal{Z}}{dt} &= (1 - \xi_2 Q) - \mathcal{Z}\end{aligned}$$

For convenience in the main text and for the remainder of this appendix we replace the above \mathcal{X} with X and likewise for \mathcal{Y} , \mathcal{Z} and t with Y , Z and t .

Piecewise equilibria for the within-host model

The equilibria for the non-dimensional model are

$$(X_{DFE}, Y_{DFE}, Z_{DFE}) = \left(\frac{1 - \tilde{\zeta}_1 Q}{\phi}, 0, 1 - \tilde{\zeta}_2 Q \right)$$

and

$$(X_{EE}, Y_{EE}, Z_{EE}) = \left(\frac{\gamma - \tilde{\zeta}_2 Q \omega + \omega}{\epsilon}, \frac{\epsilon - \tilde{\zeta}_1 Q \epsilon}{\gamma - \tilde{\zeta}_2 Q \omega + \omega} - \phi, 1 - \tilde{\zeta}_2 Q \right)$$

We define X' to be the equilibrium state of within-host cells in an uninfected individual in the absence of infection. Under increasing Q , the solution for X' is defined until $\frac{1 - \tilde{\zeta}_1 Q}{\phi} = 0$ (after which the solution would be negative) and hence we set the value equal to zero after this point:

$$X' = \begin{cases} \frac{1 - \tilde{\zeta}_1 Q}{\phi}, & \text{if } 1 - \tilde{\zeta}_1 Q > 0 \\ 0, & \text{otherwise} \end{cases}$$

We define X^* to be the equilibrium state of within-host cells in an infected individual. The solution depends on whether or not the infection is present within the host, and whether or not the immune system has been depleted to zero. If the immune system Z is nonzero ($1 - \tilde{\zeta}_2 Q > 0$), X^* is the solution defined by X_{EE} . However, once the immune system is

depleted, then the ODEs become

$$\begin{aligned}\frac{dX}{dt} &= (1 - \xi_1 Q) - X(\phi + Y) \\ \frac{dY}{dt} &= Y(\epsilon X - \gamma)\end{aligned}$$

which has a solution at

$$(X_{EE2}, Y_{EE2}) = \left(\frac{\gamma}{\epsilon}, \frac{-\gamma\phi - \xi_1 Q\epsilon + \epsilon}{\gamma} \right)$$

Hence if $Z = 0$ at $1 - \xi_2 Q = 0$ and the parasite density is above zero, then X^* is the solution defined by X_{EE2} . However, once the infection is removed from the system by the toxicant, the ODE system becomes

$$\frac{dX}{dt} = (1 - \xi_1 Q) - \phi X$$

which has a solution at

$$X_{DFE} = \frac{1 - \xi_1 Q}{\phi}$$

After $Y^* = 0$ the solution for X^* becomes identical to X' . Collecting these three conditions together yields the piecewise equilibria defined as:

$$X^* = \begin{cases} \frac{\gamma - \zeta_2 Q \omega + \omega}{\epsilon}, & \text{if } 1 - \zeta_2 Q > 0 \\ \frac{\gamma}{\epsilon}, & \text{if } 1 - \zeta_2 Q \leq 0 \text{ \& } Y^* > 0 \\ X', & \text{if } 1 - \zeta_2 Q \leq 0 \text{ \& } Y^* = 0 \end{cases}$$

Similarly Y^* is the equilibrium state of parasite density in an infected individual. This is determined by the status of immunity and by the point at which the infection is removed from the system. If $Z > 0$ at $1 - \zeta_2 Q > 0$ then Y^* is defined by Y_{EE1} . However if the immune system is depleted then the ODE system becomes 2 dimensional and the solution for Y^* becomes Y_{EE2} . This solution is defined until $Y_{EE2} = 0$, at which point the infection is completely removed from the host and remains at 0 indefinitely. Collecting these conditions together yields the piecewise equilibria for the parasite density:

$$Y^* = \begin{cases} \frac{\epsilon - \zeta_1 Q \epsilon}{\gamma - \zeta_2 Q \omega + \omega} - \phi, & \text{if } 1 - \zeta_2 Q > 0 \\ \frac{-\gamma \phi - \zeta_1 \epsilon + \epsilon}{\gamma}, & \text{if } 1 - \zeta_2 Q \leq 0 \text{ \& } \frac{-\gamma \phi - \zeta_1 \epsilon + \epsilon}{\gamma} > 0 \\ 0, & \frac{-\gamma \phi - \zeta_1 \epsilon + \epsilon}{\gamma} \leq 0 \end{cases}$$

The basic reproduction number

We will use the next generation matrix method to derive the basic reproduction number. The disease free equilibrium for the between-host model is

$$(S^{DFE}, I^{DFE}) = \left(\frac{\Lambda + k\Lambda X'}{u}, 0 \right)$$

The next generation matrix G is comprised of two parts: F and V^{-1} where F represents the new infections and V represents the transfer of individuals between compartments:

$$F = \begin{pmatrix} 0 & 0 \\ IY^*\theta & SY^*\theta \end{pmatrix}$$

$$V = \begin{pmatrix} \frac{u}{kX'+1} + IY^*\theta & SY^*\theta \\ 0 & \frac{u}{kX^*+1} \end{pmatrix}$$

$$V^{-1} = \begin{pmatrix} \frac{kX'+1}{u+I(kX'+1)Y^*\theta} & -\frac{S(kX'+1)(kX^*+1)Y^*\theta}{u(u+I(kX'+1)Y^*\theta)} \\ 0 & \frac{kX^*+1}{u} \end{pmatrix}$$

so that

$$G = FV^{-1} = \begin{pmatrix} 0 & 0 \\ IY^*\theta & SY^*\theta \end{pmatrix} \begin{pmatrix} \frac{kX'+1}{u+I(kX'+1)Y^*\theta} & -\frac{S(kX'+1)(kX^*+1)Y^*\theta}{u(u+I(kX'+1)Y^*\theta)} \\ 0 & \frac{kX^*+1}{u} \end{pmatrix}$$

$$G = \begin{pmatrix} 0 & 0 \\ 1 - \frac{u}{u+I(kX'+1)Y^*\theta} & \frac{S(kX^*+1)Y^*\theta}{u+I(kX'+1)Y^*\theta} \end{pmatrix}$$

The eigenvalues of G are

$$\left(0, \frac{\theta SY^*(kX^* + 1)}{\theta IY^*(kX' + 1) + u}\right)$$

The largest eigenvalue of G evaluated at the DFE is the basic reproduction number. $\frac{\theta SY^*(kX^*+1)}{\theta IY^*(kX'+1)+u}$ evaluated at $(S^{DFE}, I^{DFE}) = (\frac{\Lambda+k\Lambda X'}{u}, 0)$ gives the basic reproduction number:

$$R_0 = \frac{\theta \Lambda Y^*(1+kX')(1+kX^*)}{u^2}$$

Co-author contributions and declarations

Date: 09/09/2018

Please allow Ross Booton to include the following paper(s) which have been published (or submitted for publication), of which I was a co-author in his doctoral thesis. I confirm that Ross Booton conceived the initial idea for the paper(s) and was the primary contributor to the design and conduct of the reported research. All authors contributed its development. Ross Booton constructed the model(s) and analysed and interpreted the material. Ross Booton wrote the manuscript(s), with contributions from all authors.

Chapter 2: R. Booton, Y. Iwasa, J. Marshall, and D. Childs. Stress-Mediated Allee Effects Can Cause the Sudden Collapse of Honey Bee Colonies. *Journal of Theoretical Biology*, 420:213–219, 2017.

Chapter 3: R. Booton, D. Childs, R. Yamaguchi, Y. Tachiki, and S. Iwami. Multiple routes of transmission synergistically increase infection within the honey bee hive: a mathematical model. Manuscript submitted for publication, 2018.

Chapter 4: R. Booton, R. Yamaguchi, J. Marshall, D. Childs, and Y. Iwasa. Interactions between immunotoxicants and parasite stress: implications for host health. *Journal of Theoretical Biology*, 445: 120–127, 2018.

Chapter 5: R. Booton, Y. Iwasa, and D. Childs. How do toxicants affect epidemiological dynamics? Manuscript submitted for publication, 2018.

Name: Dr Dylan Childs



Signed:

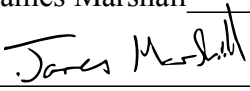
Date: 10/9/2018

Please allow Ross Booton to include the following paper(s) which have been published (or submitted for publication), of which I was a co-author in his doctoral thesis. I confirm that Ross Booton conceived the initial idea for the paper(s) and was the primary contributor to the design and conduct of the reported research. All authors contributed its development. Ross Booton constructed the model(s) and analysed and interpreted the material. Ross Booton wrote the manuscript(s), with contributions from all authors.

Chapter 2: R. Booton, Y. Iwasa, J. Marshall, and D. Childs. Stress-Mediated Allee Effects Can Cause the Sudden Collapse of Honey Bee Colonies. *Journal of Theoretical Biology*, 420:213–219, 2017.

Chapter 4: R. Booton, R. Yamaguchi, J. Marshall, D. Childs, and Y. Iwasa. Interactions between immunotoxicants and parasite stress: implications for host health. *Journal of Theoretical Biology*, 445: 120–127, 2018.

Name: James Marshall

Signed: 

Date: September 8, 2018

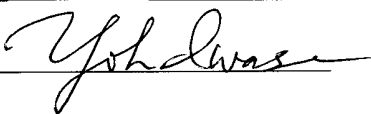
Please allow Ross Booton to include the following paper(s) which have been published (or submitted for publication), of which I was a co-author in his doctoral thesis. I confirm that Ross Booton conceived the initial idea for the paper(s) and was the primary contributor to the design and conduct of the reported research. All authors contributed its development. Ross Booton constructed the model(s) and analysed and interpreted the material. Ross Booton wrote the manuscript(s), with contributions from all authors.

Chapter 2: R. Booton, Y. Iwasa, J. Marshall, and D. Childs. Stress-Mediated Allee Effects Can Cause the Sudden Collapse of Honey Bee Colonies. *Journal of Theoretical Biology*, 420:213–219, 2017.

Chapter 4: R. Booton, R. Yamaguchi, J. Marshall, D. Childs, and Y. Iwasa. Interactions between immunotoxicants and parasite stress: implications for host health. *Journal of Theoretical Biology*, 445: 120–127, 2018.

Chapter 5: R. Booton, Y. Iwasa, and D. Childs. How do toxicants affect epidemiological dynamics? Manuscript submitted for publication, 2018.

Name: Yoh Iwasa

Signed: 


Date: 08/09/18

Please allow Ross Booton to include the following paper(s) which have been published (or submitted for publication), of which I was a co-author in his doctoral thesis. I confirm that Ross Booton conceived the initial idea for the paper(s) and was the primary contributor to the design and conduct of the reported research. All authors contributed its development. Ross Booton constructed the model(s) and analysed and interpreted the material. Ross Booton wrote the manuscript(s), with contributions from all authors.

Chapter 3: R. Booton, D. Childs, R. Yamaguchi, Y. Tachiki, and S. Iwami. Multiple routes of transmission synergistically increase infection within the honey bee hive: a mathematical model. Manuscript submitted for publication, 2018.

Chapter 4: R. Booton, R. Yamaguchi, J. Marshall, D. Childs, and Y. Iwasa. Interactions between immunotoxicants and parasite stress: implications for host health. *Journal of Theoretical Biology*, 445: 120–127, 2018.

Name: Ryo Yamaguchi

Signed: 

Date: 11 / 9 / 2018

Please allow Ross Booton to include the following paper(s) which have been published (or submitted for publication), of which I was a co-author in his doctoral thesis. I confirm that Ross Booton conceived the initial idea for the paper(s) and was the primary contributor to the design and conduct of the reported research. All authors contributed its development. Ross Booton constructed the model(s) and analysed and interpreted the material. Ross Booton wrote the manuscript(s), with contributions from all authors.

Chapter 3: R. Booton, D. Childs, R. Yamaguchi, Y. Tachiki, and S. Iwami. Multiple routes of transmission synergistically increase infection within the honey bee hive: a mathematical model. Manuscript submitted for publication, 2018.

Name: Shingo Iwami

Signed: 岩見真吾

Date: 9 Sep 2018

Please allow Ross Booton to include the following paper(s) which have been published (or submitted for publication), of which I was a co-author in his doctoral thesis. I confirm that Ross Booton conceived the initial idea for the paper(s) and was the primary contributor to the design and conduct of the reported research. All authors contributed its development. Ross Booton constructed the model(s) and analysed and interpreted the material. Ross Booton wrote the manuscript(s), with contributions from all authors.

Chapter 3: R. Booton, D. Childs, R. Yamaguchi, Y. Tachiki, and S. Iwami. Multiple routes of transmission synergistically increase infection within the honey bee hive: a mathematical model. Manuscript submitted for publication, 2018.

Name: YUUYA TACHIKI

Signed: 立花 結子

